Aus dem Institut für Physik der Universität Potsdam

Statistical Properties and Scaling
of the Lyapunov Exponents
in Stochastic Systems

Dissertation

zur Erlangung des akademischen Grades

Doktor der Naturwissenschaften (Dr. rer. nat.)

in der Wissenschaftsdisziplin Theoretische Physik

eingereicht an der

Mathematisch-Naturwissenschaftlichen Fakultät

der Universität Potsdam

von

RÜDIGER ZILLMER

geboren am 21. März 1969 in Schwedt

Potsdam, im Oktober 2003

Abstract

This work incorporates three treatises which are commonly concerned with a stochastic theory of the Lyapunov exponents. With the help of this theory universal scaling laws are investigated which appear in coupled chaotic and disordered systems.

First, two continuous-time stochastic models for weakly coupled chaotic systems are introduced to study the scaling of the Lyapunov exponents with the coupling strength (coupling sensitivity of chaos). By means of the the Fokker-Planck formalism scaling relations are derived, which are confirmed by results of numerical simulations.

Next, coupling sensitivity is shown to exist for coupled disordered chains, where it appears as a singular increase of the localization length. Numerical findings for coupled Anderson models are confirmed by analytic results for coupled continuous-space Schrödinger equations. The resulting scaling relation of the localization length resembles the scaling of the Lyapunov exponent of coupled chaotic systems.

Finally, the statistics of the exponential growth rate of the linear oscillator with parametric noise are studied. It is shown that the distribution of the finite-time Lyapunov exponent deviates from a Gaussian one. By means of the generalized Lyapunov exponents the parameter range is determined where the non-Gaussian part of the distribution is significant and multiscaling becomes essential.

Kurzfassung

Die vorliegende Arbeit umfaßt drei Abhandlungen, welche allgemein mit einer stochastischen Theorie für die Lyapunov-Exponenten befaßt sind. Mit Hilfe dieser Theorie werden universelle Skalengesetze untersucht, die in gekoppelten chaotischen und ungeordneten Systemen auftreten.

Zunächst werden zwei zeitkontinuierliche stochastische Modelle für schwach gekoppelte chaotische Systeme eingeführt, um die Skalierung der Lyapunov-Exponenten mit der Kopplungsstärke (*coupling sensitivity of chaos*) zu untersuchen. Mit Hilfe des Fokker-Planck-Formalismus werden Skalengesetze hergeleitet, die von Ergebnissen numerischer Simulationen bestätigt werden.

Anschließend wird gezeigt, daß *coupling sensitivity* im Fall gekoppelter ungeordneter Ketten auftritt, wobei der Effekt sich durch ein singuläres Anwachsen der Lokalisierungslänge äußert. Numerische Ergebnisse für gekoppelte Anderson-Modelle werden bekräftigt durch analytische Resultate für gekoppelte raumkontinuierliche Schrödinger-Gleichungen. Das resultierende Skalengesetz für die Lokalisierungslänge ähnelt der Skalierung der Lyapunov-Exponenten gekoppelter chaotischer Systeme.

Schließlich wird die Statistik der exponentiellen Wachstumsrate des linearen Oszillators mit parametrischem Rauschen studiert. Es wird gezeigt, daß die Verteilung des zeitabhängigen Lyapunov-Exponenten von der Normalverteilung abweicht. Mittels der verallgemeinerten Lyapunov-Exponenten wird der Parameterbereich bestimmt, in welchem die Abweichungen von der Normalverteilung signifikant sind und Multiskalierung wesentlich wird.

Contents

1 Introduction

In the beginning of the 20th century unpredictability entered physics as a fundamental property of many processes in nature. The new theoretical basis for all science, quantum mechanics, has as a basic ingredient a statistical interpretation. But also in the realm of classical mechanics the possibility of chaos has destroyed the hope for an unlimited prediction of deterministic processes. The irregularity of a chaotic system usually forbids a detailed analysis of its motion. In many practical applications, however, one is interested in averaged quantities, such as the mean electrical current in an electronic device or the Lyapunov exponent of a chaotic system, the latter being the focus of this work. In theoretical models the influence of the respective irregular process may then be represented by an ensemble of fluctuating functions, which gave rise to the concept of stochastic processes. Usually noise is used to model the effect of fast degrees of freedom which are too involved to describe in more detail. As a consequence only the statistical properties of the irregular force are preserved which is usually sufficient to determine the motion of averaged quantities. This idea has helped to understand the motion of a particle suspended in water, the famous Brownian motion (see [31] for details), or the influence of noise in electrical circuits. An example for the effect of spatial irregularities on linear equations is given by Anderson localization in quantum systems: Due to the disordered potential the wavefunction decays exponentially (on average), characterized by a localization length which can be related to the corresponding Lyapunov exponent.

For some phenomena in chaotic dynamics, universal scaling relations exist that are valid for a wide range of different specific systems. A prominent example is the sequence of period doubling bifurcations characterized by the universal Feigenbaum constant [47]. A further example, which is studied in this work, is the scaling of the Lyapunov exponents of weakly coupled chaotic and disordered systems. In the case of coupled chaotic systems the role of chaos is to provide temporal or spatiotemporal fluctuations in the linearized dynamics.

It has been found that in several cases it is possible to model the chaotic fluctuations by random variables, which explains the universality of the observed phenomena and often allows an analytic treatment [22, 19]. This approach is to some extent comparable with the methods of statistical mechanics. However, there exists no general formalism for the stochastic modelling of chaotic fluctuations, mainly because one is often in the finite-size regime where specific properties of the respective systems have to be taken into account.

In this work the statistical approach is used to investigate the Lyapunov exponents of chaotic systems and of one-dimensional disordered chains. The remaining chapters are

organized as follows.

In chapter 2 a brief review of dynamical systems and chaos is given. The main focus is on concepts that are used in this work. Furthermore, the idea of stochastic modelling of chaotic fluctuations is reviewed and references to the literature of stochastic dynamics are given.

In chapter 3 we study the strong dependence of the Lyapunov exponents of weakly coupled chaotic systems on the coupling strength. DAIDO coined the notion "coupling sensitivity of chaos" for this behaviour which he first observed in 1984 [23]. Although some theoretical explanations of this effect have been given since, we gain further insight by using a very simple stochastic model that includes the key ingredients of the dynamics: fluctuations and coupling. We then compare the theoretical predictions of our model with results of numerical simulations.

Chapter 4 is concerned with weakly coupled disordered quantum systems which possess a quasi-one-dimensional geometry. This problem is formally similar to coupled chaotic Hamiltonian systems treated in chapter 3. As a consequence the localization length also shows coupling sensitivity, which to our knowledge has not been reported before. We perform numerical simulations of disordered chains which agree with the analytic results for a continuous-space model.

In chapter 5 we turn our attention to the linear oscillator with parametric noise, which serves as a model in localization theory as well as in the theory of chaotic Hamiltonian systems. The fluctuations lead to an exponential growth of the oscillations which is characterized by the Lyapunov exponent. We focus on the finite-time (local) Lyapunov exponent which fluctuates according to a time-dependent distribution. The deviations of this distribution from a Gaussian one are examined with the help of the generalized Lyapunov exponents. We identify the parameter range where the deviations are significant and multiscaling becomes essential.

Chapter 6 gives a summary of our main results and shows directions for further research. In addition, each of the chapters 3, 4, and 5 closes with a brief summary. The possible experimental relevance of our theoretical results is discussed in some detail in these summaries.

Finally, the two appendices A.1 and A.2 review some basic methods for the numerical calculation of Lyapunov exponents and for the treatment of stochastic differential equations. On page 73 an overview of the notation used in this work can be found.

2 Stochastic Theory of the Lyapunov Exponent

This chapter introduces the basic statistical formalism of this work. First a brief review of some of the main concepts of nonlinear dynamics is given, paying particular attention to the Lyapunov exponents as a measure of the stability of dynamical systems. Then two stochastic approaches to the Lyapunov exponents are presented whose extensions are studied in the following chapters.

2.1 Dynamical Systems

2.1.1 Differential Equations and Maps

A dynamical system describes the temporal evolution of a physical system, which is characterized by a number of state variables. Typical examples are coordinates for mechanical systems or voltages and currents for electrical ones. The d variables form a state vector $\boldsymbol{u} \in \mathbf{M} \subset \mathbf{R}^d$ that determines the system. Each possible state of the system corresponds to a point in the d-dimensional phase space, the temporal evolution of a state is described by a trajectory $\boldsymbol{u}(t)$ in this phase space. In a deterministic dynamical system the state of the system unequivocally determines its future evolution. The temporal evolution is typically either described by a set of differential equations or by a discrete map acting on the state vector.

In the case of ordinary differential equations (ODEs) it is sufficient to consider sets of first order ODEs,

$$\mathrm{d}\boldsymbol{u}(t)/\mathrm{d}t = \boldsymbol{f}(\boldsymbol{u}(t)), \tag{2.1}$$

where $t \in \mathbf{R}$ is the continuous time and $\boldsymbol{f} : \mathbf{M} \to \mathbf{R}^d$ is a function that is in general nonlinear. Equations including higher order derivatives or explicit time dependences can be transformed into this form by introducing additional state variables. If one observes the system at discrete time instants, one can describe the temporal evolution by a map,

$$\boldsymbol{u}(t+1) = \boldsymbol{f}(\boldsymbol{u}(t)), \tag{2.2}$$

where $t \in \mathbf{Z}$ is the discrete time and $\boldsymbol{f} : \mathbf{M} \to \mathbf{M}$ is again a function that is in general nonlinear. Given an initial condition $\boldsymbol{u}(0)$, it is clear that the temporal evolution of $\boldsymbol{u}(t)$ for $t > 0$ is determined unequivocally. A discrete map can be attributed to a continuous-time dynamical system via the Poincaré surface of section (see, e.g. Ref. [47]).

2.1.2 Lyapunov Exponents

An important characteristic of chaotic dynamics is the exponential divergence of initially adjacent trajectories. This can be mathematically characterized with the help of a stability analysis. A trajectory $u(t)$ is called asymptotically stable if there exists a phase space volume around it such that trajectories $u'(t)$ in this volume approach $u(t)$ in the long time limit,

$$\lim_{t \to \infty} \| u(t) - u'(t) \| = 0.$$

We first limit our attention to differential equations of the form (2.1). We consider a reference trajectory $u(t)$ and a second trajectory $u(t) + w(t)$, where $w(t)$ is a small perturbation or inaccuracy. By means of the Taylor expansion

$$f(u + w) = f(u) + \mathbf{J}(u)w + O(\| w \|^2)$$

(where $\mathbf{J}$ is the Jacobian of f) we can study the time evolution of the perturbation vector in linear approximation,[1]

$$\mathrm{d}w(t)/\mathrm{d}t = \mathbf{J}(u(t))w(t).$$

Note that the Jacobian $\mathbf{J}(u(t))$ is in general time-dependent. If the reference trajectory consists of a fixed point, $u(t) = u_0$, its stability depends on the real parts of the eigenvalues γ_i ($i = 1, \ldots, d$) of the constant Jacobian $\mathbf{J}(u_0)$:

$$\max_i\{\Re\gamma_i\} \begin{cases} < 0: & \text{asymptotically stable,} \\ = 0: & \text{marginally stable,} \\ > 0: & \text{unstable.} \end{cases}$$

In the case of marginal stability one has to consider higher order terms in the Taylor expansion of $f(u + w)$ to decide about the stability of the fixed point.

In the case of discrete maps of the form (2.2), we can also use the Taylor expansion of $f(u + w)$ and obtain in linear approximation

$$w(t + 1) = \mathbf{J}(u(t))w(t).$$

If the reference trajectory consists of a fixed point u_0, the stability again depends on the eigenvalues γ_i ($i = 1, \ldots, d$) of the constant Jacobian $\mathbf{J}(u_0)$. Here, however, the logarithms of the absolute eigenvalues are of interest:

$$\max_i\{\ln|\gamma_i|\} \begin{cases} < 0: & \text{asymptotically stable,} \\ = 0: & \text{marginally stable,} \\ > 0: & \text{unstable.} \end{cases}$$

---

[1] We write an equal sign here and understand $w(t)$ as a "linear perturbation".

If the reference trajectory is not a fixed point, its stability is measured by the Lyapunov exponents. We first concentrate on discrete maps of the form (2.2). Given the initial conditions $u_0 = u(0)$ and $w_0 = w(0)$ (with $\| w_0 \| = 1$), we define the local (or finite-time) Lyapunov exponents as

$$\lambda(t, u_0) = \frac{1}{t} \ln \| w(t) \| = \frac{1}{t} \ln \| \mathbf{P}(t, u_0) w_0 \| = \frac{1}{2t} \ln(w_0^T \mathbf{P}^T(t, u_0) \mathbf{P}(t, u_0) w_0), \qquad (2.3)$$

where the upper index T denotes the transpose and

$$\mathbf{P}(t, u_0) = \prod_{\tau=0}^{t-1} \mathbf{J}(u(\tau)).$$

The real nonnegative symmetric matrix $\mathbf{P}^T \mathbf{P}$ has real nonnegative eigenvalues $\gamma_i(t, u_0)$ ($i = 1, \ldots, d$) and eigenvectors which are orthogonal to each other. Choosing w_0 in the direction of the eigenvector corresponding to the eigenvalue $\gamma_i(t, u_0)$, we have

$$\lambda_i(t, u_0) = \frac{1}{2t} \ln(w_0^T \gamma_i(t, u_0) w_0) = \frac{1}{2t} \ln \gamma_i(t, u_0).$$

In the long-time limit we obtain the Lyapunov exponents

$$\lambda_i = \lim_{t \to \infty} \lambda_i(t, u_0)$$

which are according to Oseledec's multiplicative ergodic theorem independent of u_0 for almost all u_0 (see, e.g. Ref. [33]). We sort the Lyapunov exponents with decreasing magnitude, $\lambda_1 \geq \lambda_2 \geq \cdots \geq \lambda_d$. A generic perturbation w_0 will have components in the directions of all eigenvectors and thus rapidly align in the direction of fastest growth. Due to ergodicity, we also obtain the largest Lyapunov exponent by means of averaging its finite-time value with respect to the invariant measure of u,

$$\lambda_1 = \langle \lambda_1(t, u_0) \rangle . \qquad (2.4)$$

A numerical method for the calculation of Lyapunov exponents is given in App. A.1.

In the case of differential equations of the form (2.1) Lyapunov exponents are defined in nearly the same way. The only difference is that $\mathbf{P}(t, u_0)$ has to be replaced by $\mathbf{O}(t, u_0)$, which is the matrix solution of the differential equation

$$d\mathbf{O}(t, u_0)/dt = \mathbf{J}(u(t))\mathbf{O}(t, u_0)$$

with the initial condition $\mathbf{O}(0, u_0) = \mathbf{I}$ (where $\mathbf{I}$ is the unit matrix). For trajectories of autonomous continuous-time systems one Lyapunov exponent is always zero (except for trajectories that consist of single fixed points); this accounts for the phase space motion along the trajectory.

The concept of Lyapunov exponents is one of the most direct tools to characterize dynamical systems. Although the Lyapunov exponents themselves have no physical meaning, many physically relevant quantities, such as the correlation time and the entropy, depend on them (see, e.g. Ref. [22]). Furthermore, the Lyapunov exponents are used to classify dynamical systems with respect to their stability properties in the following way. After a transient time a system typically settles on an attractor. Without going into mathematical details, an attractor can be seen as a set of phase space points that is approached by all trajectories starting from a surrounding phase space volume (the basin of attraction). The Lyapunov exponents are average quantities that describe the stretching and shrinking of phase space volumes in different directions. For dissipative systems the sum of Lyapunov exponents is negative, while it is zero for conservative systems. The Lyapunov exponents provide a criterion to decide about the nature of an attractor. As chaos is characterized by a sensitive dependence of the system behaviour on initial conditions, it can be associated with a positive largest Lyapunov exponent λ_1. For continuous-time systems we have the following classification:

$$\lambda_1 < 0 : \quad \text{attractive fixed point,}$$
$$\lambda_1 = 0, \ \lambda_2 < 0 : \quad \text{attractive limit cycle,}$$
$$\lambda_1 = \lambda_2 = 0 : \quad \text{quasiperiodic attractor,}$$
$$\lambda_1 > 0 : \quad \text{chaotic attractor.}$$

Finally we remark that the Lyapunov exponents play a crucial role in the context of localization, see Sec. 4.1 below.

The estimation of Lyapunov exponents from time series of experimental systems is very difficult, although some methods exist for the estimation of at least the largest Lyapunov exponent [34]. Therefore, the Lyapunov exponents are most useful for systems which mathematical models are known for.

If only the largest Lyapunov exponent is considered, we set for simplicity $\lambda \equiv \lambda_1$ in the following.

2.1.3 Generalized Lyapunov Exponents

The local Lyapunov exponent $\lambda(t)$, Eq. (2.3), is a fluctuating quantity with a probability density $P(\lambda;t)$ (defined by sampling all initial conditions $\boldsymbol{u}_0$ in phase space according to the invariant measure). A possible way to extract information about a distribution is to consider higher moments. Within the framework of Lyapunov exponents this leads to the generalized Lyapunov exponents, defined as

$$L(q) = \frac{1}{q} \lim_{t \to \infty} \frac{1}{t} \ln \langle \| \boldsymbol{w}(t) \|^q \rangle \ , \tag{2.5}$$

where the average refers to $P(\lambda;t)$. These exponents give the exponential growth rate of higher moments of the perturbation $\boldsymbol{w}(t)$, and because of the fluctuations of $\lambda(t)$ they are

not equal to the usual largest Lyapunov exponent, $L(q) \neq \lambda_1$. For large q this is intuitively clear, because the growth of high moments of the perturbation amplitude is dominated by rare events that correspond to the tail of $P(\lambda; t)$. However, the largest Lyapunov exponent is included in the above definition as a special case,

$$\lambda_1 = \lim_{q \to 0} L(q) \ .$$

For a detailed discussion of the exponents $L(q)$ we rewrite Eq. (2.3) as $\| w(t) \| = \exp[t\lambda(t)]$. Thus the cumulants $K_q(t)$ of the process $\lambda(t)$ can be related to the moments of the norm $\| w(t) \|$ (see [65] for details concerning the cumulant expansion):

$$\langle \| w(t) \|^q \rangle \ = \ \langle \exp[q\lambda(t)t] \rangle \ = \ \exp \left[\sum_{n=1}^{\infty} \frac{q^n t^n}{n!} K_n(t) \right] \ .$$

The first two cumulants which correspond to the mean and the variance of $\lambda(t)$, respectively, scale for large times as follows:

$$K_1(t) = \langle \lambda(t) \rangle \xrightarrow[t \to \infty]{} \lambda_1 \ , \quad K_2(t) = \langle [\lambda(t) - \lambda_1]^2 \rangle \xrightarrow[t \to \infty]{} D/t \ ; \tag{2.6}$$

with the diffusion constant D. The variance K_2 vanishes for large times in accordance with the self-averaging property of the largest Lyapunov exponent. Hence, by definition (2.5), the generalized Lyapunov exponent is the asymptotic cumulant-generating function of $P(\lambda; t)$:

$$L(q) \ = \ \lim_{t \to \infty} \sum_{n=1}^{\infty} \frac{q^{n-1} t^{n-1}}{n!} K_n(t) \ = \ \lambda_1 + \frac{q}{2} D + \lim_{t \to \infty} \sum_{n=3}^{\infty} \frac{q^{n-1} t^{n-1}}{n!} K_n(t) \ . \tag{2.7}$$

In other words, $L(q)$ can be expanded in a power series around $q = 0$ with coefficients given by the cumulants of the local Lyapunov exponent. It immediately follows that

$$\lambda_1 = L(0) \ , \quad D = 2L'(0) \ .$$

There is still a more direct connection between $L(q)$ and the distribution of $\lambda(t)$. For $t \gg 1$ the probability density $P(\lambda; t)$ can be written in a scaling form as (see e.g. [28, 10])

$$P(\lambda; t) \sim \exp[-t f(\lambda)] \ .$$

The entropy function $f(\lambda)$ is connected with the generalized Lyapunov exponent via a Legendre transformation [48, 22]:

$$f(\lambda) \ = \ q\lambda - qL(q) \ , \quad \frac{\mathrm{d}}{\mathrm{d}q} qL(q) = \lambda \ . \tag{2.8}$$

The expansion of the entropy function around $\lambda = \lambda_1$ reads $f \approx (\lambda - \lambda_1)^2 / 2D$, which yields a Gaussian distribution of the local Lyapunov exponent. In the tails, however, deviations from the Gaussian will be present in general.

Ususally the generalized exponents are difficult to compute numerically, which is not the case for the largest exponent because it is a self-averaged quantity (see Eq. (2.4)). The effect of non-Gaussian fluctuations of the exponential growth rate on the $L(q)$ are discussed in more detail in Ch. 5. For a comprehensive overview see [48, 49].
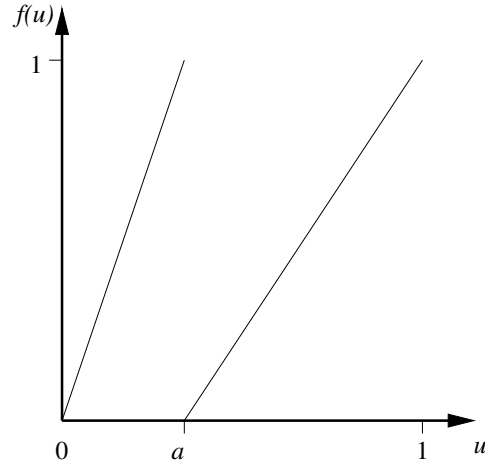
Figure 2.1: The skew Bernoulli map.

2.1.4 Example: Skew Bernoulli Map

A simple example which allows analytical calculations of Lyapunov exponents is given by the one-dimensional skew Bernoulli map (see Fig. 2.1)

$$f : [0,1] \to [0,1] \quad , \quad u \mapsto \begin{cases} u/a & \text{if } u \leq a, \\ (u-a)/(1-a) & \text{if } u > a. \end{cases} \tag{2.9}$$

The map depends on a parameter $a \in (0,1)$. Due to the uniform invariant measure of the map, the absolute derivative is given by

$$|f'(u)| = \begin{cases} 1/a & \text{with probability } a, \\ 1/(1-a) & \text{with probability } 1-a. \end{cases}$$

The Lyapunov exponent is easily calculated by averaging the one step (finite-time) Lyapunov exponent according to Eq. (2.4),

$$\lambda = \langle \lambda(1,u_0) \rangle = \langle \ln|f'(u_0)| \rangle = -a \ln a - (1-a) \ln(1-a).$$

The Lyapunov exponent is positive for all values of $a \in (0,1)$ and has a maximum at $a = 1/2$. The variance of the one step Lyapunov exponent can also be calculated,

$$2\sigma^2 = \langle [\lambda(1,u_0) - \lambda]^2 \rangle = a(1-a)\left(\ln\frac{a}{1-a}\right)^2.$$

The variance is zero only for $a = 0.5$ and has maxima at $a \approx 0.5 \pm 0.417$.

The generalized Lyapunov exponents can be calculated by noting that the $|f'(u)|$ are not correlated:

$$L(q) = \frac{1}{q} \ln \left[a^{1-q} + (1-a)^{1-q} \right] = \alpha + \frac{\beta}{2} q + O(q^2) \ .$$

For the coefficients α, β one obtains,

$$\alpha = -a \ln a - (1-a) \ln(1-a) = \lambda \ , \quad \beta = a(1-a) \left(\ln \frac{a}{1-a} \right)^2 = 2\sigma^2 \ ,$$

in accordance with the statements of section 2.1.3.

2.2 Stochastic Modelling of the Exponential Instability in Chaotic Systems

In Ch. 3 we focus on the coupling sensitivity of the Lyapunov exponents. It turns out, that this effect is within a large range independent of the nature of the underlying chaotic dynamics. It is thus appropriate to use simple models for the chaotic behavior. In recent years it turned out that for several problems it is possible to model chaotic fluctuations by random variables [52, 12, 49, 66, 29] (for an introduction see Ref. [22]). The phenomena studied in this work are found in the perturbation dynamics (Lyapunov exponents) rather than in the dynamics of the state variables. We therefore aim at stochastic models of the perturbation dynamics of chaotic systems. Lyapunov exponents are widely used in the context of random dynamical systems [22, 7].

In the following sections we introduce two stochastic models for the perturbation dynamics of dissipative and Hamiltonian chaotic systems, resp. The particular models used to study the phenomena of coupling sensitivity of chaos are introduced in Ch. 3. To be able to make use of the Fokker-Planck equation, we choose continuous-time models with Gaussian white noise. This choice is motivated by the observation that the effects we study are found for discrete-time as well as continuous-time dynamics, and do not seem to depend on the distribution of fluctuations of particular systems. For low-dimensional dynamics very simple stochastic models can already be sufficient. In Ch. 3 this is demonstrated for the case of two weakly coupled chaotic systems. In the high-dimensional case, however, spatial diffusion often plays an important role, which can be incorporated by the use of spatially extended stochastic models [54].

Problems are encountered for systems with long temporal correlations, in which white noise is not appropriate to replace the fluctuations. An example is given by strange non-chaotic attractors [53, 68]. Most chaotic systems, however, show a rapid decay of temporal correlations and are thus adequately modelled by a Langevin approach.

2.2.1 Dissipative Systems

Here we aim at a simple stochastic model for the dynamics of perturbations, which should reproduce the long time behavior (with the Lyapunov exponent λ),

$$w(t) \to w(0)e^{\lambda t} \quad \text{for} \quad t \to \infty \,,$$

but also allow for finite-time fluctuations. The amplitude $w(t)$ is understood as the component of the perturbation vector in the direction of the fastest growth. The simplest ansatz seems to be the linear Stratonovich stochastic differential equation (see App. A.2 and Ref. [65, 31])

$$\mathrm{d}w(t)/\mathrm{d}t = [\lambda + \xi(t)]w(t)\,, \tag{2.10}$$

where $\xi(t)$ is a Gaussian stochastic process with

$$\langle \xi(t) \rangle = 0 \,, \qquad \langle \xi(t)\xi(t') \rangle = 2\sigma^2 \delta(t - t')$$

(the averages are over different realizations of the noise). We notice that $w(t)$ stays positive if $w(0) > 0$. Integration leads to

$$w(t) = w(0)\exp\left(\lambda t + \int_0^t \xi(\tilde{t})\,\mathrm{d}\tilde{t}\right) = w(0)\exp\left(\lambda t + \sqrt{2\sigma^2}W(t)\right)\,, \tag{2.11}$$

where $W(t)$ is the Wiener process (see App. A.2). The local Lyapunov exponent is according to definition (2.3) given by

$$\lambda(t) = \lambda + \frac{\sqrt{2\sigma^2}}{t}W(t)\,. \tag{2.12}$$

Since $W(t)/t \to 0$ for $t \to \infty$ with probability one, we have

$$w(t) \to w(0)e^{\lambda t} \quad \text{for} \quad t \to \infty \,.$$

The distribution of $\lambda(t)$ is a Gaussian, defined by its mean and variance:

$$\langle \lambda(t) \rangle = \lambda \,, \qquad \langle [\lambda(t) - \lambda]^2 \rangle = \frac{2\sigma^2}{t}\,.$$

Thus the higher cumulants vanish in Eq. (2.7) and the generalized Lyapunov exponents assume the simple form,

$$L(q) = \lambda + \frac{q}{2}\sigma^2 \,.$$

Now we have the somewhat paradoxical result that the $L(q)$ are nonzero even for $\lambda = 0$. This, however, is due to the diffusion of the logarithm $\ln w(t) \propto t\lambda(t)$ about its mean growth $t\lambda$ (see Eq. 2.12) caused by the fluctuating term $(\sqrt{2\sigma^2}/t)W(t)$. The expression for the $L(q)$ also reflects the statement that they contain information about the whole distribution of the

local Lyapunov exponent. That is, the exponents $L(q)$ depend on both, the mean λ and the variance σ^2.

The correspondence to a real chaotic system can be achieved by setting λ and σ^2 equal to the Lyapunov exponent and the diffusion constant (see section 2.1.3), respectively, of the system under consideration. It should be noted that the noise $\xi(t)$ does not explicitly model the chaotic system. It mimics the fluctuations of the Jacobian, that is, nearby trajectories evolve with the same realization of the noise (see [15] for a detailed discussion of this problem). This model of the perturbation dynamics is strikingly simple, what of course restricts its adaptability. It ignores inhomogeneities of the chaotic attractor as well as correlations of the chaotic process. It is, however, sufficient to describe the phenomenon of coupling sensitivity as will be shown in Ch. 3.

2.2.2 Hamiltonian Systems

An important property of Hamiltonian systems is the conservation of the phase space volume corresponding to Liouville's theorem. In terms of Lyapunov exponents this requires the sum of the exponents to be zero (cf. sec. 2.1.2),

$$\sum_{i=1}^{2N} \lambda_i = 0 \, ,$$

where N is the number of degrees of freedom. Moreover, due to the symplectic structure of the equations of motion the Lyapunov exponents are pairwise conjugated[2]: $\lambda_i = -\lambda_{2N+1-i}$. This property gives rise to very distinct signatures of Hamiltonian chaos, such as homoclinic points, and it is thus advisable to include the phase volume conservation in a model of the perturbation dynamics.

Hence the model should be characterized by a fluctuating exponential growth, a Hamiltonian structure, and linearity; taking these minimal requirements into account a simple *ansatz* is the parametrically excited linear oscillator (also designated as random frequency oscillator) [65, 63]:

$$\mathrm{d}^2 w / \mathrm{d} t^2 + [E + \xi(t)]w = 0 \, , \quad \langle \xi(t)\xi(t') \rangle = 2\sigma^2 \delta(t - t') \, . \tag{2.13}$$

Generally we will assume that E can take on all values of the real axis. With the momentum variable $v \equiv \dot{w}$, the Hamiltonian of this system reads

$$H(w, v, t) = \frac{1}{2}v^2 + \frac{1}{2}[E + \xi(t)]w^2 \, .$$

The random modulations of the frequency lead via parametric instability to an exponential increase of the amplitude,

$$\sqrt{w^2 + v^2} \sim e^{\lambda t} \, ,$$

---

[2]an introduction into this topic can be found in [6]

characterized by the (Lyapunov) exponent λ. Unfortunately, the exponent λ can be expressed analytically only up to quadratures. Moreover, the non-Gaussian distribution of the local Lyapunov exponent,

$$\lambda(t) = \frac{1}{2t} \ln(w^2 + v^2) \,,$$

brings about multiscaling, which hampers a simple correspondence to real systems. These problems are treated in Ch. 5, where also analytic expressions for the Lyapunov exponents can be found.

However, there exists a correspondence between the random frequency oscillator and Hamiltonian systems with many degrees of freedom with a Hamiltonian of the form

$$H = \frac{1}{2} \sum_{1}^{N} p_i^2 + V(q_1, \ldots, q_N) \,,$$

where the q, p are the coordinates and conjugate momenta, resp. CASETTI et al. [19] used a geometric approach to derive Eq. (2.13) as an approximation to the perturbation dynamics. For this the authors assumed the system to be chaotic with a quasi-isotropic manifold. The parameters of Eq. (2.13) are then connected with the curvature of the potential V as follows,

$$E = \frac{1}{N} \langle \Delta V \rangle_\mu \,, \quad 2\sigma^2 = \frac{\tau}{N} \left(\langle (\Delta V)^2 \rangle_\mu - \langle \Delta V \rangle_\mu^2 \right) \,,$$

where τ is a characteristic correlation time scale and μ denotes the microcanonical average. This method has been succesfully applied to lattice systems, see e.g. [18, 9].

The random frequency oscillator also serves as a model in the theory of Anderson localization; an application in the case of coupled chains is the subject of Ch. 4.

3 Coupling Sensitivity of Chaotic Systems

In 1985 DAIDO discovered by means of numerical simulations that the Lyapunov exponents of weakly coupled chaotic maps show a very strong dependence on the strength of the coupling [23]. He was able to find an approximate logarithmic scaling relation and coined the notion "coupling sensitivity of chaos" for this behaviour. Further studies with different systems indicated that the effect is very general [24, 25, 26].

In the first part of this chapter a stochastic continuous-time model is presented that captures the essential aspects of the perturbation dynamics (the basic idea of stochastic modelling of chaotic fluctuations is explained in Sec. 2.2). This approach yields a general scaling relation which includes as a limiting case the logarithmic scaling found by DAIDO. The model further allows one to trace the origin of this effect and to identify the significant small parameter as the coupling strength divided by the strength of the fluctuations. Thus an application of perturbative methods such as the small noise expansion [8] is excluded. Results of numerical simulations using chaotic maps are presented that confirm the predictions of the derived scaling relation. Finally, a random walk picture is introduced that sheds light on the origin of the logarithmic singularity.

It will be further shown that coupling sensitivity is absent for the null Lyapunov exponent of continuous-time systems. This is qualitatively explained by taking into account the role of fluctuations.

In the remaining part of the chapter analytic and numerical results for coupled Hamiltonian systems will be presented. The analytic approach employs a coupled version of the second-order Langevin equation introduced in Sec. 2.2.2. The results prove the coupling sensitivity of the non-zero Lyapunov exponents for Hamiltonian systems.

Parallel to our work, a similar stochastic model has been used by CECCONI and POLITI to estimate the Lyapunov exponent of a coupled map lattice in the limit of weak coupling [21] (see also Sec. 3.1.2). The numerical computations in Sec. 3.1.4 have been carried out by VOLKER AHLERS and are described in detail in his dissertation [2]. Some of the results of this chapter have been published in Refs. [68, 3, 69].

3.1 Coupled Dissipative Systems

3.1.1 The Effect

DAIDO studied a system consisting of two coupled one-dimensional maps,

$$
\begin{aligned}
u_1(t+1) &= f(u_1(t)) + \kappa g(u_2(t), u_1(t)) \,, \\
u_2(t+1) &= f(u_2(t)) + \kappa g(u_1(t), u_2(t)) \,,
\end{aligned}
\tag{3.1}
$$

where $t \in \mathbf{Z}$ is the discrete time variable, κ is the coupling parameter (the coupling strength), u_1 and u_2 are the state variables, f is a nonlinear map, and g is a coupling function. The map f is assumed to be chaotic with a positive Lyapunov exponent Λ. In the following we always choose the coupling to be diffusive:[1] $g(u_2, u_1) = f(u_2) - f(u_1)$. It should be emphasized, however, that the effects described in this chapter are also found for other coupling functions.

Without coupling, $\kappa = 0$, we have two identical systems with equal Lyapunov exponents Λ. When coupling is introduced, the Lyapunov exponents are in general different. Furthermore, their values depend on the coupling parameter κ. We thus have the two Lyapunov exponents $\lambda_1(\kappa)$ and $\lambda_2(\kappa)$.

The observation of Daido was that for small values of the coupling parameter, $\kappa \ll 1$, the Lyapunov exponents diverge from each other and from the zero coupling value Λ according to

$$
\lambda_1 - \lambda_2 \sim \frac{1}{|\ln \kappa|} \,, \quad \lambda_{1,2} - \Lambda \sim \frac{1}{|\ln \kappa|} \,.
\tag{3.2}
$$

He found this to be a common behaviour of different maps f and different coupling functions g [23].

As a simple example we study the dependence of two coupled skew Bernoulli maps on the coupling parameter. The skew Bernoulli map is defined as (see also Sec. 2.1.4)

$$
f : [0,1] \to [0,1] \quad , \quad u \mapsto
\begin{cases}
u/a & \text{if } u \le a \,, \\
(u-a)/(1-a) & \text{if } u > a \,,
\end{cases}
\tag{3.3}
$$

with the parameter $a \in (0,1)$. The Lyapunov exponents of the system 3.1 of coupled maps are calculated by standard numerical methods (cf. App. A.1). In Fig. 3.1 the differences of the Lyapunov exponents $\lambda_{1,2}$ from the single map value Λ are shown as functions of the coupling parameter κ. From Fig. 3.1(b) it can be seen that for small values of coupling these differences indeed scale according to

$$
\lambda_i - \Lambda \sim \frac{1}{|\ln \kappa|} \,, \quad i = 1, 2 \,.
$$

---

[1] Naively choosing $g(u_2, u_1) = u_2 - u_1$ would give rise to the possibility that the $u_{1,2}(t+1)$ lie outside of the interval that the map f is acting on.
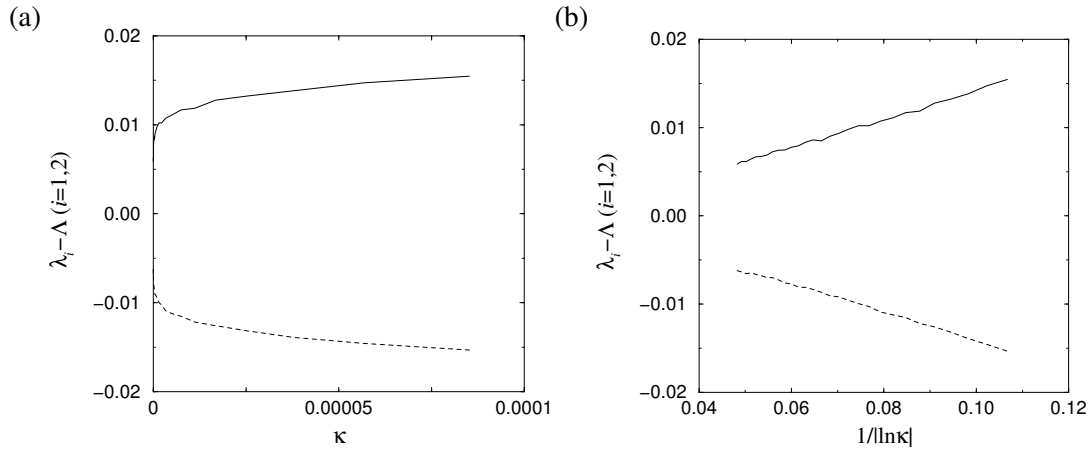
Figure 3.1: Coupled skew Bernoulli maps, Eq. (3.3). (a) The Lyapunov exponents $\lambda_1 - \Lambda_1$ (solid line) and $\lambda_2 - \Lambda_2$ (dashed line) *vs.* κ for $a = 1/4$. (b) The same data in scaled coordinates.

3.1.2 Previous Theoretical Results

The first theoretical approaches to understand the origin of the coupling sensitivity stem from DAIDO, who used an expansion of the local Lyapunov exponents of coupled maps and hence was able to reproduce the $1/|\ln\kappa|$ dependence [24]. He pointed out the importance of fluctuations of the local expansion rates and stressed that this prerequisite distinguishes the coupling sensitivity from the usual sensitive dependence on initial conditions. He later introduced a discrete-time stochastic model that shows the logarithmic singularity, but not the quantitative dependence on the magnitude of fluctuations of the local expansion rate [26].

Further theoretical investigations have focused on the largest Lyapunov exponent of coupled map lattices with weak coupling. In that context, which corresponds to the limit of infinitely many (instead of just two) coupled systems, a similar logarithmic singularity (with different prefactors) is observed.

LIVI et al. found an analogy to the problem of directed polymers in random media. They used a mean field approach and a tree approximation to estimate the dependence of the Lyapunov exponent on the coupling strength [43]. While their model approximately shows the $1/|\ln\kappa|$ dependence, it wrongly predicts a phase transition at a critical coupling strength. Subsequently CECCONI and POLITI were able to improve the previous approach by using an n-tree approximation [20]. They found that the critical coupling strength of the spurious phase transition shifts to higher values of κ with increasing tree depth n.

Finally, CECCONI and POLITI used a continuous-time approximation of a discrete-time model [21]. Parallel to our work, they found a relation similar to our result (3.12) (including the quantitative dependence on the magnitude of fluctuations of the local expansion rate), but with different prefactors because of the high dimensionality. Furthermore, they were able to find an approximate result for coupled maps which have derivatives with fluctuating

signs.

Our own approach does not start from coupled maps, but uses a simple continuous-time stochastic model of the perturbation dynamics with the key ingredients of exponential growth, finite-time fluctuations, and coupling. It further allows for different Lyapunov exponents of the coupled systems, which is needed to understand the phenomenon of avoided crossing of Lyapunov exponents [2].

3.1.3 Analytical Approach

Stochastic Model

The universality of the effect of coupling sensitivity of chaos indicates that there exists an underlying mechanism not connected with any special system. Furthermore, the effect has been found for both two- and higher-dimensional systems. The basic ingredients common to all studied systems are temporal fluctuations (due to the chaotic nature of the dynamics) and weak coupling. The first property is provided by the stochastic model (2.10) in section 2.2.1. In the following we propose an extension of this model to a system of two diffusive coupled Langevin equations:

$$
\begin{aligned}
\mathrm{d}w_1(t)/\mathrm{d}t &= [\Lambda_1 + \xi_1(t)]w_1(t) + \kappa[w_2(t) - w_1(t)] \ , \\
\mathrm{d}w_2(t)/\mathrm{d}t &= [\Lambda_2 + \xi_2(t)]w_2(t) + \kappa[w_1(t) - w_2(t)] \ .
\end{aligned}
\tag{3.4}
$$

Here the random processes ξ are normally distributed with zero mean and δ-correlated,

$$
\left\langle \xi_i(t)\xi_j(t') \right\rangle = 2\sigma_i^2 \delta_{ij}\delta(t - t') \ , \quad i,j \in \{1,2\} \ .
$$

These equations have to be interpreted in the Stratonovich sense. The Langevin approach allows the application of the Fokker-Planck equation and hence allows an analytic expression for the Lyapunov exponents, as is shown in the following section.

Three groups of parameters describe three important ingredients of the dynamics:

1. The *Lyapunov exponents* of the uncoupled systems are described by the constants $\Lambda_{1,2}$.

2. The *diffusion constants* $D_{1,2}$ of the logarithmic growth of the uncoupled systems (cf. section 2.2.1) are given by the parameters $\sigma_{1,2}^2$. They account for the fluctuations of local expansion rates. The value of σ^2 can thus be calculated from the variance of local Lyapunov exponents of a given chaotic system. In connection with the numerical simulations in Sec. 3.1.4, the parameters σ^2 will be calculated for different systems.

3. The *coupling* is described by the coupling parameter κ. For a while a symmetrical coupling is assumed, the case of asymmetrical coupling is considered in section 3.1.3. Coupling sensitivity of the Lyapunov exponent is expected for $\kappa \to 0$.

It has to be stressed that we assume the statistical properties of the individual systems (characterized by the distributions of the stochastic processes $\xi_{1,2}$) to be independent of the coupling. This assumption can be justified by means of results from a perturbation analysis of weakly coupled maps [17], indicating that the invariant measure depends on the coupling strength in a nonsingular way. In other words, the logarithmic singularity of the splitting of the Lyapunov exponents, $\sim 1/|\ln \kappa|$, is much stronger than possible changes of the statistics of the subsystems. Nevertheless, our model will certainly fail for strong coupling.

Without fluctuations, $\sigma_1^2 = \sigma_2^2 = 0$, and equal Lyapunov exponents of the uncoupled systems, $\Lambda_1 = \Lambda_2 = \Lambda$, we have a two-dimensional system of linear differential equations,

$$\frac{\mathrm{d}}{\mathrm{d}t} \begin{pmatrix} w_1 \\ w_2 \end{pmatrix} = \begin{pmatrix} \Lambda - \kappa & \kappa \\ \kappa & \Lambda - \kappa \end{pmatrix} \begin{pmatrix} w_1 \\ w_2 \end{pmatrix} .$$

The Lyapunov exponents are just the eigenvalues of the time-independent real symmetric matrix (cf. section 2.1.2). We thus obtain

$$\lambda_1 = \Lambda , \quad \lambda_2 = \Lambda - 2\kappa$$

for the Lyapunov exponents of the coupled systems. This means that without fluctuations of the local expansion rates there is no coupling sensitivity of chaos, a result that was already observed by DAIDO [23].

Analytical Expression for the Lyapunov Exponent

In the following the coupling dependence of the Lyapunov exponent will be explicitly derived, using the stationary probability density of the associated Fokker-Planck equation. The largest Lyapunov exponent is defined by

$$\lambda_1 = \lim_{t \to \infty} \frac{1}{2t} \left\langle \ln(w_1^2 + w_2^2) \right\rangle = \lim_{t \to \infty} \frac{1}{2t} \ln(w_1^2 + w_2^2) , \tag{3.5}$$

where the last equality corresponds to the self-averaging property of λ_1 [46]. The averages are over different realizations of the noise processes $\xi_{1,2}$.

First we perform a transformation to new variables,

$$v_1 = \ln(w_1/w_2) , \quad v_2 = \ln(w_1 w_2) .$$

For this it should be noted, that the regions $w_1, w_2 > 0$ and $w_1, w_2 < 0$ are absorbing ones because for $w_1 = 0$ we have $\dot{w}_1 = \kappa w_2$ and for $w_2 = 0$ we have $\dot{w}_2 = \kappa w_1$ in Eq. (3.4). This transformation leads to a partial decoupling of system (3.4):

$$\mathrm{d}v_1/\mathrm{d}t = \chi_1 - 2\kappa \sinh v_1 + \Lambda_1 - \Lambda_2 , \tag{3.6}$$

$$\mathrm{d}v_2/\mathrm{d}t = \chi_2 + 2\kappa \cosh v_1 + \Lambda_1 + \Lambda_2 - 2\kappa , \tag{3.7}$$

where $\chi_1 = \xi_1 - \xi_2$ and $\chi_2 = \xi_1 + \xi_2$. The equation for the evolution of v_1 is a closed Langevin equation for a random walk in the potential $\Phi = 2\kappa \cosh v_1 - (\Lambda_1 - \Lambda_2)v_1$. Thus we can write the Fokker-Planck equation for the probability density $\rho(v_1;t)$ [58] (see also App. A.2),

$$\frac{\partial \rho(v_1;t)}{\partial t} = \left[2\kappa \cosh v_1 + 2\kappa \sinh v_1 \frac{\partial}{\partial v_1} - (\Lambda_1 - \Lambda_2)\frac{\partial}{\partial v_1} + 2\sigma^2 \frac{\partial^2}{\partial v_1^2} \right] \rho(v_1;t) , \qquad (3.8)$$

where $\sigma^2 = (\sigma_1^2 + \sigma_2^2)/2$. The stationary solution of (3.8) is given by [67]

$$\rho_{\text{stat}}(v_1) = N \exp\left(l v_1 - \frac{\kappa}{\sigma^2} \cosh v_1 \right) , \qquad (3.9)$$

where $l = (\Lambda_1 - \Lambda_2)/(2\sigma^2)$ and N is a normalization constant. In order to calculate the Lyapunov exponent we first express it in terms of v_1 and v_2:

$$\ln(w_1^2 + w_2^2) = \ln\left(w_1 w_2 \left(\frac{w_1}{w_2} + \frac{w_2}{w_1} \right) \right) = v_2 + \ln(2\cosh v_1) .$$

According to the definition (3.5) the Lyapunov exponent is given by

$$\lambda_1 = \lim_{t\to\infty} \left\{ \frac{1}{2t}\langle v_2 \rangle + \frac{1}{2t}\langle \ln(2\cosh v_1) \rangle \right\} .$$

The second term vanishes for $t \to \infty$ because $\langle \ln(2\cosh v_1) \rangle_{\text{stat}}$ is finite and time-independent. Since one is interested in the long-time limit, the stationary distribution (3.9) of v_1 may be used. In the first term, $\langle v_2/t \rangle$ can thus be replaced by $\langle \dot{v}_2 \rangle_{\text{stat}}$. Hence the Lyapunov exponent can be calculated by averaging the r.h.s. of Eq. (3.7),

$$\lambda_1 = \frac{1}{2}\langle \dot{v}_2 \rangle_{\text{stat}} = \kappa \langle \cosh v_1 \rangle_{\text{stat}} + \frac{1}{2}(\Lambda_1 + \Lambda_2 - 2\kappa) . \qquad (3.10)$$

Averaging with the stationary distribution $\rho_{\text{stat}}(v_1)$ yields (see Ref. [67] for details)

$$\langle \cosh v_1 \rangle_{\text{stat}} = \frac{K_{1-|l|}(\kappa/\sigma^2) + K_{1+|l|}(\kappa/\sigma^2)}{2K_{|l|}(\kappa/\sigma^2)} ,$$

where the K_l are modified Bessel functions (Macdonald functions) [1]. Substituting this in Eq. (3.10) we obtain a final analytical formula for the largest Lyapunov exponent. We write it in a scaling form,

$$\frac{\lambda_1 - (\Lambda_1 + \Lambda_2 - 2\kappa)/2}{\sigma^2} = \frac{\kappa}{\sigma^2} \frac{K_{1-|l|}(\kappa/\sigma^2) + K_{1+|l|}(\kappa/\sigma^2)}{2K_{|l|}(\kappa/\sigma^2)} . \qquad (3.11)$$

This form demonstrates that the essential parameters of the problem are the coupling parameter and the Lyapunov exponents' mismatch normalized to the fluctuation of the exponents,

$$\frac{\kappa}{\sigma^2} \quad \text{and} \quad l = \frac{\Lambda_1 - \Lambda_2}{2\sigma^2} , \quad \text{respectively.}$$

If the Lyapunov exponents of the two interacting systems are equal, $\Lambda_1 = \Lambda_2 = \Lambda$, the parameter l vanishes and we obtain (cf. [21])

$$\lambda_1 - \Lambda = \kappa \frac{K_1(\kappa/\sigma^2)}{K_0(\kappa/\sigma^2)} - \kappa \, . \tag{3.12}$$

Further insight into the scaling behaviour can be gained by approximating the modified Bessel functions. Simplified expressions can be obtained in the following limiting cases:

Small coupling, equal Lyapunov exponents. In the limit $\kappa/\sigma^2 \ll 1$, the functions K_1 and K_0 in Eq. (3.12) can be expanded [1], resulting in

$$\lambda_1 - \Lambda \approx \frac{\sigma^2}{|\ln(\kappa/\sigma^2)|} \, . \tag{3.13}$$

This formula corresponds to DAIDO's singular dependence of the Lyapunov exponent on the coupling parameter [23, 24, 25] and will be checked by means of numerical simulations in section 3.1.4. It is valid in all cases when identical chaotic systems are coupled symmetrically, provided that the Lyapunov exponents in these systems fluctuate ($\sigma^2 > 0$). Moreover, even for different systems having, however, equal Lyapunov exponents (but not necessarily equal fluctuations of the exponents) we get the same singularity as for identical systems. DAIDO arrived at a similar result in his analytical treatment of coupled one-dimensional maps, cf. Eq. (19) of Ref. [26].

No fluctuations. With vanishing fluctuations, $\sigma^2 \to 0$, and fixed coupling parameter, we have $\kappa/\sigma^2 \to \infty$. In this case the fraction in Eq. (3.12) becomes unity, $K_1(\kappa/\sigma^2)/K_0(\kappa/\sigma^2) \to 1$, and for the Lyapunov exponent we obtain

$$\lambda_1 = \Lambda \, .$$

This is consistent with the result one directly gets from the model without fluctuations, see previous section.

Small coupling, different Lyapunov exponents. The expansion (3.13) remains valid for small values of mismatch $|l|$, more precisely if $(\kappa/\sigma^2)^{|l|}$ is close to 1. For larger mismatch, when

$$\left(\frac{\kappa}{\sigma^2} \right)^{|l|} \ll 1 \, ,$$

the largest Lyapunov exponent becomes

$$\lambda_1 \approx 2\sigma^2 |l| \frac{\Gamma(1-|l|)}{\Gamma(1+|l|)} \left(\frac{\kappa}{2\sigma^2} \right)^{2|l|} + \underbrace{\frac{1}{2}(|\Lambda_1 - \Lambda_2| + \Lambda_1 + \Lambda_2)}_{=\max\{\Lambda_1, \Lambda_2\}} \, . \tag{3.14}$$
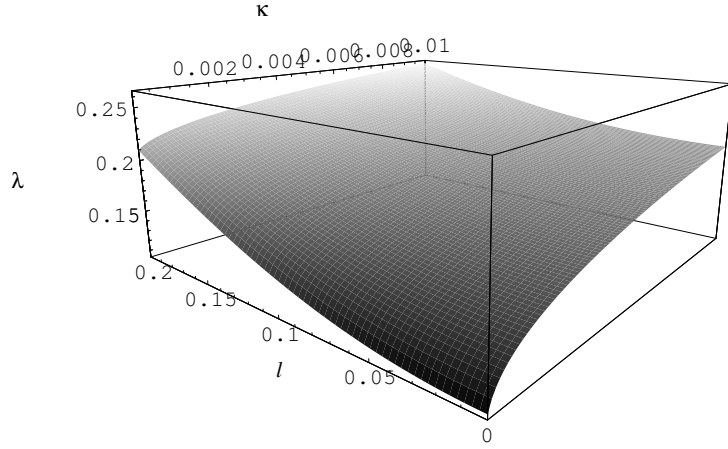
Figure 3.2: The dependence of λ_1 on the mismatch $|l|$ and the coupling κ; $\sigma^2 = 1$.

The singularity is now of the power-law type, with the power depending on the systems' mismatch. With increasing difference $|l|$ the influence of the coupling on λ_1 decreases. For large $|l|$ we thus have $\lambda_1 \approx \max \Lambda_{1,2}$, such that the l.h.s. of Eq. (3.11) becomes (for $\kappa/\sigma^2 \ll |l|$)

$$\frac{\lambda_1 - (\Lambda_1 + \Lambda_2 - 2\kappa)/2}{\sigma^2} \approx \frac{|\Lambda_1 - \Lambda_2|/2 + \kappa}{\sigma^2} \approx |l| \,,$$

which can also be seen in Fig. 3.2.

The Second Lyapunov Exponent

The sum of Lyapunov exponents can be calculated from the divergence of the phase space volume using Eqs. (3.4),

$$\lambda_1 + \lambda_2 = \left\langle \frac{\partial \dot{w}_1}{\partial w_1} + \frac{\partial \dot{w}_2}{\partial w_2} \right\rangle = \Lambda_1 + \Lambda_2 - 2\kappa \,.$$

This enables us to find an expression for the second Lyapunov exponent,

$$\lambda_2 - \Lambda_2 = -(\lambda_1 - \Lambda_1) - 2\kappa \,. \tag{3.15}$$

The singularity is the same as for the first Lyapunov exponent but with opposite sign. The linear decrease corresponds to the synchronization effect, leading to a negative λ_2 for coupling strengths larger than some critical κ_c.

Asymmetrical Coupling

An interesting generalization of the stochastic model not covered so far is the case of asymmetrical coupling,

$$dw_1(t)/dt = [\Lambda_1 + \xi_1(t)]w_1(t) + \kappa_1[w_2(t) - w_1(t)] \, ,$$
$$dw_2(t)/dt = [\Lambda_2 + \xi_2(t)]w_2(t) + \kappa_2[w_1(t) - w_2(t)] \, .$$

We can reduce this problem to the symmetric case by means of the transformation

$$\widetilde{w}_1 = \sqrt{\kappa_2}w_1 \, , \quad \widetilde{w}_2 = \sqrt{\kappa_1}w_2 \, .$$

Hence for the Lyapunov exponent we obtain (cf. Eq. (3.11))

$$\frac{\lambda_1 - (\Lambda_1 + \Lambda_2 - \kappa_1 - \kappa_2)/2}{\sigma^2} = \frac{\kappa}{\sigma^2}\frac{K_{1-|l|}(\kappa/\sigma^2) + K_{1+|l|}(\kappa/\sigma^2)}{2K_{|l|}(\kappa/\sigma^2)} \, ,$$

with the effective coupling parameter and the effective mismatch

$$\kappa = \sqrt{\kappa_1\kappa_2} \quad \text{and} \quad l = \frac{1}{2\sigma^2}[(\Lambda_1 - \kappa_1) - (\Lambda_2 - \kappa_2)] \, ,$$

respectively [68].

An interesting limit is given by unidirectional coupling. Then one can calculate the Lyapunov exponents directly from the system,

$$dw_1(t)/dt = [\Lambda_1 + \xi_1(t)]w_1(t) \, ,$$
$$dw_2(t)/dt = [\Lambda_2 + \xi_2(t)]w_2(t) + \kappa[w_1(t) - w_2(t)] \, .$$

For the first autonomous equation we obtain $\lambda_1 = \Lambda_1$. The sum of both Lyapunov exponents can again be calculated from the divergence of the phase space volume. This gives us the value of the second Lyapunov exponent: $\lambda_2 = \Lambda_2 - \kappa$. Thus for unidirectionally coupled systems there is no coupling sensitivity [68].

3.1.4 Numerical Simulations

In this section the results obtained for the system of continuous-time Langevin equations are compared with numerical calculations for discrete-time deterministic systems. The Lyapunov exponents are calculated as described in App. A.1.

We first study systems of two diffusively coupled one-dimensional maps $f_{1,2}$, Eq. (3.1). To have a good correspondence to the theory, we use only mappings with a constant sign of f' below, so that the fluctuations of the local expansion rate are the only source of irregularity in the perturbation dynamics. Another source could be irregular changes of the sign of the derivative f' (as for the logistic and the tent maps). Such an irregularity is not covered by our continuous-time approach, but also leads to a logarithmic singularity similar to Eq. (3.13), see Ref. [21].
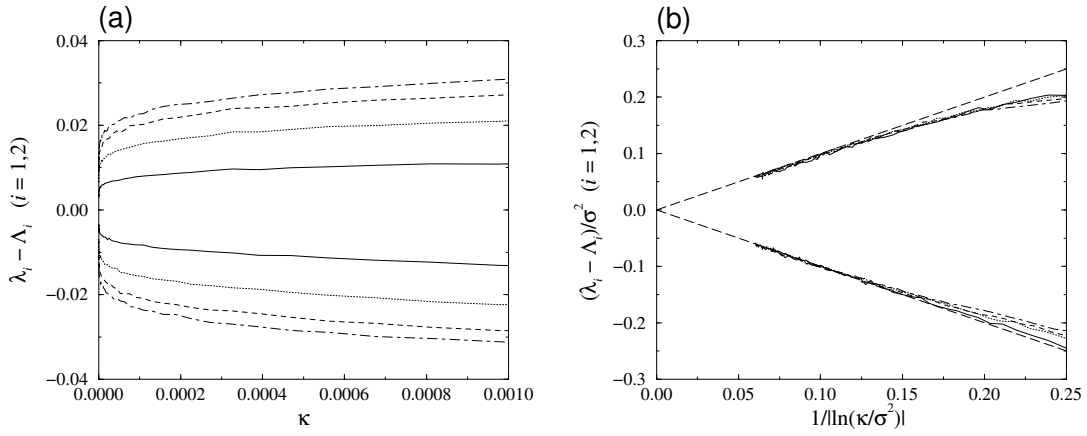
Figure 3.3: Coupled identical skew Bernoulli maps. (a) The Lyapunov exponents $\lambda_1 - \Lambda$ and $\lambda_2 - \Lambda$ *vs.* κ for $a = 1/3$ (solid lines), $a = 1/4$ (dotted lines), $a = 1/5$ (dashed lines), and $a = 1/6$ (dash-dotted lines). (b) The same graphs in scaled coordinates. The long-dashed lines show the analytic results $(\lambda_1 - \Lambda)/\sigma^2 = 1/|\ln(\kappa/\sigma^2)|$ and $(\lambda_2 - \Lambda)/\sigma^2 = -1/|\ln(\kappa/\sigma^2)|$, see Eqs. (3.13) and (3.15).

Skew Bernoulli Maps

We consider the skew Bernoulli map (3.3). For the uncoupled map, the Lyapunov exponent and the magnitude of fluctuations are given by (see Sec. 2.1.4)

$$\Lambda = -a\ln a - (1-a)\ln(1-a) \, , \tag{3.16}$$

and

$$\sigma^2 = \frac{1}{2}a(1-a)\left(\ln\frac{a}{1-a}\right)^2 \, , \tag{3.17}$$

respectively. For $a = 1/2$ we obtain the ordinary Bernoulli map. In this case, there are no fluctuations of the local multipliers ($\sigma^2 = 0$), and no coupling sensitivity of the Lyapunov exponents is observed.

Figure 3.3(a) shows the differences $\lambda_{1,2} - \Lambda$ versus κ for maps with different values of $a \neq 1/2$. From Fig. 3.3(b) it can be seen that different curves collapse onto single lines for both exponents when plotted in the rescaled form according to (3.11). The resulting lines are in very good agreement with the leading term of the theoretical prediction $(\lambda_1 - \Lambda)/\sigma^2 = 1/|\ln(\kappa/\sigma^2)|$, which is also shown.

Different Maps

One main result of the analytic approach is, that the singularity does only depend on the average $\sigma^2 = (\sigma_1^2 + \sigma_2^2)/2$ of the fluctuations of local expansion rates and on the mismatch

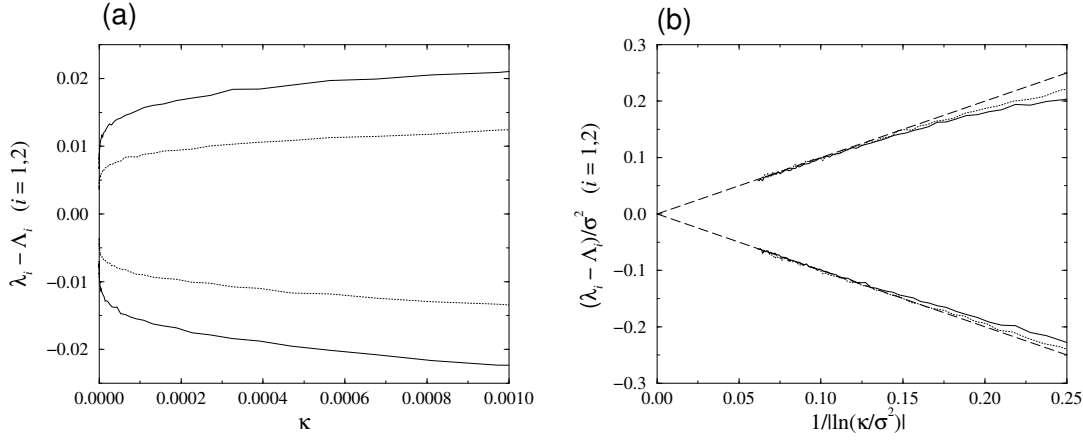**Figure 3.4:** Different maps. (a) $\lambda_1 - \Lambda$ and $\lambda_2 - \Lambda$ *vs.* κ for two coupled skew Bernoulli maps with $a = 1/4$ (solid lines) as well as one skew Bernoulli map with $a = 1/4$ coupled with the different map (3.18) (dotted lines). (b) $(\lambda_1 - \Lambda)/\sigma^2$ and $(\lambda_2 - \Lambda)/\sigma^2$ *vs.* $1/|\ln(\kappa/\sigma^2)|$ for the same examples as in Fig. 3.4(a). The long-dashed lines show the analytic results as in Fig. 3.3(b).

$l = (\Lambda_1 - \Lambda_2)/(2\sigma^2)$ of the Lyapunov exponents of the uncoupled systems. Although no singularity occurs if $\sigma^2 = 0$, one can expect to observe coupling sensitivity in the case of one system with fluctuations ($\sigma_1^2 > 0$) coupled to a different one without fluctuations ($\sigma_2^2 = 0$), given that the mismatch l is sufficiently small.

In order to check this prediction we again numerically iterate the system (3.1) and its linearized version, now choosing two different maps. The first map is again the skew Bernoulli map (3.3), while the second map is defined as

$$f_2(u) = e^{\Lambda} u \pmod{1}, \tag{3.18}$$

where Λ is set equal to the Lyapunov exponent of the skew Bernoulli map (see Eq. (3.16)). With this choice we have the parameters $\sigma_1^2 > 0$, $\sigma_2^2 = 0$, and $l = 0$ (because $\Lambda_1 = \Lambda_2 = \Lambda$).

In Fig. 3.4 the result is compared with the previous result for two coupled identical skew Bernoulli maps ($a = 1/4$ in either case). As expected, the logarithmic singularity is observed in both cases, although the deviation $|\lambda_i - \Lambda|$ is smaller if $\sigma_2^2 = 0$. When rescaled with the average σ^2, however, the curves collapse onto single lines for the first and second Lyapunov exponents, as can be seen in Fig. 3.4(b).

3.1.5 Random Walk Picture

The stochastic model allows to understand the origin of the logarithmic singularity by means of a qualitative consideration [68, 3]. For simplicity we assume $\Lambda_1 = \Lambda_2 = 0$ and $\sigma_1^2 = \sigma_2^2 =$

$\sigma^2 \gg \kappa$, leading to the system

$$dw_1/dt = \sigma\eta_1(t)w_1 + \kappa[w_2 - w_1] \,,$$
$$dw_2/dt = \sigma\eta_2(t)w_2 + \kappa[w_1 - w_2] \,,$$

with

$$\langle\eta_i(t)\rangle = 0 \,, \quad \langle\eta_i(t)\eta_j(t')\rangle = 2\delta_{ij}\delta(t-t') \,, \quad i,j \in \{1,2\} \,.$$

Now we perform a time rescaling $t \to t/\sigma^2$, where we have also to rescale $\eta \to \sigma\eta$ because of the δ-correlation. Dividing by σ^2 we then obtain

$$dw_1/dt = \eta_1(t)w_1 + \frac{\kappa}{\sigma^2}[w_2 - w_1] \,,$$
$$dw_2/dt = \eta_2(t)w_2 + \frac{\kappa}{\sigma^2}[w_1 - w_2] \,. \tag{3.19}$$

Since the amplitudes of the noise processes $\eta_{1,2}$ are of order one and $\kappa/\sigma^2 \ll 1$, the coupling in the first equation of (3.19) only influences the dynamics of w_1 if $w_2 \sim \sigma^2 w_1/\kappa \gg w_1$. In this case the influence of the coupling on the dynamics of w_2 in the second equation of (3.19) is small. The opposite situation occurs if $w_1 \sim \sigma^2 w_2/\kappa \gg w_2$. Thus the coupling leads to a reflection of w_1 and w_2 in the direction of growing amplitude if the system reaches the lines $w_2 = \sigma^2 w_1/\kappa$ and $w_1 = \sigma^2 w_2/\kappa$ in phase space, as illustrated in Fig. 3.5(a).
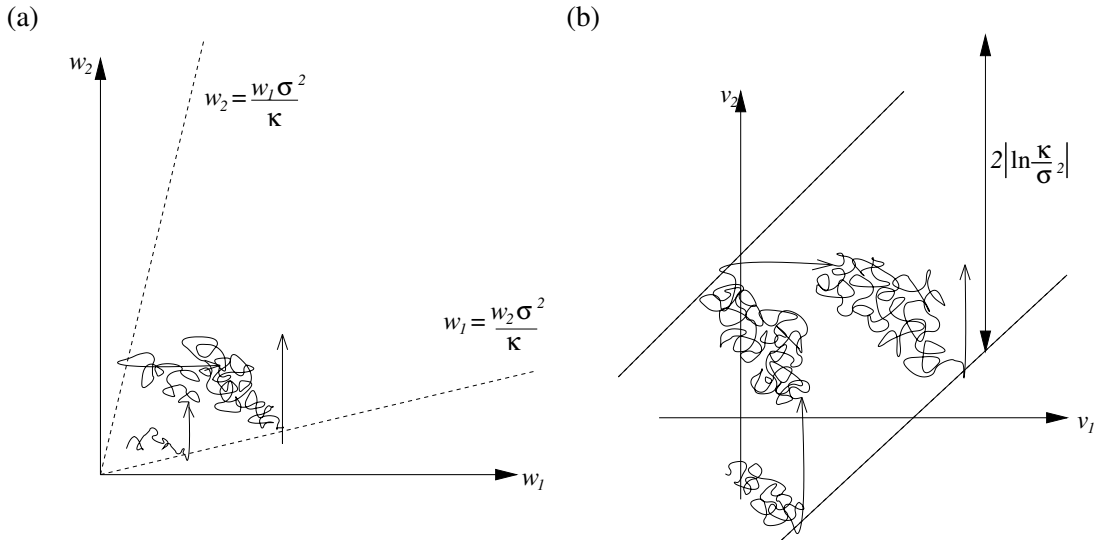

Figure 3.5: A sketch of the perturbation dynamics in coupled systems. Curly lines show the random walk not influenced by coupling; straight arrows demonstrate the effect of coupling.

For logarithmic variables $v_{1,2} = \ln w_{1,2}$ the model (3.19) is transformed to

$$
\begin{aligned}
\mathrm{d}v_1/\mathrm{d}t &= \eta_1(t) + \frac{\kappa}{\sigma^2}\left(e^{v_2-v_1} - 1\right) \;, \\
\mathrm{d}v_2/\mathrm{d}t &= \eta_2(t) + \frac{\kappa}{\sigma^2}\left(e^{v_1-v_2} - 1\right) \;.
\end{aligned}
\tag{3.20}
$$

Now the coupling in the first equation only influences the dynamics of v_1 if $v_2 \sim v_1 + |\ln(\kappa/\sigma^2)|$, and vice versa. Thus the dynamics of the system is restricted to a strip of vertical and horizontal width $2|\ln(\kappa/\sigma^2)|$, see Fig. 3.5(b). Due to the additive noise processes in system (3.20), the dynamics between the reflections correspond to a two-dimensional random walk. The average time to reach the boundary from the middle diagonal is $[\ln(\kappa/\sigma^2)]^2$ [31]. The reflections introduce a drift in direction of growing $v_{1,2}$, the contribution of each reflection to the way travelled due to this drift being $|\ln(\kappa/\sigma^2)|$. Thus the mean drift velocity (corresponding to the largest Lyapunov exponent λ_1) is $1/|\ln(\kappa/\sigma^2)|$. Inverting the time rescaling, $t \to \sigma^2 t$, we have to multiply the Lyapunov exponent by σ^2 and we finally obtain

$$
\lambda_1 \sim \frac{\sigma^2}{|\ln(\kappa/\sigma^2)|} \;,
$$

in perfect agreement with our theoretical result, Eq. (3.13). Furthermore, the random walk picture underlines the connection between σ^2 in the model and the diffusion constant of the logarithmic growth in the corresponding chaotic system.

3.1.6 Scaling of the Null Lyapunov Exponent

In continuous-time systems one Lyapunov exponent is zero; it corresponds to perturbations tangential to the trajectory. We also expect that the fluctuations of the corresponding growth rate are suppressed. Following the argumentation of the previous section, this means that there is no coupling sensitivity of the null Lyapunov exponent. In terms of the stochastic model (3.4) such a behavior can be achieved by using high pass filtered noise. The corresponding power spectrum vanishes at zero frequency which induces a vanishing diffusion constant.

As an example we studied a system of two coupled one-dimensional delay differential equations. Such an equation has an infinite number of Lyapunov exponents of which usually a finite number is positive. In Ref. [68] it is shown that for coupled Ikeda equations the positive and negative Lyapunov exponents exhibit coupling sensitivity whereas for the null exponents no singular deviations are found.

One can also consider complex discrete maps with a null Lyapunov exponent. An example is the following map:

$$
z(n+1) = \alpha\left(1 - |z(n)|\right)\left(1 + i|z(n)|\right)z(n) \;, \quad z \equiv x + iy \in \mathbf{C} \;.
\tag{3.21}
$$

In terms of amplitude and phase defined by $z = A \exp(i\phi)$, Eq. (3.21) reads

$$A(n+1) = \alpha A(n)[1-A(n)]\sqrt{1+A^2(n)} \equiv f[A(n)] , \quad \phi(n+1) = \phi(n) + \arctan A(n) .$$

For $\alpha \in [0, 3.54]$ the amplitude is confined to the interval $[0,1]$. The map $f(A)$ is plotted in Fig. 3.6. For $\alpha = 3.5$ it is chaotic with a positive Lyapunov exponent Λ_1. The phase ϕ, however, has a vanishing Lyapunov exponent. That is, for the map (3.21) we have the exponents $\Lambda_1 > 0$, $\Lambda_2 = 0$.
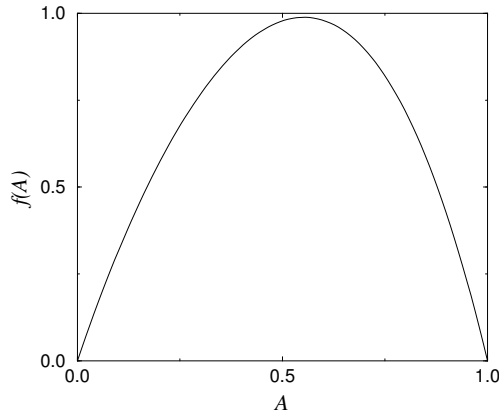
Figure 3.6: The amplitude map $f(A)$; $\alpha = 3.5$.

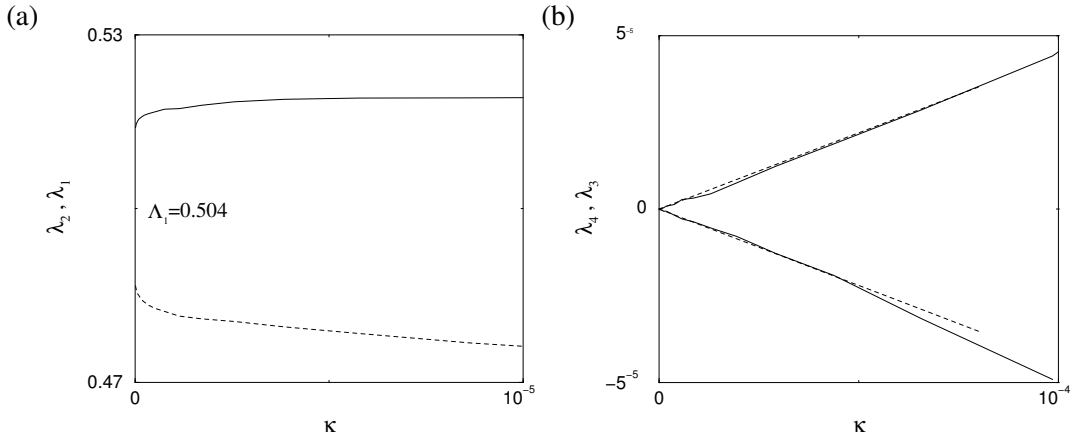**Figure 3.7:** Two coupled complex maps. (a) λ_1 and λ_2 *vs.* κ for $\alpha = 0.35$.
(b) λ_3 and λ_4 *vs.* κ for the same examples as in (a). The dashed lines show the linear fit with slope ± 0.44, resp.

For the components x, y the map (3.21) assumes the following form:

$$x(n+1) = g[x(n), y(n)] \ , \quad y(n+1) = h[x(n), y(n)] \quad \text{with}$$

$$g(x,y) = \alpha \left[x - (x+y)\sqrt{x^2 + y^2} + y(x^2 + y^2) \right] \ ,$$

$$h(x,y) = \alpha \left[y + (x-y)\sqrt{x^2 + y^2} - x(x^2 + y^2) \right] \ .$$

We introduce diffusive coupling of two maps (3.21) according to Eqs. (3.1):

$$x_1(n+1) = g[x_1(n), y_1(n)] + \kappa \left(g[x_2(n), y_2(n)] - g[x_1(n), y_1(n)] \right), \ y_1(n+1) = h[x_1(n), y_1(n)],$$

$$x_2(n+1) = g[x_2(n), y_2(n)] + \kappa \left(g[x_1(n), y_1(n)] - g[x_2(n), y_2(n)] \right), \ y_2(n+1) = h[x_2(n), y_2(n)].$$

Now we have four Lyapunov exponents which are in the absence of coupling given by $\lambda_{1,2} = \Lambda_1$ and $\lambda_{3,4} = 0$.

The numerical results are plotted in Fig. 3.7. They confirm the singular splitting of the positive Lyapunov exponents, whereas the null exponent λ_3 increases linearly with the coupling. The coupling gives rise to nonlinear terms affecting the dynamics of the phases ϕ and leads thus to an increase of λ_3. The former null exponent λ_4 decreases linearly with the same rate as λ_3. This is in contrast to continuous-time systems where at least one Lyapunov exponent has to remain zero.

3.2 Hamiltonian Systems

3.2.1 Example: Standard Map

Here we show coupling sensitivity to exist in the case of weakly coupled standard maps. This symplectic map (see [57] for details), which is a paradigm of Hamiltonian chaos, is defined by

$$q(n+1) = q(n) + p(n+1) \ , \quad p(n+1) = p(n) + K\sin q(n) \ ,$$

where n is the discrete time and K is the parameter. The phase space is invariant under shifts $q \to q \pm 2\pi$, $p \to p \pm 2\pi$, which is why we consider only the sqare $q, p \in [0 : 2\pi)$. This map arises, for example, from a standard discretization of the pendulum equation. For large values of K the phase space is chaotic and the Lyapunov exponent can be approximated, $\Lambda_1 \approx \ln(K/2)$. In order to check the coupling behavior, we consider the following symplectically coupled version:

$$q_1(n+1) = q_1(n) + p_1(n+1) \ , \ p_1(n+1) = p_1(n) + K\sin q_1(n) + \kappa \sin[q_2(n) - q_1(n)] \ ,$$

$$q_2(n+1) = q_2(n) + p_2(n+1) \ , \ p_2(n+1) = p_2(n) + K\sin q_2(n) + \kappa \sin[q_1(n) - q_2(n)] \ .$$

Without coupling there are two positive degenerate Lyapunov exponents, $\Lambda_1 = \Lambda_2$. For small coupling we expect a singular splitting according to Eq. (3.2) into $\lambda_1(\kappa)$ and $\lambda_2(\kappa)$.

(a)   (b)
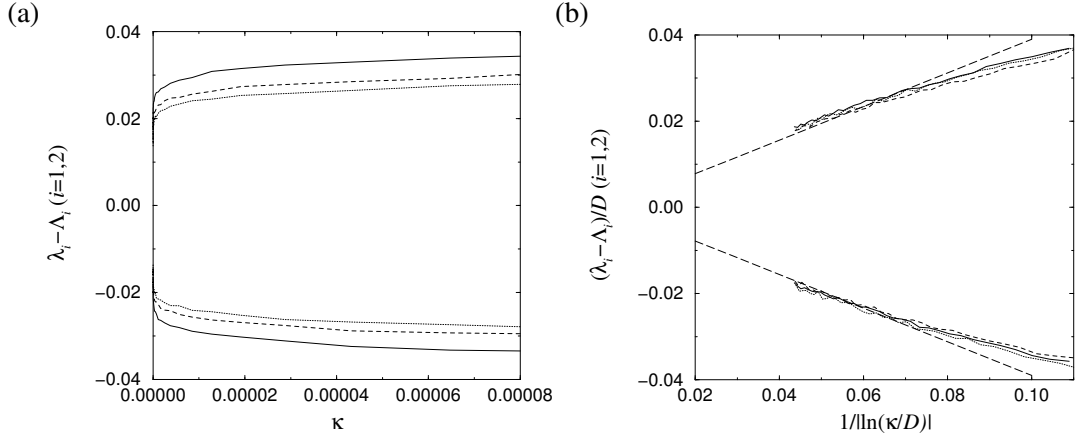
Figure 3.8: Two coupled standard maps. (a) $\lambda_1 - \Lambda_1$ and $\lambda_2 - \Lambda_1$ *vs.* κ for $K = 35$ (solid lines), $K = 40$ (dotted lines), $K = 45$ (dashed lines). (b) $(\lambda_1 - \Lambda_1)/D$ and $(\lambda_2 - \Lambda_1)/D$ *vs.* $1/|\ln(\kappa/D)|$ for the same examples as in (a). The long-dashed lines show the linear fits with slopes ± 0.39, resp.

The Lyapunov exponents of the coupled system have been numerically computed as a function of the coupling strength and for different values of K.

The results are shown in Fig. 3.8. There is indeed a singular splitting of the Lyapunov exponents and the rescaled plot Fig. 3.8 (b) suggests the form

$$\lambda_1 - \Lambda_1 = A \frac{D}{|\ln(\kappa/D)|} \quad , \quad \lambda_2 - \Lambda_1 = -A \frac{D}{|\ln(\kappa/D)|} \; , \tag{3.22}$$

with the diffusion constant D as defined by Eq. (2.6). This corresponds to the result (3.13) for two coupled dissipative systems up to the value of $A \approx 0.39$, which is no longer unity. This is not surprising; there are several examples (e.g. [21]) which confirm the singular splitting with a magnitude depending on the details of the coupling and of the subsystems.

3.2.2 Analytical Approach

Here we consider a simple stochastic model for the dynamics of perturbations which should also take into account the Hamiltonian structure. We propose the following extension of model (2.13):

$$\begin{aligned} \mathrm{d}^2 w_1/\mathrm{d}t^2 + [\omega^2 + \xi_1(t)]w_1 &= \kappa(w_2 - w_1) \; , \\ \mathrm{d}^2 w_2/\mathrm{d}t^2 + [\omega^2 + \xi_2(t)]w_2 &= \kappa(w_1 - w_2) \; . \end{aligned} \tag{3.23}$$

The white noise is defined by

$$\left\langle \xi_i(t)\xi_j(t')\right\rangle = 2\sigma^2 \delta_{ij}\delta(t - t') \; , \quad i,j \in \{1,2\} \; .$$

For the following we assume

$$\kappa \ll 1 \quad \text{and} \quad \omega \gg 1 \; ,$$

which will allow an analytic estimate of the Lyapunov exponent. In the limit of large ω the Lyapunov exponent of the uncoupled systems is given by $\Lambda_1 = \sigma^2/4\omega^2$ (cf. [41] and Ch. 5). For the system (3.23) the exponent is defined by

$$\lambda_1 = \lim_{t\to\infty} \frac{1}{2t} \left\langle \ln(w_1^2 + \dot{w}_1^2 + w_2^2 + \dot{w}_2^2) \right\rangle .$$

The dependence of λ_1 on coupling can be derived as follows.

First we transform to action and angle variables of the uncoupled systems,

$$w_i = \sqrt{2I_i/\tilde{\omega}} \sin\theta_i , \quad \dot{w}_i = \sqrt{2I_i\tilde{\omega}} \cos\theta_i , \quad i = 1,2 ,$$

with $\tilde{\omega}^2 \equiv \omega^2 + \kappa$. The equations of motion in the new variables read

$$\frac{dI_1}{dt} = \frac{-1}{\tilde{\omega}} \xi_1 I_1 \sin 2\theta_1 + 2\frac{\kappa}{\tilde{\omega}} \sqrt{I_1 I_2} \sin\theta_2 \cos\theta_1 ,$$

$$\frac{d\theta_1}{dt} = \tilde{\omega} + \frac{1}{\tilde{\omega}} \xi_1 \sin^2\theta_1 - \frac{\kappa}{\tilde{\omega}} \sqrt{I_2/I_1} \sin\theta_1 \sin\theta_2 ,$$

$$\frac{dI_2}{dt} = \frac{-1}{\tilde{\omega}} \xi_2 I_2 \sin 2\theta_2 + 2\frac{\kappa}{\tilde{\omega}} \sqrt{I_1 I_2} \sin\theta_1 \cos\theta_2 ,$$

$$\frac{d\theta_2}{dt} = \tilde{\omega} + \frac{1}{\tilde{\omega}} \xi_2 \sin^2\theta_2 - \frac{\kappa}{\tilde{\omega}} \sqrt{I_1/I_2} \sin\theta_1 \sin\theta_2 .$$

In order to simplify further calculations we change to the logarithms of the actions,

$$2u_i = \ln I_i .$$

To avoid a clumsy notation we temporarily define $x^t = (x_1, x_2, x_3, x_4)^t \equiv (u_1, u_2, \theta_1, \theta_2)^t$. The non-vanishing Kramers-Moyal coefficients (see App. A.2) read

$$D_1 = \frac{\kappa}{\tilde{\omega}} e^{u_2 - u_1} \sin\theta_2 \cos\theta_1 - \frac{\sigma^2}{\tilde{\omega}^2} \sin^2\theta_1 \cos 2\theta_1 ,$$

$$D_2 = \frac{\kappa}{\tilde{\omega}} e^{u_1 - u_2} \sin\theta_1 \cos\theta_2 - \frac{\sigma^2}{\tilde{\omega}^2} \sin^2\theta_2 \cos 2\theta_2 ,$$

$$D_3 = \tilde{\omega} - \frac{\kappa}{\tilde{\omega}} e^{u_2 - u_1} \sin\theta_1 \sin\theta_2 + \frac{\sigma^2}{\tilde{\omega}^2} \sin^2\theta_1 \sin 2\theta_1 ,$$

$$D_4 = \tilde{\omega} - \frac{\kappa}{\tilde{\omega}} e^{u_1 - u_2} \sin\theta_1 \sin\theta_2 + \frac{\sigma^2}{\tilde{\omega}^2} \sin^2\theta_2 \sin 2\theta_2 ,$$

$$D_{11} = \frac{\sigma^2}{4\tilde{\omega}^2} \sin^2 2\theta_1 , \quad D_{13} = -\frac{\sigma^2}{2\tilde{\omega}^2} \sin 2\theta_1 \sin^2\theta_1 , \quad D_{33} = \frac{\sigma^2}{\tilde{\omega}^2} \sin^4\theta_1 ,$$

$$D_{22} = \frac{\sigma^2}{4\tilde{\omega}^2} \sin^2 2\theta_2 , \quad D_{24} = -\frac{\sigma^2}{2\tilde{\omega}^2} \sin 2\theta_2 \sin^2\theta_2 , \quad D_{44} = \frac{\sigma^2}{\tilde{\omega}^2} \sin^4\theta_2 .$$

The corresponding Fokker-Planck equation, which governs the evolution of the probability density $\rho(\boldsymbol{x};t)$, is defined by these coefficients as

$$\frac{\partial \rho(\boldsymbol{x};t)}{\partial t} = -\sum_{i=1}^{4} \frac{\partial}{\partial x_i} D_i \rho(\boldsymbol{x};t) + \sum_{i,j=1}^{4} \frac{\partial^2}{\partial x_i \partial x_j} D_{ij} \rho(\boldsymbol{x};t) \ .$$

The motion of the phases $\theta_{1,2}$ is dominated by a fast rotation with the large frequency $\tilde{\omega}$. Thus the coefficients may be averaged with respect to $\theta_{1,2}$ over the small period $2\pi/\tilde{\omega}$, where we first consider terms which are not mixed in θ_1 and θ_2. This leads to a simplified Fokker-Planck equation $\dot{\rho}(u_1, u_2, \theta_1, \theta_2; t) = \mathbf{L}\rho$, where the operator $\mathbf{L}$ reads

$$\begin{aligned}
\mathbf{L} = & -\frac{\partial}{\partial u_1} \left(\frac{\kappa}{\tilde{\omega}} e^{u_2 - u_1} \cos\theta_1 \sin\theta_2 + \frac{\sigma^2}{4\tilde{\omega}^2} \right) - \frac{\partial}{\partial u_2} \left(\frac{\kappa}{\tilde{\omega}} e^{u_1 - u_2} \sin\theta_1 \cos\theta_2 + \frac{\sigma^2}{4\tilde{\omega}^2} \right) \\
& -\frac{\partial}{\partial \theta_1} \left(\tilde{\omega} - \frac{\kappa}{\tilde{\omega}} e^{u_2 - u_1} \sin\theta_1 \sin\theta_2 \right) - \frac{\partial}{\partial \theta_2} \left(\tilde{\omega} - \frac{\kappa}{\tilde{\omega}} e^{u_1 - u_2} \sin\theta_1 \sin\theta_2 \right) \\
& +\frac{\sigma^2}{8\tilde{\omega}^2} \frac{\partial^2}{\partial u_1^2} + \frac{\sigma^2}{8\tilde{\omega}^2} \frac{\partial^2}{\partial u_2^2} + \frac{3\sigma^2}{8\tilde{\omega}^2} \frac{\partial^2}{\partial \theta_1^2} + \frac{3\sigma^2}{8\tilde{\omega}^2} \frac{\partial^2}{\partial \theta_2^2} \ .
\end{aligned}$$

Next we separate the directed motion by means of the following transformation:

$$v_1 = u_2 - u_1 \ , \quad v_2 = u_2 + u_1 \ , \quad \phi = \theta_2 - \theta_1 \ , \quad \varphi = \theta_1 + \theta_2 \ .$$

The Fokker-Planck equation defined by $\mathbf{L}$ is statistically equivalent to a new set of Langevin equations which in the new variables reads

$$\begin{aligned}
\frac{dv_1}{dt} &= \frac{\sigma}{2\tilde{\omega}} \eta_1(t) - \frac{\kappa}{\tilde{\omega}} \sin\varphi \sinh v_1 - \frac{\kappa}{\tilde{\omega}} \sin\phi \cosh v_1 \ , \\
\frac{dv_2}{dt} &= \frac{\sigma^2}{2\tilde{\omega}^2} + \frac{\sigma}{2\tilde{\omega}} \eta_2(t) + \frac{\kappa}{\tilde{\omega}} \sin\varphi \cosh v_1 + \frac{\kappa}{\tilde{\omega}} \sin\phi \sinh v_1 \ , \\
\frac{d\phi}{dt} &= \frac{\sqrt{3}\sigma}{2\tilde{\omega}} \eta_3(t) - \frac{\kappa}{\tilde{\omega}} \cos\varphi \sinh v_1 + \frac{\kappa}{\tilde{\omega}} \cos\phi \sinh v_1 \ , \\
\frac{d\varphi}{dt} &= 2\tilde{\omega} + \frac{\sqrt{3}\sigma}{2\tilde{\omega}} \eta_4(t) + \frac{\kappa}{\tilde{\omega}} \cos\varphi \cosh v_1 - \frac{\kappa}{\tilde{\omega}} \cos\phi \cosh v_1 \ ,
\end{aligned}$$

where the white noise sources fulfill $\langle \eta_i(t) \eta_j(t') \rangle = 2\delta_{ij}\delta(t - t')$, $i, j \in \{1, 2, 3, 4\}$. There are still fast oscillating terms left (those depending on φ) which stem from the mixed terms that have not been averaged above. By virtue of the separation of the fast and slow angle variables these terms can now be averaged, yielding a closed dissipative set of equations for the variables v_1 and ϕ:

$$\frac{dv_1}{dt} = \frac{\sigma}{2\tilde{\omega}} \eta_1(t) - \frac{\kappa}{\tilde{\omega}} \sin\phi \cosh v_1 \ , \tag{3.24a}$$

$$\frac{d\phi}{dt} = \frac{\sqrt{3}\sigma}{2\tilde{\omega}} \eta_3(t) + \frac{\kappa}{\tilde{\omega}} \cos\phi \sinh v_1 \ . \tag{3.24b}$$
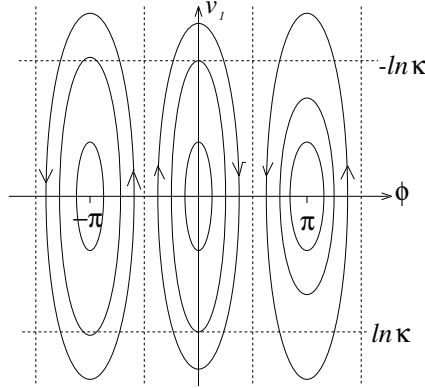
Figure 3.9: The dynamics of system (3.24) without noise.

The deterministic dynamics of this system, i.e. the case $\eta_{1,3} = 0$, is sketched in Fig. 3.9. There exists a stationary distribution of v_1 which will be caclulated in the following. Our initial goal to calculate the Lyapunov exponent should now be reformulated in terms of the new variables. The Lyapunov exponent is hence given by (cf. derivation of Eq. (3.10))

$$\lambda_1 = \left\langle \frac{\mathrm{d}}{\mathrm{d}t} \ln(I_1 + I_2) \right\rangle_{\text{stat}} = \frac{1}{2} \langle \dot{v}_2 \rangle_{\text{stat}} + \frac{\mathrm{d}}{\mathrm{d}t} \langle \ln \cosh(v_1/2) \rangle_{\text{stat}} \ .$$

The last term vanishes due to stationarity and we are left with $\lambda_1 = \frac{1}{2} \langle \dot{v}_2 \rangle_{\text{stat}}$, which can be rewritten as

$$\lambda_1 = \frac{\sigma^2}{4\tilde{\omega}^2} + \left\langle \frac{\kappa}{2\tilde{\omega}} \sin\phi \sinh v_1 \right\rangle_{\text{stat}} = \Lambda_1 + \left\langle \frac{\kappa}{2\omega} \sin\phi \sinh v_1 \right\rangle_{\text{stat}} + O(\kappa) \ , \qquad (3.25)$$

where $\Lambda_1 = \sigma^2/(4\omega^2)$ is the Lyapunov exponent of the subsystems. Because we are interested in the leading order in κ, we set $\tilde{\omega} = \omega$ in the following. To determine λ_1 we need to find from Eqs. (3.24) the stationary density $\rho(\phi, v_1)$.

Unfortunately, we were not able to find the stationary solution in a closed analytic form. We present here an estimate, using the smallness of κ. In order to normalize the noise terms we rescale the time as $t \to (\omega^2/\sigma^2)t$, thus obtaining for Eqs. (3.24)

$$\frac{\mathrm{d}v_1}{\mathrm{d}t} = \frac{1}{2}\eta_1(t) - \frac{\kappa\omega}{\sigma^2}\sin\phi\cosh v_1 \ , \qquad \frac{\mathrm{d}\phi}{\mathrm{d}t} = \frac{\sqrt{3}}{2}\eta_3(t) + \frac{\kappa\omega}{\sigma^2}\cos\phi\sinh v_1 \ . \qquad (3.26)$$

The stationary Fokker-Planck equation now reads

$$\left[\frac{\kappa\omega}{\sigma^2}\frac{\partial}{\partial v_1}\sin\phi\sinh v_1 - \frac{\kappa\omega}{\sigma^2}\frac{\partial}{\partial\phi}\cos\phi\sinh v_1 + \frac{1}{4}\frac{\partial^2}{\partial v_1^2} + \frac{3}{4}\frac{\partial^2}{\partial\phi^2} \right]\rho(\phi, v_1) = 0 \ . \qquad (3.27)$$

Because $\kappa \ll 1$, the deterministic transport terms in (3.26) are small for $v_1 < |\ln(\kappa\omega/\sigma^2)|$. Thus in this range (termed region I) of v_1 we write the stationary density in the form $\rho_I \approx C\exp[\kappa f(v_1, \phi)]$. Inserting this *ansatz* in Eq. (3.27) we obtain in the leading order in κ

$$f = (4\omega/\sigma^2) \sin\phi \sinh v_1 \, .$$

Now we consider the outer region II: There $v_1 > |\ln(\kappa\omega/\sigma^2)|$, thus the $\cosh v_1$ term is large and we neglect the noise terms of Eqs. (3.26) here. Due to the symmetry of the deterministic motion (cf. Fig. 3.9) this part does not contribute to the average $\langle \sin\phi \sinh v_1 \rangle$. By virtue of the transformation $z = \tanh v_1$ the deterministic motion is governed by a Hamiltonian $H = \sqrt{1 - z^2} \cos\phi = \cos\phi/\cosh v_1$, whereupon the density in region II can be written as $\rho_{II} \sim \cosh^{-2} v_1 F(\cos\phi/\cosh v_1)$. Here F is a limited function corresponding to the probability of the orbits with $\cos\phi/\cosh v_1 = const$. Hence $\rho_{II} \ll \rho_I$ and we can estimate the normalization constant C by considering only region I:

$$C^{-1} \approx \int_{-\pi/2}^{\pi/2} d\phi \int_{-|\ln(\kappa\omega/\sigma^2)|}^{|\ln(\kappa\omega/\sigma^2)|} dv_1 \exp[(4\kappa\omega/\sigma^2) \sin\phi \sinh v_1] \approx 2\pi |\ln(\kappa\omega/\sigma^2)| \, .$$

The average in Eq. (3.25) is finally given by

$$\left\langle \frac{\kappa}{2\omega} \sin\phi \sinh v_1 \right\rangle \approx C^{-1} \int_{-\pi/2}^{\pi/2} d\phi \int_{-|\ln(\kappa\omega/\sigma^2)|}^{|\ln(\kappa\omega/\sigma^2)|} dv_1 \frac{\kappa}{2\omega} \sin\phi \sinh v_1 \exp[(4\kappa\omega/\sigma^2) \sin\phi \sinh v_1]$$

$$\approx \frac{1}{16\pi\omega^2} \frac{\sigma^2}{|\ln(\kappa\omega/\sigma^2)|} \, . \tag{3.28}$$

Using that for $\omega \gg 1$ the diffusion constant is $D = \Lambda_1 = \sigma^2/4\omega^2$ (see Sec. 5.5), the result (3.28) can be rewritten as

$$\lambda_1 - \Lambda_1 = \frac{1}{4\pi} \frac{D}{|\ln(\kappa/D)|} \, ,$$

in exact agreement with the logarithmic singularity (3.22).

3.3 Summary and Perspectives

In order to gain insight into universal scaling properties of the Lyapunov exponents of weakly coupled dynamical systems we used a Langevin approach. In this way we neglected the specific properties of the chaotic systems by only taking into account the coupling and the fluctuations of the exponential growth rate of perturbations. For the simplest system of two coupled stochastic equations it is possible to obtain an analytical expression for the Lyapunov exponents, for different values of parameters (coupling, Lyapunov exponents of uncoupled systems, fluctuations of finite-time Lyapunov exponents). The logarithmic singularity, first discovered by DAIDO, is shown to exist even if rather different systems are

coupled, provided their Lyapunov exponents coincide. We also gave a qualitative explanation of the effect, based on the interpretation of the perturbations' dynamics as random walks which are confined due to the coupling.

An extension of the stochastic model to three coupled identical systems as well as numerical simulations led to the asymptotic result [68]

$$\lambda_1 - \Lambda \sim \frac{4}{3} \frac{\sigma^2}{|\ln(\kappa/\sigma^2)|} \quad \text{for} \quad \frac{\kappa}{\sigma^2} \to 0 .$$

We also investigated into a set of coupled Langevin equations of second order, which reflect the symplectic structure of Hamiltonian chaotic systems. The numerical results for coupled standard maps confirm the existence of coupling sensitivity of the Lyapunov exponents for simplectic systems. The analytic approach yielded a scaling relation for the Lyapunov exponent which is of the same form as for dissipative systems.

Together with the results for the Largest Lyapunov exponent of weakly coupled CMLs [43, 21], it can be summarized that the coupling sensitivity of chaos is a general phenomenon of coupled fluctuating systems.

In the case of coupled continuous-time systems an interesting quantity is the null Lyapunov exponent. It can be used as an indicator for the onset of phase-synchronization. Our numerical results show that this exponent scales regularly with weak coupling, as one would expect from a perturbation expansion. We attribute this to the fact that the fluctuations of the null Lyapunov exponent are suppressed in an autonomous system. Recently it has been shown by LIU et al. [42] that the null Lyapunov exponent of coupled chaotic oscillators with multiple scrolls increases quadratically with the coupling.

The singular splitting of equal Lyapunov exponents for weak coupling leads to the interesting phenomenon of avoided crossings of the Lyapunov exponents when a system parameter is varied. This is similar to the effect of energy level repulsion in quantum systems. Details concerning this effect can be found in [4].

An interesting consequence of the coupling sensitivity of chaos is found in the context of Anderson localization in disordered systems which is treated in the following chapter.

Lyapunov exponents are very hard to estimate from experimental time series. It is therefore difficult to directly observe the rather small effect of coupling sensitivity in experiments. The coupling dependence of the localization length, however, may be observable via its influence on transport coefficients like the electrical conductivity.

4 Coupling Sensitivity of the Localization Length

This chapter is devoted to weakly coupled disordered quantum systems which possess a quasi-one-dimensional geometry. Such systems have been the subject of intense research, mainly due to their nontrivial conductance properties and their accessibility to theoretical investigations. The one-particle wave function in a disordered system can be exponentially localized at zero temperature, where coupling to phonons and particle-particle interactions are negligible. This problem was first discussed by ANDERSON 1958 [5] who addressed quantum diffusion in random lattices. Physically the disorder can be connected, e.g., with impurities or vacancies in the crystal lattice. Localized states cannot contribute to transport and can thus lead to a vanishing DC conductivity. This concept is important for the understanding of the transition between insulating and metallic states of matter. The exponential decay of the wavefunction is characterized by a localization length, which is an averaged quantity corresponding to different realizations of the disorder. Following BORLANDs conjecture [16], the localization length is given by the inverse of the Lyapunov exponent, which will be employed in the following sections.

Quantum localization is mainly due to interference effects of the wavefunction, which implies the possibility to observe localization also for classical waves. These are experimentally accessible; see e.g. [44]. An experimental realization of one-dimensional quantum localization provide carbon nanotubes (see [35] and references therein). General theoretical aspects of disordered systems are treated in [37, 41, 22, 11].

Considering weakly coupled one-dimensional chains we demonstrate in the following that the localization length singularly increases as $1/|\ln \kappa|$ with the coupling strength κ. The form of this singularity resembles the scaling of the Lyapunov exponent of coupled chaotic systems, therefore we call the effect coupling sensitivity of the localization length. Numerical evidence will be given for coupled random chains with different statistics of the site potential. An analytic approach will be developed based on the Fokker-Planck treatment of coupled stationary Schrödinger equations with δ-correlated random potentials. The effect on the conductance will be discussed, allowing for different average definitions. Some of the results of this chapter have been published in [70].

4.1 Anderson Localization

A discrete description of a quantum particle in a periodic lattice potential is given by the tight-binding approach. There one starts with the eigenstates of the on-site potentials as a basis and treats the overlap energy between the sites as perturbation (see [56] for details). The Anderson model allows for random on-site potentials, which can be described in a dimensionless form by the following one-dimensional (single-band) Hamiltonian,

$$H = \sum_m \left[\varepsilon_m |m><m| - |m><m+1| - |m+1><m| \right] . \tag{4.1}$$

Here ε_m are the random energies of the states at the site m of the lattice, and the non-diagonal terms describe the nearest-neighbor tunneling amplitude. The stationary Schrödinger equation for the state $\Psi = \sum \psi_m |m>$ and eigenenergy e follows as

$$-\psi_{m+1} - \psi_{m-1} + \varepsilon_m \psi_m = e \psi_m . \tag{4.2}$$

The same equation appears also in the Kronig-Penney model, with a sligthly different interpretation of ε_m and e. For the random potential we assume $\langle \varepsilon_m \varepsilon_n \rangle = \langle \varepsilon_m^2 \rangle \delta_{mn}$ and consider several distributions. In the ordered case, i.e. $\varepsilon_m \equiv 0$, the eigenstates are periodic with wavenumber k and energies $e = -2\cos k \in [-2, 2]$. For $k \to 0$ the eigenfunctions wavelength ($\propto 1/k$) becomes much larger than the lattice spacing, and Eq. (4.2) can be replaced by a continuous stochastic equation:
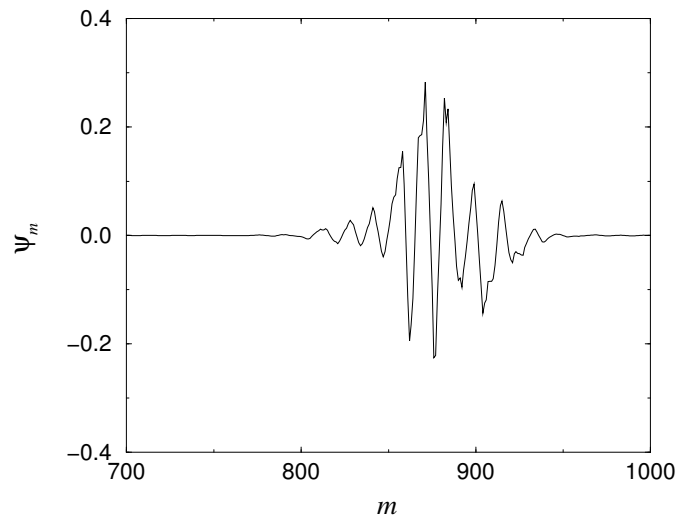
$$-\psi'' + U(x)\psi = (e+2)\psi ; \tag{4.3}$$

Figure 4.1: Amplitudes ψ_m of a localized state, obtained by numerical diagonalization of (4.1) for $e = 1.89$. The ε_m are box distributed with width $w = 1$.

with a properly chosen random potential $U(x)$. This equation can also be interpreted as the continuous Schrödinger equation for a particle in the random potential $U(x)$. It will be used in the theoretical part of this chapter.

Equation (4.2) can be written in recursive form with a transfer matrix $\mathbf{T}$ as

$$\begin{pmatrix} \psi_{m+1} \\ \psi_m \end{pmatrix} = \begin{pmatrix} \varepsilon_m - e & -1 \\ 1 & 0 \end{pmatrix} \begin{pmatrix} \psi_m \\ \psi_{m-1} \end{pmatrix} \equiv \mathbf{T} \begin{pmatrix} \psi_m \\ \psi_{m-1} \end{pmatrix} .$$

Thus the spatial evolution of ψ_m is given by a product of random matrices and the theorem of OSELEDEC holds. That is, for almost any initial condition, ψ_m grows exponentially with a rate given by the largest Lyapunov exponent defined by

$$\lambda_1 = \lim_{m \to \infty} \frac{1}{2m} \ln(\psi_m^2 + \psi_{m-1}^2) .$$

Furthermore the transfer matrix $\mathbf{T}$ is symplectic, so that for the second Lyapnov exponent the relation holds

$$\lambda_2 = -\lambda_1 .$$

The above statement 'almost any' allows for some initial conditions leading to states which obey the boundary conditions connected with Eq. (4.2); a typical localized state is depicted in Fig. 4.1. These states correspond to discrete energy eigenvalues e and decrease exponentially at large distances from their maximum,

$$|\psi_m| \sim |\psi_{\max}| e^{-|m|/l} ,$$

with the localization length l. It is plausible that the most probable decrease is determined by the smallest in absolute value Lyapunov exponent, here given by λ_1. This leads to BOR-LANDs conjecture [16], namely that

$$l = \lambda_1^{-1} .$$

This relation is the basis of the following sections which focus on the behavior of the Lyapunov exponent.

4.2 Coupled Disordered Chains

4.2.1 Quasi-One-Dimensional Model

Starting from the Anderson model (4.2) we propose the following quasi-one-dimensional model for two coupled disordered chains:

$$-\psi_{1,m+1} - \psi_{1,m-1} + \varepsilon_{1,m}\psi_{1,m} + \kappa\psi_{2,m} = e\psi_{1,m} , \tag{4.4a}$$

$$-\psi_{2,m+1} - \psi_{2,m-1} + \varepsilon_{2,m}\psi_{2,m} + \kappa\psi_{1,m} = e\psi_{2,m} . \tag{4.4b}$$
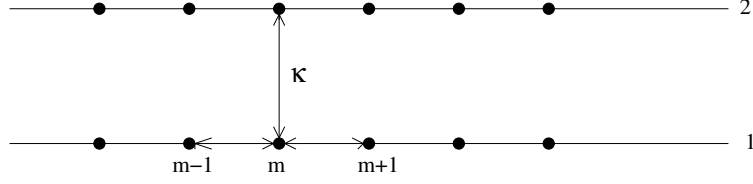
Figure 4.2: Two coupled chains corresponding to Eqs. (4.4); the arrows indicate nearest-neighbor hopping.

Here the local site energies $\varepsilon_{1,m}$, $\varepsilon_{2,m}$ are assumed to be independent and equally distributed in both chains. The amplitudes of the wave functions are now given by $\psi_{n,m}$ where $n = 1,2$ labels the chains. We assume that the chains are coupled via the nearest-neighbor hopping amplitude $\kappa \ll 1$, i.e. the inter-chain hopping probability is much smaller than the intra-chain one. The geometry of this model is sketched in Fig. 4.2. Because the inter-chain coupling is close to zero, the model is not well described by the DMPK [1] equation (see [11] and references therein), which presumes isotropic scattering by neglecting the length scale of transverse diffusion. The spatial evolution of the state $\Psi_m \equiv (\psi_{1,m}, \psi_{2,m}, \psi_{1,m-1}, \psi_{2,m-1})^t$ is determined by a symplectic transfer matrix, $\Psi_{m+1} = \mathbf{T}_m \Psi_m$, with

$$\mathbf{T}_m = \begin{pmatrix} \varepsilon_{1,m} - e & \kappa & -1 & 0 \\ \kappa & \varepsilon_{2,m} - e & 0 & -1 \\ 1 & 0 & 0 & 0 \\ 0 & 1 & 0 & 0 \end{pmatrix} .$$

Thus there are two positive Lyapunov exponents λ_1, λ_2 and the negative exponents are related to the positive ones by $\lambda_{4,3} = -\lambda_{1,2}$, resp. For vanishing coupling, $\kappa = 0$, the exponents λ_1 and λ_2 coincide; we denote the largest exponent of the uncoupled system as Λ.

The localization length of the whole lattice is given by the smallest positive exponent: $l = 1/\lambda_2$. Our main interest lies in the deviations of this length from that of the uncoupled system (4.2), which is $1/\Lambda$. By the results of Sec. 3.2 we expect a singular decrease of the second Lyapunov exponent,

$$\lambda_2 - \Lambda \sim -A(e) \frac{D}{|\ln \kappa|} , \tag{4.5}$$

with an energy-dependent strength A and a diffusion constant D defined by

$$\langle (\ln \|\Psi_m\| - m\Lambda)^2 \rangle \propto Dm \quad \text{for} \quad m \to \infty .$$

This behavior transforms into a singular increase of the localization length,

$$l(\kappa) - l_0 \sim l_0^2 \, A(e) \frac{D}{|\ln \kappa|} . \tag{4.6}$$

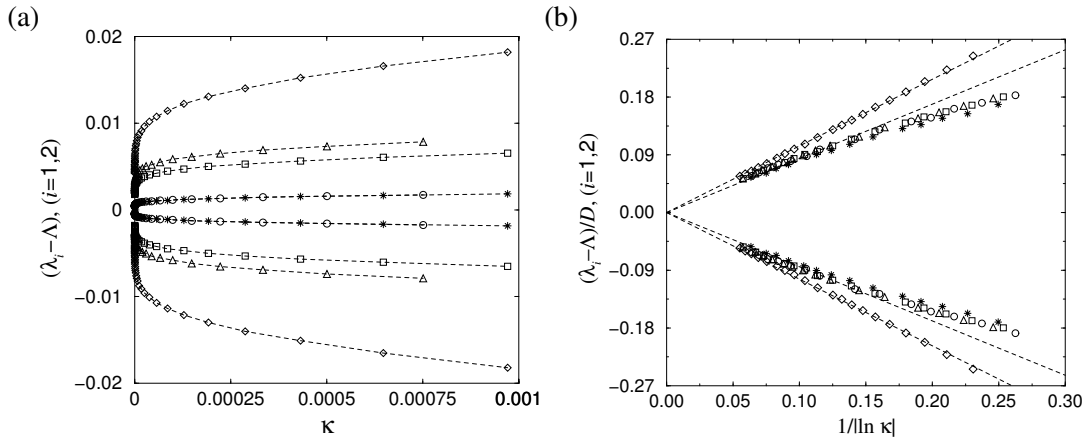[1] DMPK stands for Dorokhov-Mello-Pereyra-Kumar.

(a)

(b)

Figure 4.3: (a) The upper graphs show the splitting $\lambda_1(\kappa) - \Lambda$ *vs.* κ at $e = -0.09$ for a two-point (circles), a Gaussian (stars) and a box distribution of $\varepsilon_{k,m}$; the latter with widths $w = 2.6$ (squares) and $w = 3.0$ (triangles). At $e = 2.5$ the splitting is shown for the box distribution with $w = 1.6$ (diamonds). The lower graphs show $\lambda_2(\kappa) - \Lambda$ for the same values of w and e. The dashed lines are to improve readability.
(b) The same as (a) but in rescaled coordinates: $(\lambda_1(\kappa) - \Lambda)/D$ (upper graphs) and $(\lambda_2(\kappa) - \Lambda)/D$ (lower graphs) *vs.* $1/|\ln\kappa|$. The dashed lines are linear fits with slopes ± 0.85 for $e = -0.09$ and ± 1.04 for $e = 2.5$, resp. The valid range of scaling (4.5) depends on e: in the band centre it is $\kappa < 10^{-5}$, while at the band edge ($|e| = 2$) it expands up to $\kappa \approx 10^{-3}$.

We show in the following that this effect indeed exists, which we call coupling sensitivity of the localization length.

4.2.2 Numerical Evidence of Coupling Sensitivity

In order to check relation (4.5) we calculated the Lyapunov exponents by iterating the vector Ψ_m with the transfer matrix $\mathbf{T}_m$, where we used a modified Gram-Schmidt algorithm (see App. A.1). Additionally, for each setup of statistics we calculated the diffusion constant D by iterating the uncoupled system (4.2). We considered several distributions of the random potential $\varepsilon_{n,m}$, namely a box distribution, $P(\varepsilon) = \Theta(w - |\varepsilon|)/2w$,[2] a two-point distribution, $P(\varepsilon) = \delta(\varepsilon - a)/2 + \delta(\varepsilon + a)/2$, and a Gaussian distribution. In Fig. 4.3(a) we present the results for the different distributions of the site potential $\varepsilon_{n,m}$ and different energies e. The figure clearly demonstrates singular splitting of the first and second Lyapunov exponents. Fig. 4.3(b) shows the same data in the scaled coordinates: $(\lambda_{1,2}(\kappa) - \Lambda)/D$ vs $1/|\ln\kappa|$. Here the curves for the different distributions and the same e collapse on straight lines, as expected according to Eq. (4.5). The linear fit, also shown in the figure, reveals that the splitting is symmetric, i.e. $\lambda_2(\kappa) - \Lambda = -(\lambda_1(\kappa) - \Lambda)$.

---

[2]Here Θ denotes the Heaviside function.

(a)

(b)
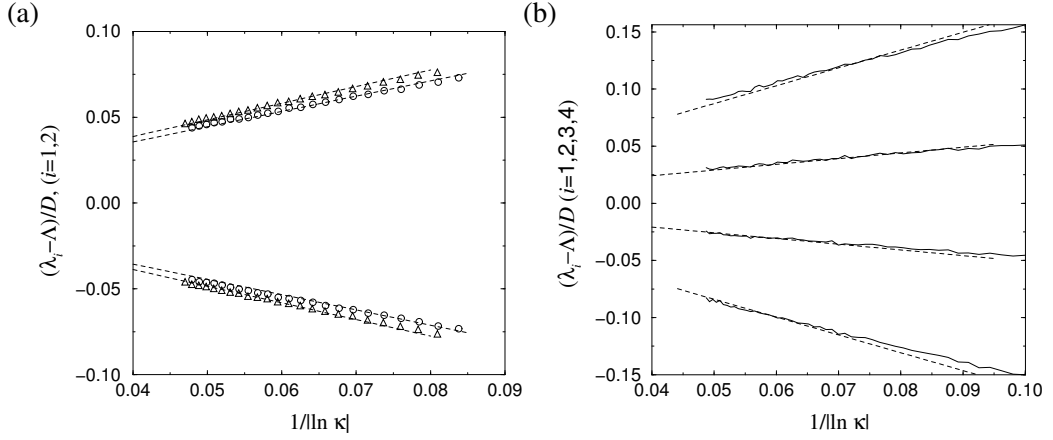
Figure 4.4: (a) Splitting of $\lambda_{1,2}$ in rescaled coordinates for two channels with random coupling for $e = 0$ (circles) and $e = -1.8$ (triangles). The dashed lines are linear fits with slopes ± 0.89 and ± 0.97, resp. The on-site potential was choosen box distributed with $w = \sqrt{3}/2$.
(b) Four coupled channels: Splitting of the positive Lyapunov exponents in rescaled coordinates with $e = -0.08$, $w = 1.6$. The dashed lines have slope ± 1.56 and ± 0.44 resp.

This symmetry, important for the analytic approach below, can be explained as follows. The sum of positive Lyapunov exponents is related to the density of states via a generalization of the Thouless formula [22]. Because the eigenstates non-singularly depend on the coupling, the sum of the positive Lyapunov exponents also depends on κ in a non-singular way. Therefore, in order to cancel out in the sum, the singular deviations of λ_1 and λ_2 are to be symmetric.

Randomly Coupled Chains

Coupling sensitivity also appears in the case of fluctuating coupling, which underlines the robustness of the effect. We investigated the following generalization of model (4.4):

$$-\psi_{1,m+1} - \psi_{1,m-1} + \varepsilon_{1,m}\psi_{1,m} + \kappa\xi_{1,m}\psi_{2,m} = e\psi_{1,m} \,,$$
$$-\psi_{2,m+1} - \psi_{2,m-1} + \varepsilon_{2,m}\psi_{2,m} + \kappa\xi_{2,m}\psi_{1,m} = e\psi_{2,m} \,.$$

The random numbers $\xi_{n,m}$ are again assumed to be independent equally distributed in both chains. The rescaled plot of the positive Lyapunov exponents is shown in Fig. 4.4(a) for two values of the energy. The linear fits confirm the singular behavior according to relation (4.5).

N Coupled Chains

The model (4.4) can be straightforwardly generalized to the case of N coupled chains. We still assume that the hopping amplitudes κ between the chains are much less than those inside the chains; furthermore periodic boundary conditions in the transverse direction are used: $\psi_{N+1,m} = \psi_{1,m}$. Now one has to deal with N positive Lyapunov exponents which coincide for $\kappa = 0$.[3] The rescaled plot Fig. 4.4(b) shows a different slope for the splitting of $\lambda_{1,4}$ and $\lambda_{2,3}$, resp. Again the splitting is symmetric. The localization length determined by λ_4 thus increases according to relation (4.6).

4.2.3 Two-Site Hopping Model

A slight modification of the geometry in Fig. 4.2 allows an interpretation in terms of two-site coupling as follows (see [50] for numerical results). We consider the system of weakly coupled chains as shown below. The inter-chain hopping amplitude, indicated by the dashed
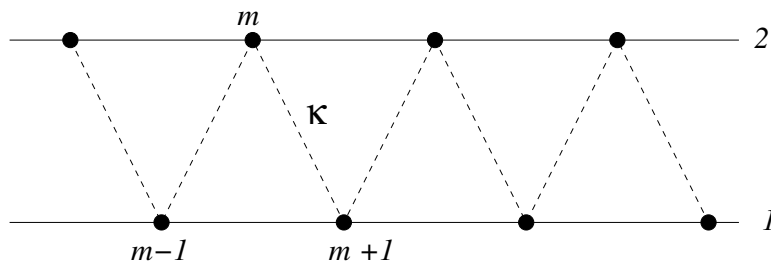
lines, is again much smaller than the intra-chain one.

This coupling scheme is equivalent to one chain with next-neighbor and second-neighbor coupling as sketched below. The next-neighbor coupling is indicated by the dashed curves,
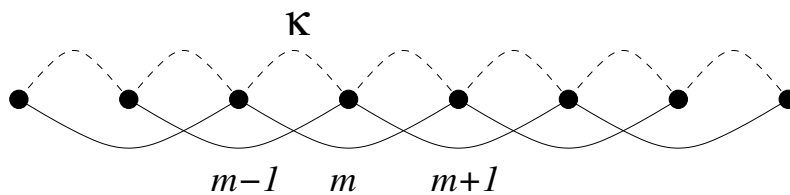
the second-neighbor coupling by the solid curves. Thus we have the somewhat uncommon situation that the second-neighbor tunneling is favored compared to the next-neighbor one.

---

[3]For the relation of these exponents to electrical conductance properties see [51, 36].

Numerical simulations [50] confirmed the expectation that this two-site hopping model shows coupling sensitivity of the localization length for weak coupling.

4.2.4 Qualitative Picture

The results of the numerical simulations can be explained with the help of qualitative considerations similar to the random walk picture in Sec. 3.1.5. We consider two weakly coupled channels. The wave functions in both channels $\psi_{1,m}$, $\psi_{2,m}$ spatially decrease exponentially in average, with the same rate given by the Lyapunov exponent. However, due to different fluctuations in statistically independent channels, it may happen that the wave function in one channel attains much larger values than in the other one, i.e. $\| \psi_{1,m} \| / \| \psi_{2,m} \| > \kappa^{-1}$. In this case it is favorable for the wave function to concentrate in channel 1, which is accomplished by hopping from 2 to 1. Then the decrease continues until the ratio between the wave functions will be again of order of κ^{-1} and a new hopping occurs, etc. Because the values $\ln(\psi_{1,m}^2 + \psi_{1,m-1}^2)$ and $\ln(\psi_{2,m}^2 + \psi_{2,m-1}^2)$ perform biased random walks in space with the diffusion constant D, a characteristic length to reach a distance $|\ln \kappa|$ between them is $m_h \approx (\ln \kappa)^2/D$. This is a characteristic distance between inter-channel hopping. At each hopping the quantity $\ln \| \Psi_m \|$ increases by $\Delta(\ln \| \Psi_m \|) \approx |\ln \kappa|$. Thus the logarithmic decay rate of the wave function decreases by $\Delta(\ln \| \Psi_m \|)/m_h \approx D/|\ln \kappa|$, which corresponds to the singular increase (4.6) of the localization length.

In Fig. 4.5 it is demonstrated how the localized states of weakly coupled chains look like. By numerically diagonalizing the coupled version of the tight-binding Hamiltonian (4.1) the amplitudes of the localized states have been obtained for different values of coupling.
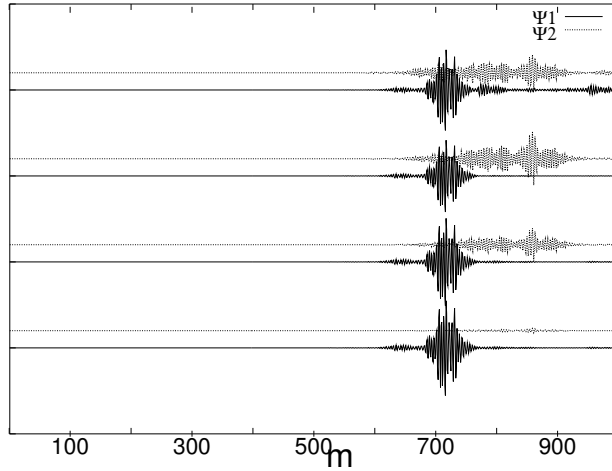

Figure 4.5: The amplitudes $\psi_{1,m}, \psi_{2,m}$ *vs.* m for different values of κ . Chain 2 is shifted w.r.t. chain 1, and this pair is shifted by a larger amount for the values (starting from the bottom) $\kappa = 10^{-5}$, 10^{-4}, 10^{-3}, 10^{-2}, resp.

The number of lattice sites has been chosen as $N = 2000$, i.e. 1000 per chain. In the figure these amplitudes are plotted for the energy value $e = 0.0944$ (at $\kappa = 0$) and the width of the box distribution $w = 0.8$. It should be stressed that the plotted amplitudes result from one realization of the random potential on a quite short lattice length N, so that there is a strong influence of finite size effects. At $\kappa = 0$ there exists a localized state only on one chain because we are dealing with a one-particle Hamiltonian. With small coupling the hopping to the other chain occurs, as described qualitatively above. For larger coupling ($\kappa = 10^{-2}$) one can also see the back-hopping. As a result, small coupling leads to a considerable spread of the localized state.

4.3 Analytical Approach

For the theory we consider a coupled version of the continuous Schrödinger equation (4.3),

$$-\mathrm{d}^2\psi_1/\mathrm{d}x^2 + U_1(x)\psi_1 + \kappa\psi_2 = (e+2)\psi_1 , \tag{4.7a}$$

$$-\mathrm{d}^2\psi_2/\mathrm{d}x^2 + U_2(x)\psi_2 + \kappa\psi_1 = (e+2)\psi_2 . \tag{4.7b}$$

For convenience we have set the lattice constant equal to unity. The random potential is assumed to be a δ-correlated Gaussian random variable: $\langle U_i(x_1)U_j(x_2)\rangle = 2\sigma^2\delta_{ij}\delta(x_1-x_2)$. Because of the symmetry (cf. Sec. 4.2.2) $\lambda_2(\kappa) - \Lambda = -(\lambda_1(\kappa) - \Lambda)$, it is sufficient to calculate the largest Lyapunov exponent in order to determine the coupling sensitivity of the localization length. We define this exponent by (cf. Eqs. (3.5),(3.10))

$$\lambda_1 = \lim_{x\to\infty}\frac{1}{x}\langle\ln\parallel\Psi(x)\parallel\rangle = \left\langle\frac{\mathrm{d}}{\mathrm{d}x}\ln\parallel\Psi(x)\parallel\right\rangle_{\mathrm{stat}} ,$$

with $\Psi = (\psi_1 + \psi_1' + \psi_2 + \psi_2')^t$, and the average on the r.h.s. refering to the stationary distribution. The Lyapunov exponent Λ of the uncoupled subsystems can be represented analytically; this is shown in more detail in Sec. 5.2.

Negative Energies
Here we develop an analytic approach for energies below the band edge and for weak coupling, i.e.

$$e < -2 , \quad \kappa \ll 1 .$$

First let us consider the subsystems without coupling. Then the variables $v_n(x) \equiv \psi_n'/\psi_n$ perform a random walk in a potential $\Phi(v)$,

$$\frac{\mathrm{d}v_n}{\mathrm{d}x} = -\frac{\mathrm{d}\Phi}{\mathrm{d}v} + U_n(x) \quad \text{with} \quad \Phi(v) = v^3/3 + (e+2)v .$$

The potential is plotted in Fig. 4.6; it has a minimum at $v_{\min} = \sqrt{|e+2|}$, however, globally it is unstable. This instability relates to the nodes of the wave function as follows. A change
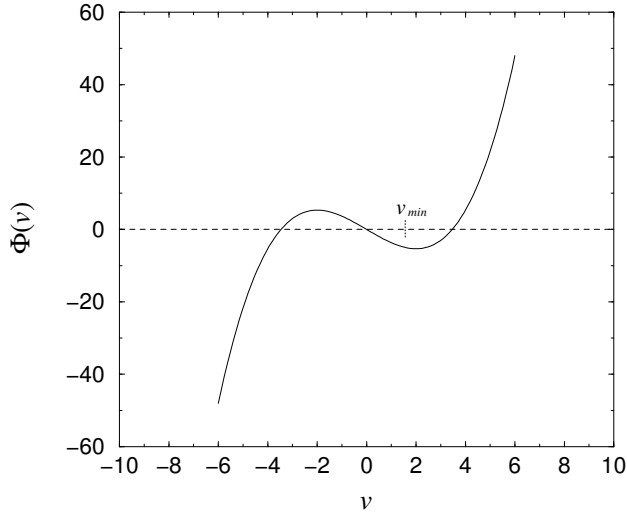
Figure 4.6: The potential $\Phi(v)$ for $e = -4$ with minimum at $v_{\min} = \sqrt{|e+2|}$.

of sign of ψ_n corresponds to the limit $v_n \to -\infty$ followed by a reinjection at $v_n = +\infty$. Thus there is a probability flow along the v-axis which is proportional to the density of nodes of the eigenfunction ψ_n.

For the stable minimum of Φ at $v_{\min}$ one can write the Kramers escape time (see e.g. [58]) as

$$T_K = |e+2|^{-1/2} \exp\left[4|e+2|^{3/2}/3\sigma^2\right] .$$

For $T_K \gg 1$ we may assume that the variable v_n is trapped sufficiently long around the minimum, i.e. absence of a node on long intervals and hence we may presume $\psi_n > 0$.

For the coupled system we now introduce the variables $w_1 = v_1 - v_2$, $w_2 = v_1 + v_2$, and $z = \ln(\psi_1/\psi_2)$, which obey the following set of differential equations:

$$dw_1/dx = U_1 - U_2 - w_1 w_2 - 2\kappa \sinh z , \tag{4.8a}$$

$$dw_2/dx = U_1 + U_2 - \frac{w_1^2 + w_2^2}{2} - 2(e+2) + 2\kappa \cosh z, \tag{4.8b}$$

$$dz/dx = w_1 . \tag{4.8c}$$

The maximal Lyapunov exponent can be written in terms of the new variables as

$$\lambda_1 = \frac{\langle w_2 \rangle}{2} .$$

We now differentiate the equation (4.8c) for z, which yields

$$\frac{d^2 z}{dx^2} = U_1 - U_2 - w_2 \frac{dz}{dx} - 2\kappa \sinh z \approx U_1 - U_2 - 2\lambda_1 \frac{dz}{dx} - 2\kappa \sinh z . \tag{4.9}$$

For the latter approximation we adopted a mean field approach by replacing w_2 by its mean value $2\lambda_1$. For this one has to neglect correlations between the variables w_1 and w_2, which is a rather crude assumption. Now z performs a Brownian motion in the potential $2\kappa\cosh z$ and the stationary solution is given by the Boltzmann distribution [31]:

$$\rho_{\text{stat}}(z) \propto \exp\left[-\frac{\lambda_1}{\sigma^2}2\kappa\cosh z\right] \ .$$

Averaging the r.h.s. of equations (4.8 a,b) with this distribution leads to,

$$
\begin{aligned}
\mathrm{d}w_1/\mathrm{d}x &= U_1 - U_2 - w_1 w_2 \ , \\
\mathrm{d}w_2/\mathrm{d}x &= U_1 + U_2 - \frac{w_1^2 + w_2^2}{2} - 2(e+2) + 2\frac{\sigma^2/2\lambda_1}{|\ln(2\lambda_1\kappa/\sigma^2)|} \ ,
\end{aligned}
$$

for small κ (for the evaluation of the corresponding integral we refer to [1]). Hence the coupling corresponds to a small shift of the effective energy, whereupon the correction to the Lyapunov exponent due to coupling is given by

$$\lambda_1(\kappa) - \Lambda = \frac{\mathrm{d}\Lambda}{\mathrm{d}|e|}\frac{\sigma^2/2\Lambda}{|\ln(2\Lambda\kappa/\sigma^2)|} \ . \tag{4.10}$$

This holds for $e < -2$, where we used the fact that the largest Lyapunov exponent is an increasing function of $|e|$. This result confirms the logarithmic singularity of the Lyapunov exponent (4.5).

To check the validity of formula (4.10) we performed numerical simulations of the coupled Anderson model (4.4). For this we used that the continuous Schrödinger equation
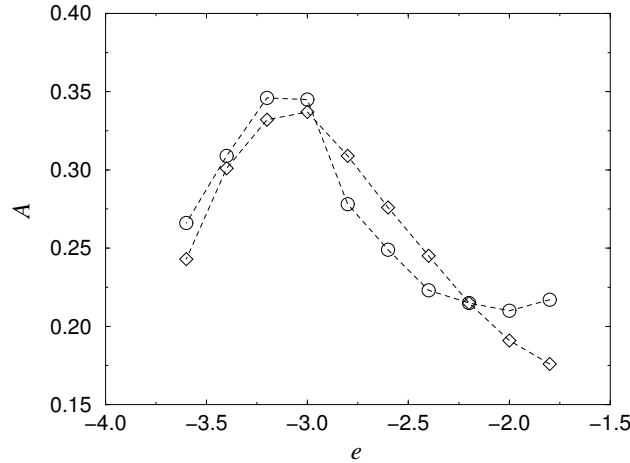
Figure 4.7: The strength *A vs. e* for box distributed potential with width $w = \sqrt{3}/2$. Shown are the numerical results (diamonds) and the analytic approach (circles).

(4.3) is a good approximation of the discrete model (4.2) at the lower band edge, i.e. for $e \leq -2$. In Fig. 4.7 the prefactor A in the relation $\lambda_1(\kappa) - \Lambda = A/|\ln \kappa|$ obtained from numerical simulations is compared with the theoretical one. The analytic results reasonably agree with the numerical calculations, while the agreement is lost with the energy tending to the band centre. As already indicated by Fig. 4.3(b), the strength A increases with $|e|$ ascending from the band centre.

Large Positive Energies
In the limit $e \gg 1$ we can adopt the results of Sec. 3.2.2 for coupled Hamiltonian systems. If we identify $\omega^2 = e - 2$, the system (3.23) is equivalent to the coupled Schrödinger equations (4.7). Hence we obtain with the result (3.28),

$$\lambda_1 - \Lambda \propto \frac{D}{|\ln(\kappa/D)|} \ ,$$

in accordance with relation (4.5). However, the strength A of the singularity (4.5) can not be determined within this approach. This is because the discrete model is not well decribed by the continuous one in the large energy limit.

4.4 Conductance Properties

The coupling sensitivity of the localization length should also affect the conductance G at small couplings, which is demonstrated in the following. We use the Landauer formula [39] for the calculation of the conductance, where G is related to the transmission of electrons through the disordered system. A detailed discussion of the conductance in disordered systems can be found in [22, 62]. Because G is a fluctuating quantity one considers proper averages. Here we consider the *typical* conductance $\tilde{G} = \exp[\langle \ln G \rangle]$ and the *average* conductance $\langle G \rangle$.

The *typical* conductance can be related to the Lyapunov exponent as [22]

$$\tilde{G} \sim e^{-2\ell\lambda_2} \quad \text{for} \quad \ell \gg 1 \ ,$$

where ℓ is the sample length. Applying relation (4.5) leads in the leading order to a singular increase of the *typical* conductance,

$$\tilde{G}/\tilde{G}_0 \sim 1 + 2\ell D/|\ln \kappa| \ ,$$

where $\tilde{G}_0$ is the conductance at zero coupling.

In order to obtain information about the *average* conductance we consider the generalized localization lengths [22], defined by

$$l_q = \lim_{x \to \infty} \frac{1}{qx} \ln \left\langle \| \Psi_{\text{loc}}(x) \|^{-q} \right\rangle \ ,$$

where Ψ_{loc} is a localized state. By employing the Borland conjecture these lengths can be related to the generalized Lyapunov exponents (introduced in Sec. 2.1.3) by

$$l_q^{-1} = L(q) .$$

Here the generalized Lyapunov exponents are defined by

$$L(q) = \lim_{x \to \infty} \frac{1}{qx} \ln \langle \parallel \Psi(x) \parallel^q \rangle ,$$

where Ψ is a generic exponentially increasing solution of the continuous Schrödinger equation (4.7).

First we consider $L(2)$ which can be deduced from the exponential growth of the second moment vector

$$Y_2 \equiv \left\langle (\psi_1^2, \psi_1 \psi_1', \psi_1'^2, \psi_2^2, \psi_2 \psi_2', \psi_2'^2, \psi_1 \psi_2, \psi_1 \psi_2', \psi_2 \psi_1', \psi_1' \psi_2')^t \right\rangle .$$

By applying the Furutsu-Novikov formula (see App. A.2), the spatial evolution of Y_2 is given by two constant matrices $\mathbf{A}, \mathbf{B}$ as

$$\frac{\mathrm{d}}{\mathrm{d}x} Y_2 = (\mathbf{A} + \kappa \mathbf{B}) Y_2 .$$

Thus $L(2)$ is given by the largest real part of the eigenvalues of this linear system. The eigenvalues, however, can be obtained by standard perturbation theory in the small coupling parameter κ, whereupon the second generalized Lyapunov exponent is given by a series expansion,

$$L(2) = L_0(2) + \sum_{j=1}^{\infty} a_j \kappa^j ,$$

where $L_0(2)$ is the value at zero coupling. The same procedure applies to higher moments.

Now, by means of the transmission coefficient t, the *average* conductance can be estimated by

$$\langle G \rangle \sim \langle |t|^2 \rangle \sim \langle \parallel \Psi_{\mathrm{loc}}^2 \parallel \rangle \sim e^{-2\ell L(2)} \quad \text{for} \quad \ell \gg 1 .$$

Thus we conclude that standard perturbation theory also holds for the *average* conductance, i.e. that it can be expanded as

$$\langle G \rangle = \langle G \rangle_0 + \sum_{j=1}^{\infty} b_j \kappa^j .$$

Hence $\langle G \rangle$ shows no coupling sensitivity.

4.5 Summary and Perspectives

In this chapter we demonstrated that small coupling of one-dimensional disordered chains yields a singular increase of the typical localization length. We have performed numerical simulations of a tight-binding model which has the form of coupled Anderson models and have demonstrated the singularity for two and four coupled chains. In order to examine the robustness of the effect we allowed for different distributions of the random potential as well as small randomized coupling. The results for the behavior of the Lyapunov exponents at small couplings agree with the analytic findings that we obtained for a continuum disordered model, whereupon the effect seems to be a general phenomenon in systems with linear localization. Formally the effect is closely related to the coupling sensitivity of chaotic Hamiltonian systems, which is treated in Sec. 3.2 (cf. also [64]).

Qualitatively, the effect results from a consideration of coupled random walks, where the "walkers" are the logarithms of the norms of the wave function in the chains. In terms of the motion of a particle, the coupling gives rise to the possibility to tunnel between the disordered subsystems when one "walker" goes far ahead, i.e. when the conditions for the particle propagation in one chain are more favorable than in the other one. This leads already for very small couplings to a considerable spread of the wave function that is reflected in the singular increase of the localization length.

An experimentally accessible quantity of disordered systems is the conductance. We deomonstrated that the *typical* conductance $\exp[\langle \ln G \rangle]$ shows coupling sensitivity, whereas the *average* conductance scales according to standard perturbation theory for weak coupling. This different scaling also underlines the role of conductance fluctuations in disordered systems. From the theoretical point of view it would be interesting to investigate into models with many coupled chains, which better reflect real systems.

5 Lyapunov Exponent Statistics of the Random Frequency Oscillator

In this chapter we focus on the exponential growth rate of the parametrically excited linear oscillator. Despite of its simplicity, this model eludes complete analytic solution. The random frequency oscillator, introduced in Sec. 2.2.2, Eq. (2.13), has already been employed in Sec. 3.2.2 as a model for the dynamics of perturbations in chaotic Hamiltonian systems, and in Sec. 4.1 as a continuous Schrödinger equation [1] for a localized particle in a disordered potential. Another field of application is the theory of parametric resonance which appears, e.g., in a pendulum with randomly vibrating suspension axis [38].

In all applications the exponential growth rate of the oscillations, determined by the Lyapunov exponents, is of major interest. Generally, one cannot characterize this rate with a single number, so one speaks of multiscaling. This property can be characterized in a twofold way. On one hand it is possible to characterize the fluctuations of the exponential growth with the local (finite-time) Lyapunov exponent $\lambda(t)$. Then one describes multiscaling in terms of the corresponding probability density. Recently it has been shown [60] that for certain parameter values the distribution of the local Lyapunov exponent deviates from the Gaussian form, leading to non-vanishing higher cumulants. Thus the usual Lyapunov exponent alone is not sufficient for a statistical characterization why we treat the problem with the help of generalized Lyapunov exponents, corresponding to growth rates of different moments of the amplitude. In the presence of multiscaling these growth rates are different, what gives a complementary characterization.

Our main goal in this chapter is to define the range of parameters where multiscaling is essential, and to relate the asymptotical scaling of the generalized exponents to the form of the tails of the density $P(\lambda; t)$. After an introduction of the generalized Lyapunov exponents we will perform a time rescaling, which leaves a noise renormed frequency as the sole relevant parameter. Some known properties of the Lyapunov exponent of the random oscillator will be recalled, which we will supplement with results for negative frequencies. The non-Gaussian properties of the distribution of the local Lyapunov exponent will be investigated, using numerical results and some analytic estimates. Some of the following results have been published in [71].

---

[1]Here the time is interpreted as the spatial variable
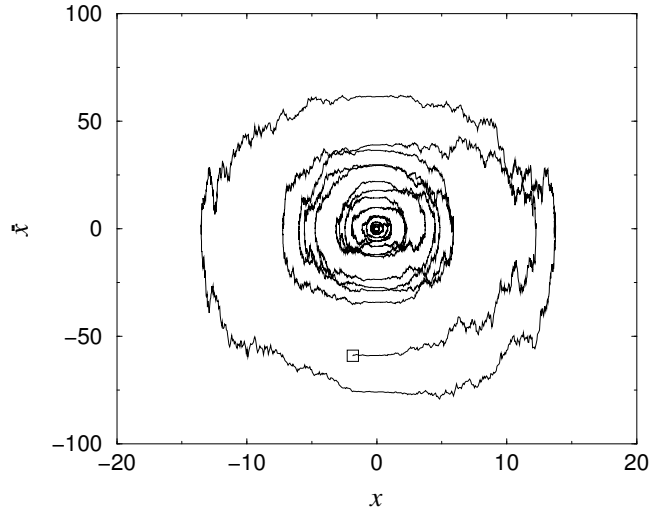
Figure 5.1: Typical orbit of the random frequency oscillator for $\mathcal{E} = 25$, $\sigma^2 = 10$; the final point is marked by the square.

5.1 Parametric Instability

The parametrically excited oscillator is defined by the following equations,

$$\mathrm{d}^2x/\mathrm{d}t^2 + [\mathcal{E} + \xi(t)]x = 0 , \quad \langle \xi(t) \rangle = 0 , \quad \langle \xi(t)\xi(t') \rangle = 2\sigma^2\delta(t - t') , \quad (5.1)$$

with the Gaussian white noise $\xi(t)$. A typical trajectory of model (5.1) obtained by numerical integration is shown in Fig. 5.1. In the following we will also allow for negative values of $\mathcal{E}$. For some applications the oscillator has a linear damping term $2\gamma\dot{x}$. However, such an equation can be transformed to Eq. (5.1) as follows.

Consider the damped oscillator

$$\ddot{x} + [\mathcal{E} + \xi(t)]x + 2\gamma\dot{x} = 0 .$$

Applying the transformation $y = e^{\gamma t}x$ yields the undamped equation,

$$\ddot{y} + [\mathcal{E} - \gamma^2 + \xi(t)]y = 0 .$$

If y grows exponentially as $\exp(\lambda t)$, the growth of x is given by $\exp[(\lambda - \gamma)t]$ where λ also depends on γ. Thus there is a threshold which divides exponential growth due to noisy pump from shrinking due to damping.

We start with the definition of quantities that characterize the growth of oscillations in our basic model. The fluctuations in (5.1) lead to an exponential (on average) growth of the
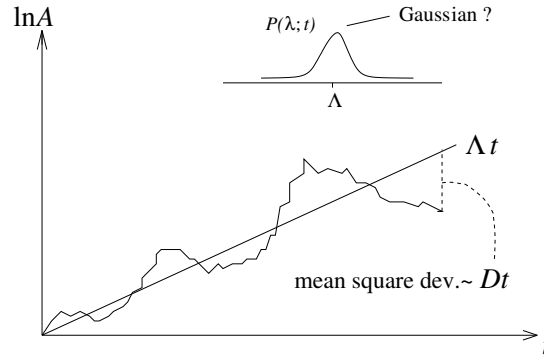
Figure 5.2: Typical fluctuations of the exponential growth with mean Λt.

amplitude:

$$A \equiv \sqrt{x^2 + \dot{x}^2} \sim \exp(\Lambda t) \ .$$

Because of the similarity to linearized equations for the growth of small perturbations in chaotic systems, the exponent Λ is called the Lyapunov exponent. The local (finite-time) Lyapunov exponent (cf. Sec. 2.3) is defined as

$$\lambda(t) \ = \ \frac{1}{t} \ln A(t) \ ; \tag{5.2}$$

it converges to Λ as time tends to infinity and is a self-averaged quantity [22]:

$$\lambda(t) \xrightarrow[t \to \infty]{} \Lambda = \left\langle \frac{\mathrm{d}}{\mathrm{d}t} \ln A \right\rangle_{\text{stat}} . \tag{5.3}$$

The average on the r.h.s. refers to the stationary distribution. Due to different realizations of the noise the local Lyapunov exponent fluctuates corresponding to its probability density $P(\lambda; t)$, and we will inspect in Sec. 5.6 to what extent this density can be approximated by a Gaussian. These relations are outlined in Fig. 5.2.

The fluctuations of $\lambda(t)$ can be characterized with the help of the generalized Lyapunov exponents (see Sec. 2.1.3), defined as the growth rate of moments of the amplitude:

$$L(q) \ = \ \frac{1}{q} \lim_{t \to \infty} \frac{1}{t} \ln \langle A^q(t) \rangle \ . \tag{5.4}$$

Because of the fluctuations these rates generally differ from Λ. Definition (5.4) includes the usual Lyapunov exponent as a special case:

$$\Lambda = \lim_{q \to 0} L(q) \ .$$

By standard theorems of probability theory it can be shown that the quantity $qL(q)$ is a convex function of q. Generally, all $L(q)$ are different and are necessary to characterize the growth of oscillations, as shall be discussed below in Sec. 5.3.

5.2 Analytic Expressions for the Lyapunov Exponents

In this section we recall some known properties of the Lyapunov exponent of the noise-driven oscillator (5.1), which we supplement with results for negative frequency $\mathcal{E}$.

5.2.1 Largest Lyapunov Exponent

The exponent Λ can be calculated as follows (see [41] for details). First we apply the Hopf-Cole transformation: $y = \dot{x}/x = \mathrm{d}\ln|x|/\mathrm{d}t$. Hence Eq. (5.1) reduces to the first-order nonlinear Langevin-type equation

$$\mathrm{d}y/\mathrm{d}t = -y^2 - \xi(t) - \mathcal{E} .$$

Here y, after reaching $-\infty$, is reinjected at $+\infty$ which corresponds to a zero-crossing of $x(t)$. This implies a probability flow along the y-axis (cf. Sec. 4.3, *Negative energies*). The next step is the application of the Fokker-Planck theory: for the distribution of y one can write the Fokker-Planck equation and find its stationary solution (which is a solution with a constant probability flow):

$$\rho_{\mathrm{stat}}(y) = \frac{1}{\sqrt{\pi}\sigma^{4/3}} \frac{e^{-y^3/3\sigma^2 - \mathcal{E}y/\sigma^2} \int_{-\infty}^{y} e^{x^3/3\sigma^2 + \mathcal{E}x/\sigma^2}\mathrm{d}x}{\int_{0}^{\infty} x^{-1/2} e^{-x^3/12 - \mathcal{E}x/\sigma^{4/3}}\mathrm{d}x} .$$

Averaging y with use of this solution yields the following expression for the Lyapunov exponent:

$$\Lambda = \left\langle \frac{\mathrm{d}\ln|x|}{\mathrm{d}t} \right\rangle_{\mathrm{stat}} = \langle y \rangle_{\mathrm{stat}} = \frac{\sigma^{2/3}}{2} \frac{\int_{0}^{\infty} x^{1/2} e^{-x^3/12 - \mathcal{E}x/\sigma^{4/3}}\mathrm{d}x}{\int_{0}^{\infty} x^{-1/2} e^{-x^3/12 - \mathcal{E}x/\sigma^{4/3}}\mathrm{d}x} . \qquad (5.5)$$

For large $|\mathcal{E}|$ one can approximate the integrals, which is shown in Sec. 5.5.

5.2.2 Generalized Lyapunov Exponents

For $q = 2, 4, 6, \ldots$ in Eq. (5.4) the following analytic approach can be used.
 Because Eq. (5.1) is a linear stochastic equation, the evolution of the moments of order q of the type $\langle x^{q-k}\dot{x}^k \rangle$ obeys a closed linear system of equations. The latter can be derived as the following (another way to derive this system is presented in [60]). Consider the temporal derivative of the moments obtained by application of Eq. (5.1):

$$\frac{\mathrm{d}}{\mathrm{d}t}\left\langle x^{q-k}\dot{x}^k \right\rangle = (q-k)\left\langle x^{q-k-1}\dot{x}^{k+1} \right\rangle - k\mathcal{E}\left\langle x^{q-k+1}\dot{x}^{k-1} \right\rangle - k\left\langle \xi(t)x^{q-k+1}\dot{x}^{k-1} \right\rangle .$$

Figure 5.3: The Lyapunov exponents Λ (solid line) and $L(2)$ (dashed line) *vs.* $\mathcal{E}$; $\sigma^2 = 1$.

The averaging of the last term can be carried out by using the Furutsu-Novikov-formula (see App. A.2),

$$k \left\langle \xi(t) x^{q-k+1} \dot{x}^{k-1} \right\rangle = -k(k-1)\sigma^2 \left\langle x^{q-k+2} \dot{x}^{k-2} \right\rangle .$$

Defining

$$M = \left\langle \left(x^q, x^{q-1}\dot{x}, \ldots, x^{q-k+1}\dot{x}^{k-1}, \ldots, \dot{x}^q \right)^t \right\rangle ,$$

the evolution of M is now determined by a $q+1 \times q+1$ matrix: $\dot{M} = \mathbf{T}M$. The sparse matrix $\mathbf{T}$ has the following form:

$$
\begin{pmatrix}
0 & q & 0 & 0 & & & & \\
-\mathcal{E} & 0 & q-1 & 0 & \ddots & & & \\
2\sigma^2 & -2\mathcal{E} & 0 & q-2 & \ddots & & & \\
0 & 2 \times 3\sigma^2 & -3\mathcal{E} & 0 & \ddots & & & \\
& \ddots & \ddots & \ddots & \ddots & & & \\
& & & & & 0 & 2 & 0 \\
& & & & & (1-q)\mathcal{E} & 0 & 1 \\
& & & & & (q-1)q\sigma^2 & -q\mathcal{E} & 0
\end{pmatrix} . \qquad (5.6)
$$

Thus the largest real part of the eigenvalues determines the exponential growth of the moments of order q. By definition (5.4) the generalized exponent $L(q)$ for even q is thus equal to this value divided by q.[2]

---

[2] For odd q follows $\langle x^q \rangle \neq \langle |x^q| \rangle$ and this approach does not provide the Lyapunov exponent.

In the simplest case of $q = 2$ the exponent $L(2)$ is a solution of the cubic equation $\gamma^3 + \mathcal{E}\gamma - 0.5\sigma^2 = 0$:

$$
L(2) = \begin{cases}
2^{-2/3}\sigma^{2/3}\left[\left(1 + \sqrt{1 + \left(\frac{4^{2/3}\mathcal{E}}{3\sigma^{4/3}}\right)^3}\right)^{1/3} - \dfrac{4^{2/3}\mathcal{E}}{3\sigma^{4/3}\left(1 + \sqrt{1 + \left(\frac{4^{2/3}\mathcal{E}}{3\sigma^{4/3}}\right)^3}\right)^{1/3}}\right] & \text{if } \frac{\mathcal{E}}{\sigma^{4/3}} \geq -\frac{3}{4^{2/3}} \\[3em]
2\sqrt{\frac{|\mathcal{E}|}{3}}\cos\left[\frac{1}{3}\arctan\sqrt{\left(\frac{4^{2/3}|\mathcal{E}|}{3\sigma^{4/3}}\right)^3 - 1}\right] & \text{if } \frac{\mathcal{E}}{\sigma^{4/3}} < -\frac{3}{4^{2/3}} \;.
\end{cases}
$$

(5.7)

For larger q one has to find the roots of the corresponding polynom of order $q+1$ numerically, but this is a straightforward task. In Fig. 5.3 the dependence of Λ and $L(2)$ on the parameter $\mathcal{E}$ is plotted.

5.3 Multiscaling in Terms of Lyapunov Exponents

What follows from the analytic expressions for the generalized Lyapunov exponents, is that they are in general different which means multiscaling. Here we remind some outcomes of Sec. 2.1.3 which deals with the relation between the generalized Lyapunov exponents and the fluctuations of $\lambda(t)$, the latter described by the probability density $P(\lambda;t)$.

It turns out that the generalized Lyapunov exponent is the asymptotic cumulant-generating function of $P(\lambda;t)$:

$$
L(q) = \lim_{t\to\infty}\sum_{n=1}^{\infty}\frac{q^{n-1}t^{n-1}}{n!}K_n(t) = \Lambda + \frac{q}{2}D + \lim_{t\to\infty}\sum_{n=3}^{\infty}\frac{q^{n-1}t^{n-1}}{n!}K_n(t) \;. \qquad (5.8)
$$

Hence $L(q)$ can be expanded in a power series around $q = 0$ with coefficients given by the cumulants of the local Lyapunov exponent. It follows that

$$
\Lambda = L(0) \;, \quad D = 2L'(0) \;.
$$

There is also a connection between $L(q)$ and the entropy function $f(\lambda)$, the latter defined by

$$
P(\lambda;t) \sim \exp[-tf(\lambda)] \quad \text{for } t \gg 1 \;.
$$

The entropy function is determined by the generalized Lyapunov exponent via a Legendre transformation [48, 22]:

$$
f(\lambda) = q\lambda - qL(q) \;, \quad \frac{\mathrm{d}}{\mathrm{d}q}qL(q) = \lambda \;. \qquad (5.9)
$$

The expansion of the entropy function around $\lambda = \Lambda$ reads $f \approx (\lambda - \Lambda)^2/2D$, which yields a Gaussian distribution of the local Lyapunov exponent. In the tails, however, deviations from the Gaussian will be present in general.

In case the Gaussian approximation holds, higher cumulants ($n \geq 3$) vanish and we obtain:

$$L(q) = \Lambda + \frac{Dq}{2} \; . \tag{5.10}$$

Then all generalized Lyapunov exponents are fully determined by the two coefficients Λ and D [or, equivalently, by Λ and $L(2)$] and this situation can be characterized as "monoscaling". However, we will show below that for the noise-driven oscillator (5.1) this holds only for $|\mathcal{E}| \gg \sigma^{4/3}$.

5.4 Reduction of Parameters

Before proceeding with the detailed analysis of the Lyapunov exponents, we explore the scaling dependence on the parameters $\mathcal{E}, \sigma$. The analytic expressions (5.5) and (5.7) suggest the scaling relation $L(q) = \sigma^{2/3} f_q(\mathcal{E}\sigma^{-4/3})$ with some q-dependend function f_q. To show that this scaling holds for all the exponents $L(q)$ we perform the time rescaling $t = (|\mathcal{E}|/\sigma^2)\tau$ in Eq. (5.1), whereupon it can be written in the following form:

$$\frac{d^2x}{d\tau^2} + \left[\left(\frac{\mathcal{E}}{\sigma^{4/3}} \right)^3 + \left(\frac{|\mathcal{E}|}{\sigma^{4/3}} \right)^{3/2} \eta(\tau) \right] x = 0 \; , \quad \langle \eta(\tau)\eta(\tau') \rangle = 2\delta(\tau - \tau') \; . \tag{5.11}$$

The Lyapunov exponents determined by Eq. (5.11) obviously depend only on the parameter $E \equiv \mathcal{E}\sigma^{-4/3}$, and we write them as $\bar{L}(q;E)$.

Returning back to time t we have to reset the time scale by multiplying these exponents with $\sigma^2/|\mathcal{E}| = \sigma^{2/3}\sigma^{4/3}/|\mathcal{E}|$; this gives for the Lyapunov exponents

$$L(q;\mathcal{E},\sigma) \;=\; \sigma^{2/3} \frac{\sigma^{4/3}}{|\mathcal{E}|} \bar{L}(q;E) \;\equiv\; \sigma^{2/3} \tilde{L}(q;E) \; . \tag{5.12}$$

The essential behavior is presented by the exponents $\tilde{L}(q;E)$; thus throughout the rest of the chapter this quantity is examined. That is, we consider the following one-parameter equation (now denoting τ as t):

$$d^2x/dt^2 + [E + \xi(t)]x = 0 \; , \quad \langle \xi(t) \rangle = 0 \; , \quad \langle \xi(t)\xi(t') \rangle = 2\delta(t - t') \; . \tag{5.13}$$

For simplicity we will omit the tilde in the sequel; relation to previous formulae can be achieved by inserting E instead of $\mathcal{E}\sigma^{-4/3}$ in the corresponding expressions (5.5) and (5.7).

5.5 Gaussian Distribution for large $|E|$

In this section we demonstrate, using approximate methods, that for $|E| \gg 1$ the Gaussian approximation to the distribution of the local Lyapunov exponent or, equivalently, Eq. (5.10) holds.

5.5.1 Large Positive Values of E

In the high-frequency limit $E \gg 1$ the fast oscillating terms can be averaged out in the same way as in Sec. 3.2.2, but now without coupling. Details can also be found in [41].

First we perform a standard transformation to amplitude and phase variables in Eq. (5.13):

$$x = A \sin \psi \,, \quad \dot{x} = \sqrt{E} A \cos \psi \,.$$

The equations of motion then become

$$\frac{\mathrm{d}\psi}{\mathrm{d}t} = \sqrt{E} + \frac{1}{\sqrt{E}} \xi(t) \sin^2 \psi \,, \quad \frac{\mathrm{d}A^q}{\mathrm{d}t} = -\frac{q}{2\sqrt{E}} \xi(t) A^q \sin 2\psi \,, \tag{5.14}$$

where the equation for the amplitude has been generalized to the equation for its qth power. With the new variable $u = \ln A$ the largest Lyapunov exponent is with Eq. (5.3) given by:

$$\Lambda = \langle \dot{u} \rangle_{\mathrm{stat}} = -\frac{1}{2\sqrt{E}} \langle \xi(t) \sin 2\psi \rangle_{\mathrm{stat}} \,. \tag{5.15}$$

For large positive E the deterministic phase velocity $\sqrt{E}$ in the l.h.s. of (5.14) dominates over the typical diffusion rate which is of order $2/E$. Thus for $E^{3/2} \gg 1$ the probability density of the phase becomes uniform on the interval $[0, 2\pi]$ and averaging the corresponding Fokker-Planck equation over ψ yields the evolution of the reduced probability density $\rho(u;t)$:

$$\frac{\partial \rho(u;t)}{\partial t} = \left[-\frac{1}{4E} \frac{\partial}{\partial u} + \frac{1}{8E} \frac{\partial^2}{\partial u^2} \right] \rho(u;t) \,.$$

This is equivalent to simple Brownian motion with a constant drift $1/4E$. Hence u and, accordingly, $\lambda(t)$ are normally distributed and for the exponents holds:

$$\Lambda = \frac{1}{4E} \,, \quad L(q) = \left(1 + \frac{q}{2} \right) \Lambda \quad \Longrightarrow \quad D = \Lambda \,. \tag{5.16}$$

The last statement is known as single parameter scaling, the distribution of the local Lyapunov exponent being determined by its mean value alone.

If one considers the parametric oscillator (5.13) as a continuous approximation to the discrete Anderson model for large wavelengths, i.e. around the lower band edge, then negative E correspond to the band gap of the Anderson model, the band edge being located at $E = 0$ (cf. Sec. 4.1). Increasing positive E translates to an approach to the band centre where single parameter scaling is known to exist. This property has been widely discussed in the context of Anderson localization [62, 27, 61].

5.5.2 Large Negative Values of E

For negative E we transform to the eigenvectors of the noiseless system:

$$x = \tilde{x} + \tilde{y} , \quad \dot{x} = |E|^{1/2}(\tilde{x} - \tilde{y}) ;$$

whereupon the equations of motion become

$$\frac{\mathrm{d}\tilde{x}}{\mathrm{d}t} = |E|^{1/2}\tilde{x} + \frac{1}{2|E|^{1/2}}\xi(t)(\tilde{x} + \tilde{y}) , \quad \frac{\mathrm{d}\tilde{y}}{\mathrm{d}t} = -|E|^{1/2}\tilde{y} - \frac{1}{2|E|^{1/2}}\xi(t)(\tilde{x} + \tilde{y}) .$$

The dynamics of $\tilde{y}$ incorporates deterministic damping and random growth due to the parametric noise. We estimate the average growth by neglecting $\tilde{x}$:

$$\langle \dot{\tilde{y}} \rangle \sim -|E|^{1/2}\langle\tilde{y}\rangle - \frac{1}{2|E|^{1/2}}\langle\xi(t)\tilde{y}\rangle = -|E|^{1/2}\langle\tilde{y}\rangle + \frac{1}{4|E|}\langle\tilde{y}\rangle ;$$

where we used the Furutsu-Novikov theorem (see App. A.2). Hence the average grows as $\exp[(|E|^{-1}/4 - |E|^{1/2})t]$, i.e. for large $|E|^{3/2}$ the damping dominates and one can neglect $\tilde{y}$ compared to $\tilde{x}$ in the equation for $\dot{\tilde{x}}$.

Hence the time evolution of $u = \ln|\tilde{x}|$ is given by

$$\frac{\mathrm{d}u}{\mathrm{d}t} = |E|^{1/2} + \frac{1}{2|E|^{1/2}}\xi(t) ,$$

which again leads to a Gaussian distribution of the local Lyapunov exponent, the latter given for large times by u/t. For the generalized Lyapunov exponents we obtain

$$\Lambda = |E|^{1/2} , \quad L(q) = |E|^{1/2} + \frac{q}{2|E|} \approx |E|^{1/2} . \tag{5.17}$$

Here there is no single parameter scaling (5.16) because $D = \Lambda^{-2}$.

Notice that in both cases, $E > 0$ and $E < 0$, the asymptotic results are obtained for

$$|E|^{3/2} \gg 1 .$$

5.6 Multiscaling of the Growth Rate

5.6.1 Non-Gaussian Fluctuations

We have demonstrated in the previous section that for large $|E|$ the distribution of the local Lyapunov exponent is nearly Gaussian. Here we will show that this does not hold for small $|E|$ (see also [60]), with two numerical tests regarding the second and the third cumulant.
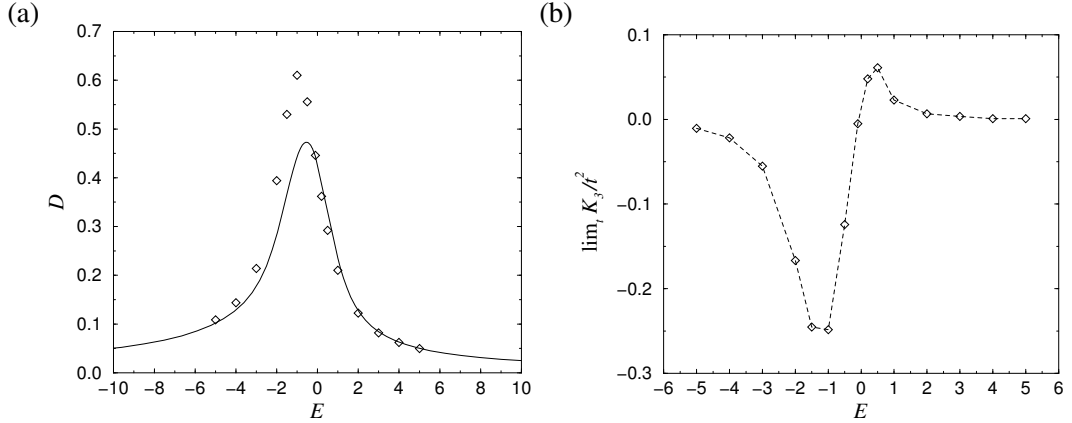
(a)

(b)

Figure 5.4: (a) The diffusion constant D as a function of the frequency E. The diamonds show the numerical result whereas the solid line depicts the Gaussian presumption $D = L(2) - \Lambda$.
(b) Numerical result for the limiting cumulant $\lim_{t \to \infty} K_3/t^2$; the dashed line is to improve readability.

Suppose that the local Lyapunov exponent is normally distributed. Then the whole set of generalized Lyapunov exponents can be expressed, according to Eq. (5.10), in terms of the analytically known exponents Λ and $L(2)$:

$$L(q) \;=\; \Lambda + \frac{D}{2}q \;=\; \Lambda + \frac{q}{2}\left[L(2) - \Lambda\right] . \tag{5.18}$$

In particular, the diffusion constant D equals $L(2) - \Lambda$ and the third cumulant K_3 in expansion (5.8) vanishes.

In Fig. 5.4(a) the numerically computed diffusion constant for the noise-driven oscillator is compared with the Gaussian assumption (5.18), indicating that there are deviations for values of E close to zero. The coefficient $\lim_{t \to \infty} K_3/t^2$ of the cumulant expansion (5.8) is plotted in Fig. 5.4(b). It is clearly different from zero for small $|E|$.

These results suggest, that in the intermediate regime, $|E| \lesssim 1$, the linear form of $L(q)$ is not correct. This is elucidated by writing explicitly the local Lyapunov exponent in terms of amplitude and phase (compare Eq. (5.15)):

$$\lambda(t) = -\frac{1}{2\sqrt{E}\,t} \int_0^t \xi(\tau) \sin 2\psi(\tau)\mathrm{d}\tau .$$

Because the noise and the phase are coupled according to Eqs. (5.14), the process $\xi(\tau)\sin 2\psi(\tau)$ resembles Gaussian white noise only for $E^{3/2} \gg 1$, as has been shown in Sec. 5.5.

In terms of the localization theory the point $E = 0$ corresponds to the band edge, where indeed a complicated behavior of the corresponding distributions is expected [62, 27, 61].
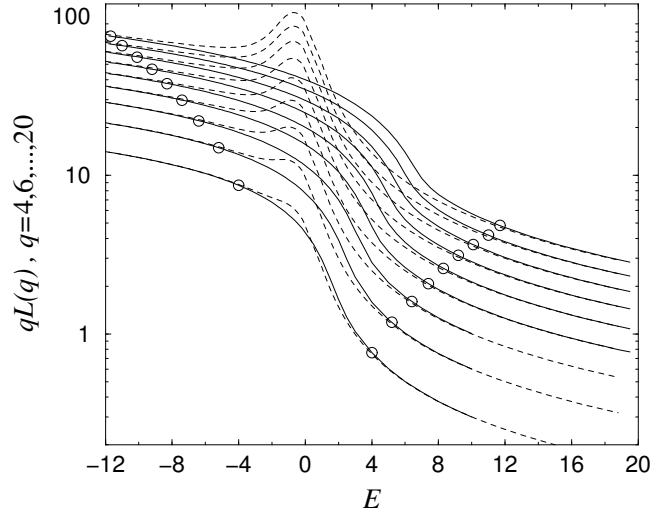
Figure 5.5: *qL(q) vs. E* for even values of *q* increasing from *q* = 4 at the bottom to *q* = 20 at the top. The solid lines show the numerical result, the dashed lines show the parabolic approximation (5.18). The threshold $q/|E|^{3/2} = 0.4$ is marked by the circles.

5.6.2 Parameter Range of Non-Gaussian Fluctuations

In Sec. 5.5 we have shown that the distribution of $\lambda(t)$ is Gaussian for $|E|^{3/2} \gg 1$. Taking this into account we assume hypothetically that the relevant scale variable is given by $|E|^{3/2}$. To be precise, we assume that the cumulants of the density $P(\lambda;t)$ vanish for large $|E|$ as

$$K_n \sim \left(\frac{1}{|E|^{3/2}} \right)^n \quad \text{for} \quad n \geq 3 \,. \tag{5.19}$$

Then the expansion (5.8) is a power series in the parameter $q/|E|^{3/2}$, and the deviation of the generalized Lyapunov exponent from the Gaussian form (5.18) scales as follows:

$$L(q) - \left\{ \Lambda + \frac{q}{2}[L(2) - \Lambda] \right\} \sim \sum_{n=3}^{\infty} a_n \left(q/|E|^{3/2} \right)^n \,;$$

with constant coefficients a_n. According to this assumption, the generalized exponent $L(q)$ deviates from the Gaussian value (5.18) when the parameter $q/|E|^{3/2}$ is large.

To test this numerically we show in Fig. 5.5 the exact generalized Lyapunov exponent together with the Gaussian approximation (5.18), as a function of *E* for several values of the parameter *q*. The indicated threshold $q/|E|^{3/2} = 0.4$ divides well the region of agreement between the correct value and the approximation from the region where these values strongly disagree, thus confirming our hypothesis.

5.6.3 Asymptotic Scaling of Generalized Lyapunov Exponents

In this section we study the asymptotic behavior of $L(q)$ for large q. This problem can be formulated as the problem of asymptotic properties of the eigenvalues of matrix (5.6) as $q \to \infty$. We expect the scaling to be a power law,

$$L(q) \sim q^{\alpha-1} , \quad \alpha(E) \in (1,2) . \tag{5.20}$$

Because the largest element of matrix (5.6) scales as q^2 for large q, $L(q) \sim q$ sets an upper limit to the scaling (5.20). This can be shown as follows (for mathematical details see [40, 13]).

We consider the matrix $\mathbf{T}$ defined by (5.6) for $\mathcal{E} = E$, $\sigma^2 = 1$. First we calculate a suitable matrix norm, which we choose as

$$\|\mathbf{T}\| = \max_j \sum_{i=1}^{q+1} |T_{ij}| ,$$

i.e. we choose the greatest column sum of absolute values of the matrix elements. Now, for $j = 2,\dots,q-1$, we have

$$\sum_{i=1}^{q+1} |T_{ij}| = q-j+2+j|E|+j(j+1) \le q-j+1+(j+1)|E|+(j+1)(j+2) = \sum_{i=1}^{q+1} |T_{i(j+1)}| .$$

Hence it is easy to see that

$$\|\mathbf{T}\| = \sum_{i=1}^{q+1} |T_{i(q-1)}| = 3+(q-1)|E|+(q-1)q \xrightarrow[q\to\infty]{} q^2 .$$
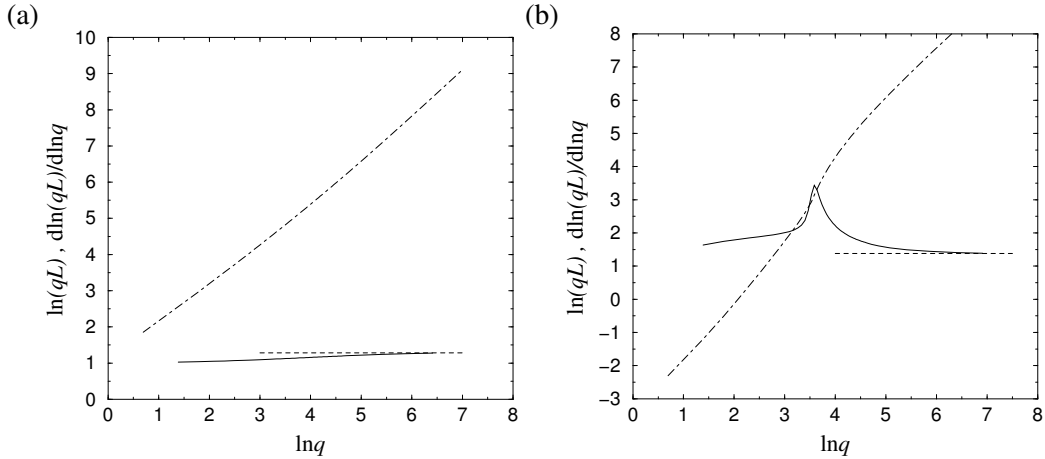

Figure 5.6: $\ln[qL(q)]$ *vs.* $\ln q$ (dot-dashed) for $E = -10$ (a) and $E = 10$ (b). The solid lines are numerical derivatives: $d\ln[qL(q)]/d\ln q$; the dashed lines correspond to $\alpha = 1.28$ and $\alpha = 1.38$, resp.
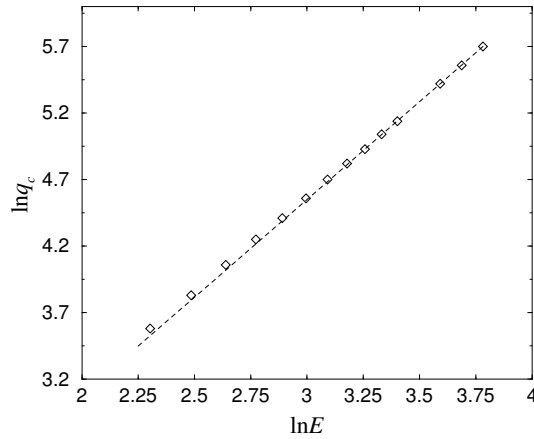
Figure 5.7: The crossover $\ln q_c$ *vs.* $\ln E$. The dashed line has slope $1.47 \approx 3/2$.

Employing a standard theorem of matrix calculus we have that for any matrix norm,

$$\|\mathbf{T}\| \geq \max_j |\gamma_j| \ ,$$

where γ_j are the eigenvalues. Because the quantity $qL(q)$ is given by the largest real part of the eigenvalues, we arrive at the above result $\alpha < 2$.

The numerical results, presented in Fig. 5.6 for two values of E, give $\alpha = 1.28$ for $E = -10$ and $\alpha = 1.38$ for $E = 10$.

The fact that asymptotically $\alpha < 2$ means that the tails of the distribution of the local Lyapunov exponent are suppressed in comparison to the Gaussian form. Indeed, by virtue of the Legendre transformation (5.9), the scaling of $L(q)$ for large q translates into a scaling of the entropy function $f(\lambda)$ for $\lambda \gg 1$:

$$f(\lambda) \sim (\alpha - 1) \left(\frac{\lambda}{\alpha} \right)^{\alpha/(\alpha-1)} \quad \text{for} \quad \lambda \gg 1 \ .$$

The linear approximation (5.18) would give $\alpha = 2$, i.e. a Gaussian form of $P(\lambda;t)$. For $\alpha < 2$, however, $f(\lambda)$ obeys a power law with an exponent $\alpha/(\alpha - 1) > 2$. That is, $P(\lambda;t)$ decays faster than the Gaussian distribution for large values of λ.

We also note a definite crossover in the scaling in Fig. 5.6 (b), which is clearly seen as a maximum in the dependence of the slope $d \ln qL/d \ln q$ on q. The position of this crossover, q_c, is plotted as a function of E in Fig. 5.7 which suggests a scaling $q_c \sim E^{3/2}$. This is another support for the scaling relation (5.19) separating Gaussian and non-Gaussian behavior of the Lyapunov exponents.

We emphasize that convergence problems of the numerical methods used to solve the eigenvalue problem stated by Eq. (5.6), did not allow us to find the asymptotic exponent α

with sufficient accuracy. This is due to the growing size of the matrix ($\sim q$) and the strong difference in magnitude of its elements ($\sim q^2$) for large values of q.

5.7 Summary and Perspectives

We presented numerical and analytic arguments confirming a nontrivial distribution of the local Lyapunov exponent in the case of the linear noise-driven oscillator (5.1). In order to describe multiscaling, we considered the generalized Lyapunov exponents $L(q)$, which characterize the fluctuations of the local Lyapunov exponent. With the help of a parameter reduction we were able to represent all the exponents $L(q)$ as functions of a renormalized "energy" $E = \mathcal{E}\sigma^{-4/3}$.

A linear form of the generalized Lyapunov exponents is equivalent to a normal distribution of the local Lyapunov exponent which, however, is valid for the noise-driven oscillator only in the limit $|E| \to \infty$. To be more precise, the normal distribution is only an approximation in the vicinity of the mean value. We have found that the parameter range where the linear approximation for the exponent $L(q)$ is valid, depends on the index q and reads $|E|^{3/2} = \mathcal{E}^{3/2}\sigma^{-2} \gg q$. In other words, the exponential growth of moments $\langle A^q \rangle$ of qth order is determined by the Gaussian part of the distribution within this parameter range.

Our numerical findings in the limit $q \gg 1$ suggest a scaling relation $L(q) \sim q^{\alpha-1}$. The corresponding exponent $\alpha \approx 1.4$ can be connected to the probability of large deviations of the local Lyapunov exponent from its average value via the Legendre transformation. We demonstrated that this results in a suppression of the tails compared to the Gaussian distribution.

Our results also shed light upon the difference between possible definitions of the exponential growth rate, given by $L(q)$ for different q. In the Gaussian regime this difference is linear in q. For $|E|^{3/2} \lesssim q$, however, this linearity is destroyed and one has to take into account multiscaling of the Lyapunov exponents.

6 Conclusion

In this work a stochastic theory of the Lyapunov exponents has been applied to weakly coupled chaotic systems and to weakly coupled disordered quantum systems. For such systems coupling sensitivity of the Lyapunov exponents is observed. The choice of the statistical framework was motivated by the observed universality, which manifests itself in scaling laws which are valid for a wide range of different systems. By replacing the chaotic fluctuations in the linearized perturbation dynamics by stochastic processes, we were able to give explanations for the observed universality and to obtain analytic or approximate results. In the case of the stochastic model for the perturbation dynamics of Hamiltonian systems, the parametrically excited oscillator, it has been examined to what extend the distribution of the finite-time Lyapunov exponent incorporates multiscaling.

In the following, we discuss our main results. Finally, we report open questions and future perspectives.

6.1 Discussion of Main Results

Coupling Sensitivity of Chaos

We have introduced a stochastic continuous-time model for the perturbation dynamics of weakly coupled chaotic systems, which includes the key ingredients of exponential growth, temporal fluctuations, and coupling (Ch. 3 and Refs. [68, 3, 69]). By means of the Fokker-Planck equation we have been able to derive a general analytic expression for the coupling dependence of the Lyapunov exponents. In contrast to previous models [26, 43, 21] it is also valid for coupled nonidentical systems. As a special case for very small coupling and identical Lyapunov exponents of the uncoupled systems, we have obtained as an approximation the $1/\ln \kappa$ dependence of the largest Lyapunov exponent known as coupling sensitivity of chaos [23]. In agreement with previous observations [23], our results underline the necessity of fluctuations of the local multipliers (or finite-time Lyapunov exponents) for this singular behaviour of the Lyapunov exponent. A comparison with results of numerical simulations for coupled maps proved the validity of our theoretical results. Finally we have shown that our simple stochastic model allows a qualitative understanding of the coupling sensitivity of chaos as a restricted random walk phenomenon.

Numerical results for coupled time-continuous systems showed that the null Lyapunov exponent exhibits no coupling sensitivity. We have also checked this for coupled complex maps, where the motion of the angle in the complex plane has a zero Lyapunov exponent.

Taking into account the role of fluctuations for the existence of coupling sensitivity, we conclude that the fluctuations of the growth rate corresponding to the null exponent are suppressed. This fact reveals a limitation of the simple stochastic approach, which assumes an unlimited diffusion in the perturbation dynamics.

Finally we have examined the coupling behavior of a stochastic Hamiltonian model for the perturbation dynamics. Numerical simulations for coupled standard maps showed coupling sensitivity of the Lyapunov exponents to occur also for symplectic maps. This has been confirmed by analytic results for the stochastic model in the limit of large frequencies.

Coupling Sensitivity of the Localization Length

Having taken into account the formal similarity to the stochastic model for Hamiltonian chaotic systems, we investigated coupled disordered quantum chains which show Anderson localization (Ch. 4 and Ref. [70]). The weak coupling regime we were interested in, is not well described by the DMPK equation [11] which presumes isotropic scattering. We have obtained numerical results for weakly coupled one-dimensional Anderson models, and found the $1/\ln \kappa$ dependence of the smallest positive Lyapunov exponent on the coupling strength κ for different distributions of the random potential. Thus the localization length, given by the inverse of this Lyapunov exponent, increases singularly with the coupling which to our knowledge has not been reported before. We have found this phenomenon also for several coupled chains and for weak random coupling.

The analytic results we have obtained for a continuum disordered model confirmed the numerical findings, whereupon the effect seems to be a general phenomenon in systems with localization due to disorder.

We have also given a qualitative explanation of this effect, which considers coupled random walks, the "walkers" being the logarithms of the norms of the wave function in the chains.

An investigation of two common conductance definitions has shown that the *typical* conductance increases singularly with the coupling in the same manner as the localization length, wheras the *average* conductance can be expanded in a power series of the coupling strength.

Lyapunov Exponents of the Noise-Driven Oscillator

Finally we have studied the linear oscillator with parametric noise, which is used as a model in the theory of localization and in the theory of Hamiltonian chaos (Ch. 5 and Ref. [71]). The noise leads to an exponential growth of the oscillations due to parametrical instability, which is described by the Lyapunov exponent.

We have investigated the distribution of the finite-time (local) Lyapunov exponent by calculating the generalized Lyapunov exponents $L(q)$. Using a time rescaling we have identified a single parameter relevant for the scaling of these exponents. Employing numerical

and analytic methods, the parameter range where the non-Gaussian part of the distribution of the local Lyapunov exponent is significant has been identified. Thus we have determined the range where the exponential growth of higher moments of the amplitude is governed by the non-Gaussian part of the distribution and multiscaling is essential.

In the limit of large q we have found a power law scaling of the exponents $L(q)$. With the help of the Legendre transformation we have related the corresponding exponent to the probability of large deviations of the local Lyapunov exponent from its mean value. This reveals that the tails of the distribution are suppressed compared to a Gaussian one.

6.2 Open Questions and Perspectives

An interesting direction of further research should be the study of manifestations of our theoretical results in physical systems. To observe directly the coupling dependence of the Lyapunov exponents (Ch. 3) in experiments with weakly coupled chaotic systems is expected to be difficult, although some methods exist to estimate at least the largest Lyapunov exponent from experimental time series [34]. A more promising approach could be to look for effects on measurable quantities that depend on the Lyapunov exponents. Here especially the Lyapunov exponents of disordered systems could be useful, as they are connected with the localization length, the electrical conductance, and correlation functions [22, 36]. The coupling sensitivity of the localization length (Ch. 4) should be accessible to experimental verification, though the realization of the weak coupling seems to be tricky. In this context optical experiments with disordered media [59] and carbon nanotubes [35] are most promising.

From the theoretical point of view the coupling dependence of the null Lyapunov exponent of continuous-time systems deserves further research. Recent results [42] have shown a quadratic increase of the null exponent of coupled attractors with multiple scrolls. If this turns out to be a universal phenomenon for such attractors, a simple model reflecting the corresponding mechanism would be desirable.

Concerning the coupling sensitivity of the localization length, it would be interesting to consider quasi-one-dimensional models with many coupled chains. It seems also promising to study in more detail the effect that the singular increase of the localization length has upon experimentally accessible quantities.

Furthermore the existence of multiscaling in the simple random frequency oscillator model (Ch. 5) suggests that such behavior should be present in a large class of chaotic systems. Especially the statistics of the local Lyapunov exponent of high dimensional Hamiltonian systems, for which the noisy oscillator serves as a model [19], is of interest. Such research, however, would demand a high numerical effort. Regarding the use of the noisy oscillator model in the theory of localization, further research is necessary to clarify the connection of our results to conductance fluctuations.

A Appendix

A.1 Numerical Calculation of Lyapunov Exponents

This work is mainly concerned with the Lyapunov exponents, the latter either as indicators for the stability properties of dynamical systems or as the inverse localization length of disordered quantum chains. Here we describe the methods used in this work to numerically calculate these exponents (see also , e.g. Ref. [47]). A comparison of different methods for calculating Lyapunov exponents can be found in Ref. [32].

A.1.1 Discrete Maps

To calculate all N Lyapunov exponents of an N-dimensional map, we have to follow the dynamics of N perturbation vectors $\boldsymbol{w}_i$, $i = 1, \ldots, N$, which for $t = 0$ are linearly independent and normalized to unit length. The largest Lyapunov exponent is then given by

$$\lambda_1 = \lim_{t \to \infty} \frac{1}{t} \ln \| \boldsymbol{w}(t) \|, \tag{A.1}$$

it does not depend on the norm. The sum of the n largest Lyapunov exponents is given by

$$\sum_{i=1}^{n} \lambda_i = \lim_{t \to \infty} \frac{1}{t} \ln V_n(t), \tag{A.2}$$

where V_n is the volume spanned up by the perturbation vectors $\boldsymbol{w}_1, \ldots, \boldsymbol{w}_n$.

At this point we face two problems. First, the norm $\| \boldsymbol{w}(t) \|$ grows or shrinks exponentially if λ_1 is greater or less than zero, respectively. So already for moderate values of t the norm can either not be calculated due to numerical overflow, or is zero due to limited numerical precision. In both cases, λ_1 cannot be calculated from Eq. (A.1). Second, if λ_1 is positive and some other perturbation vector $\boldsymbol{w}_i$, $i > 1$, has a component in the direction of $\boldsymbol{w}_1$, this component grows with a larger exponential rate than the components in all other directions. In this way the different perturbation vectors rapidly align in the direction of largest growth. As a result the calculation of volumes spanned up by different vectors becomes impossible due to limited numerical precision.

The remedy for these problems is reorthonormalization of the perturbation vectors $\boldsymbol{w}_i$ after not too long time intervals. The growth rate of the linear system is independent of the length of the vectors, such that renormalization of the vectors is a valid way to overcome

the first problem. Reorthogonalizing the vectors ensures that $\boldsymbol{w}_1$ points in the direction of largest growth, $\boldsymbol{w}_2$ points in the direction of second largest growth perpendicular to $\boldsymbol{w}_1$, and so on. Furthermore, the volumes are now rectangular and we have

$$\ln V_n = \sum_{i=1}^{n} \ln \| \boldsymbol{w}_i \| \ .$$

So we can subtract the expressions (A.2) for different n to directly calculate λ_i,

$$\lambda_i = \frac{1}{N_{\text{ort}} T_{\text{ort}}} \sum_{j=1}^{N_{\text{ort}}} \ln \| \boldsymbol{w}_i(t_j) \| \, ,$$

where $N_{\text{ort}} \gg 1$ and $T_{\text{ort}} \sim 1$ are the number of and the time interval between reorthonormalizations, and t_j is the time of the j-th reorthonormalization. The reorthonormalization method used for the numerical calculations in this work is the modified Gram-Schmidt algorithm, which is numerically more accurate than the classical Gram-Schmidt algorithm [14]. Before the calculation of the λ_i starts, a sufficiently long transient phase is necessary to ensure that the system is on its attractor. It should be kept in mind that in practice one always calculates finite-time Lyapunov exponents.

A.1.2 Differential Equations

For an N-dimensional system of ordinary differential equations the algorithm is essentially the same as for discrete maps. The numerical integration schemes used in this work (Runge-Kutta, Bulirsch-Stoer [55]) calculate $\boldsymbol{u}(t)$ at discrete times $t = t_n$. The Lyapunov exponents are calculated according to

$$\lambda_i = \frac{1}{T} \sum_{j=1}^{N_{\text{ort}}} \ln \| \boldsymbol{w}_i(t_j) \| \, ,$$

with the (long) integration time $T \gg 1$.

A.1.3 Generalized Lyapunov Exponents

The q-th generalized Lyapunov exponent is defined as

$$L(q) = \lim_{t \to \infty} \frac{1}{t} \ln \langle \| \boldsymbol{w}(t) \|^q \rangle \, ,$$

where the average is over different trajectories of the system. This average has to be carried out explicitly, i.e. there have to be computed two limits, one due to the averaging and one regarding $t \to \infty$. This makes the numerical calculation of generalized Lyapunov exponents

much more difficult than the calculation of the usual Lyapunov exponents. The standard approach consists of first calculating $L_m(q)$ by approximating (in the discrete-time case)

$$\langle \| \boldsymbol{w}(m) \|^q \rangle \approx \frac{1}{n} \sum_{j=1}^{n} \| \boldsymbol{w}_j(m) \|^q \, ,$$

where j denotes different realizations or trajectories, resp. The value of $L(q)$ is then calculated by considering $L_m(q)$ as a function of $1/m$ and extrapolating to $1/m \to 0$. Details can be found in Ref. [22].

A.2 Stochastic Differential Equations

In the following we briefly review some facts for stochastic differential equations that are needed in this work. The subject is treated in detail in Refs. [31, 58, 65].

A.2.1 Langevin Equation

Differential equations with a stochastic driving term are usually called Langevin equation. For a one-dimensional stochastic variable $x(t)$ it is given by (in Stratonovich form, see below)

$$\mathrm{d}x(t) = f(x)\mathrm{d}t + g(x) \circ \mathrm{d}W(t),$$

where $W(t)$ is a Wiener process (i.e. the displacement of a Brownian particle with starting point $W(0) = 0$). It has a Gaussian distribution characterized by

$$\langle W(t) \rangle = 0, \quad \langle W(t)W(t') \rangle = \min(t, t').$$

In general, the functions f and g can also be time-dependent. In this work, we often write Langevin equations in the intuitive form

$$\mathrm{d}x(t)/\mathrm{d}t = f(x) + g(x)\xi(t),$$

where $\xi(t) = \mathrm{d}W(t)/\mathrm{d}t$ is a Gaussian stochastic process with zero mean, unit variance, and no temporal correlations,

$$\langle \xi(t) \rangle = 0, \quad \langle \xi(t)\xi(t') \rangle = \delta(t - t'),$$

also known as white noise.

The simplest Langevin equation reads

$$\mathrm{d}x(t) = \mathrm{d}W(t).$$

Its solution is given by

$$x(t) = x(0) + \int_0^t \mathrm{d}W(\tilde{t}) = x(0) + W(t).$$

This simple example demonstrates that the variable $x(t)$ depends on $W(t)$. For the solution of a multiplicative noise equation,

$$\mathrm{d}x(t) = g(x) \circ \mathrm{d}W(t),$$

it is thus not clear how the integral in the solution

$$x(t) = x(0) + \int_0^t g(x(\tilde{t})) \circ \mathrm{d}W(\tilde{t})$$

shall be calculated. There is no definite answer to this question, one has to decide between different interpretations of the Langevin equation. In the Stratonovich interpretation the solution is given by

$$x(t) = x(0) + \lim_{N \to \infty} \sum_{n=0}^{N-1} g\left(\frac{x(t_{n+1}) + x(t_n)}{2}\right) [W(t_{n+1}) - W(t_n)] \quad \text{with} \quad t_n = \frac{nt}{N}.$$

For this choice the variable $x(t)$ can be transformed by the usual rules of calculus, which is not the case for other interpretations. One can also argue that the Stratonovich interpretation is closer to physical processes (which are never exactly δ-correlated).

In this work Langevin equations are used as models of chaotic processes. Since these models are constructed to match the properties of the chaotic processes, we have to choose one specific interpretation in advance. Throughout this work, the Stratonovich interpretation is used.

A.2.2 Furutsu-Novikov Relation

At several points in this work it is necessary to calculate averages of the form $\langle \xi(t) F[\xi] \rangle$, where $F[\xi]$ is a functional of $\xi(t)$ (e.g. an integral). For a Gaussian stochastic process $\xi(t)$ with zero mean the Furutsu-Novikov relation provides a very convenient way to evaluate averages of this kind [30, 45]. The relation reads

$$\langle \xi(t) F[\xi] \rangle = \int \langle \xi(t) \xi(t') \rangle \left\langle \frac{\delta F[\xi]}{\delta \xi(t')} \right\rangle dt' \, ,$$

where $\delta F / \delta \xi$ is the functional derivative, and the integral extends over the interval which t' is defined on.

As an example which is of particular importance for this work we study

$$dx/dt = a(x) + b(x)\xi(t)$$

with $t \in [0, \infty)$ and the Gaussian noise process $\xi(t)$:

$$\langle \xi(t) \rangle = 0 \, , \quad \langle \xi(t) \xi(t') \rangle = 2\sigma^2 \delta(t - t') \, .$$

We are interested in averages of the form $\langle f(x)\xi(t) \rangle$. Using the chain rule, the functional derivative is calculated as

$$\frac{\delta f(x)}{\delta \xi(t')} = \begin{cases} \frac{\partial f}{\partial x} \frac{\delta x}{\delta \xi(t')} = \frac{\partial f}{\partial x} b(x) & \text{if} \quad t' \in [0, t], \\ 0 & \text{else.} \end{cases}$$

The Furutsu-Novikov relation thus gives

$$\langle f(x)\xi(t) \rangle = \int_0^t 2\sigma^2 \delta(t - t') \left\langle \frac{\partial f}{\partial x} b(x) \right\rangle dt' = \sigma^2 \left\langle \frac{\partial f}{\partial x} b(x) \right\rangle$$

(note that only one half of the δ-distribution contributes to the integral).

A.2.3 Fokker-Planck Equation

Given a Langevin equation, one is usually not interested in individual trajectories. Rather averages, such as moments $\langle x^q \rangle$, which are in general time-dependent are of interest in practice. All information about the distribution of $x(t)$ can be obtained from the probability density $\rho(x;t)$. The temporal evolution of $\rho(x;t)$ is described by the Fokker-Planck equation which can be derived as follows.

Consider the one-dimensional Langevin equation

$$dx/dt = a(x,t) + b(x,t)\xi(t) , \quad \langle \xi(t)\xi(t') \rangle = 2\sigma^2 \delta(t-t') ,$$

with the Gaussian noise $\xi(t)$. The probability density is defined by

$$\rho(y;t) = \langle \delta[y - x(t)] \rangle .$$

Using the chain rule the time derivative can be written as

$$
\begin{aligned}
\frac{\partial \rho(y;t)}{\partial t} &= \frac{\partial}{\partial t} \langle \delta[y - x(t)] \rangle \\
&= \left\langle [a(x,t) + b(x,t)\xi(t)] \frac{\partial}{\partial x} \delta[y - x(t)] \right\rangle \\
&= -\frac{\partial}{\partial y} \langle [a(x,t) + b(x,t)\xi(t)] \delta[y - x(t)] \rangle \\
&= -\frac{\partial}{\partial y} a(y,t)\rho(y;t) - \frac{\partial}{\partial y} b(y,t) \langle \xi(t)\delta[y - x(t)] \rangle .
\end{aligned}
$$

The last term can be evaluated with the help of the Furutsu-Novikov theorem:

$$
\begin{aligned}
\langle \xi(t)\delta[y - x(t)] \rangle &= -\frac{\partial}{\partial y} \int_0^t dt' \, 2\sigma^2 \delta(t-t') \langle b(x,t')\delta[y - x(t)] \rangle \\
&= -\frac{\partial}{\partial y} \sigma^2 b(y,t)\rho(y;t) .
\end{aligned}
$$

Hence the Fokker-Planck equation reads as

$$\frac{\partial \rho(x;t)}{\partial t} = -\frac{\partial}{\partial x} a(x,t)\rho(x;t) + \sigma^2 \frac{\partial}{\partial x} b(x,t) \frac{\partial}{\partial x} b(x,t)\rho(x;t) = -\frac{\partial J(x,t)}{\partial x} .$$

It has the form of a continuity equation for the probability current J. A stationary distribution requires the probability current to be constant. The quantities

$$D_1 = a(x,t) + \frac{\partial b(x,t)}{\partial x} b(x,t) , \quad D_2 = b^2(x,t)$$

are known as drift and diffusion coefficient, resp.

Notation

t	time
x	space
$\boldsymbol{u}$	state vector with components u_i
$\boldsymbol{w}$	perturbation vector
$\boldsymbol{f}$	nonlinear function
$\mathbf{J}$	Jacobian of f
$\mathbf{P}$	product matrix $\prod \mathbf{J}$
$\mathbf{P}^T$	transpose of $\mathbf{P}$
A	amplitude
ϕ, θ	phase
Ψ	quantum state
$\delta(x)$	DIRAC delta-function
κ	coupling parameter
D	diffusion constant
ε	site energy (Ch. 4)
E	frequency parameter (Ch. 5)
λ_i	Lyapunov exponents
Λ_i	Lyapunov exponents of uncoupled systems
$\lambda(t)$	local (finite-time) Lyapunov exponent
$L(q)$	generalized Lyapunov exponents
χ, ξ, η	stochastic processes
$2\sigma^2$	intensity of δ-correlated stochastic process
$W(t)$	Wiener process
$\rho(s)$	probability density of stochastic variable s
ODE	ordinary differential equation
PDE	partial differential equation

Bibliography

[1] M. Abramowitz and I. A. Stegun, *Handbook of Mathematical Functions*, Department of Commerce USA, Washington, D.C., 1964.

[2] V. Ahlers, *Scaling and Synchronization in Deterministic and Stochastic Nonlinear Dynamical Systems*, Ph.D. thesis, Universität Potsdam, 2001.

[3] V. Ahlers, R. Zillmer, and A. Pikovsky, *Statistical theory for the coupling sensitivity of chaos*, Stochastic and Chaotic Dynamics in the Lakes: STOCHAOS (D. S. Broomhead, E. A. Luchinskaya, P. V. E. McClintoc, and T. Mullin, eds.), AIP Conference Proceedings, vol. 502, AIP, Melville, NY, 2000, p. 450.

[4] V. Ahlers, R. Zillmer, and A. Pikovsky, *Lyapunov exponents in disordered chaotic systems: Avoided crossing and level statistics*, Phys. Rev. E **63** (2001), 036213.

[5] P. W. Anderson, *Absence of diffusion in certain random lattices*, Phys. Rev. **109** (1958), 1492.

[6] J. Argyris, G. Faust, and M. Haase, *An Exploration of Chaos*, North-Holland, Amsterdam, 1994.

[7] L. Arnold, *Random Dynamical Systems*, Springer, Berlin, 1998.

[8] L. Arnold, M. M. Doyle, and N. S. Namachchivaya, *Small noise expansion of moment Lyapunov exponents for two-dimensional systems*, Springer, Berlin, 1998.

[9] J. Barre and T. Dauxois, *Lyapunov exponents as dynamical indicator of a phase transition*, Europhys. Lett **55** (2001), 154.

[10] C. Beck and F. Schlögel, *Thermodynamics of Chaotic Systems: An Introduction*, Cambridge University, Cambridge, 1993.

[11] C. W. J. Beenakker, *Random-matrix theory of quantum transport*, Rev. Mod. Phys. **69** (1997), no. 3, 731.

[12] G. Benettin, *Power-law behavior of Lyapunov exponents in some conservative dynamical systems*, Physica D **13** (1984), no. 1-2, 211.

[13] R. Bhatia, *Matrix Analysis*, Springer, New York, 1997.

[14] Å. Björck, *Numerics of Gram-Schmidt orthogonalization*, Linear Algebra Appl. **197/198** (1994), 297.

[15] G. Boffetta, M. Cencini, M. Falcioni, and A. Vulpiani, *Predictability: a way to characterize complexity*, Phys. Rep. **356** (2002), 367.

[16] R. E. Borland, Proc. R. Soc. London A **274** (1963), 529.

[17] L. A. Bunimovich and Ya. G. Sinai, *Spacetime chaos in coupled map lattices*, Nonlinearity **1** (1988), no. 4, 491–516.

[18] L. Casetti, R. Livi, and M. Pettini, *Gaussian model for chaotic instability of hamiltonian flows*, Phys. Rev. Lett. **74** (1995), 375.

[19] L. Casetti, M. Pettini, and E. G. D. Cohen, *Geometrical approach to hamiltonian dynamics and statistical mechanics*, Phys. Rep. **337** (2000), 237.

[20] F. Cecconi and A. Politi, *n-tree approximation for the largest Lyapunov exponent of a coupled map lattice*, Phys. Rev. E **56** (1997), no. 5, 4998.

[21] F. Cecconi and A. Politi, *Analytic estimate of the maximum Lyapunov exponent in products of tridiagonal random matrices*, J. Phys. A: Math., Gen. **32** (1999), no. 44, 7603–7622.

[22] A. Crisanti, G. Paladin, and A. Vulpiani, *Products of random matrices in statistical physics*, Springer, Berlin, 1993.

[23] H. Daido, *Coupling sensitivity of chaos*, Prog. Theor. Phys. **72** (1984), no. 4, 853–856.

[24] H. Daido, *Coupling sensitivity of chaos*, Prog. Theor. Phys. Suppl. **79** (1984), 75–95.

[25] H. Daido, *Coupling sensitivity of chaos and the Lyapunov dimension: the case of coupled two-dimensional maps*, Phys. Lett. A **110** (1985), no. 1, 5–9.

[26] H. Daido, *Coupling sensitivity of chaos: Theory and further numerical evidence*, Phys. Lett. A **121** (1987), no. 2, 60.

[27] L. I. Deych, A. A. Lisyansky, and B. L. Altshuler, *Single parameter scaling in one-dimensional localization revisited*, Phys. Rev. Lett. **84** (2000), no. 12, 2678.

[28] R. S. Ellis, *Entropy, large deviations, and statistical mechanics*, Springer, Berlin, 1985.

[29] H. Fujisaka, H. Ishii, M. Inoue, and T. Yamada, *Intermittency caused by chaotic modulation II*, Prog. Theor. Phys. **76** (1986), no. 6, 1198–1209.

[30] K. Furutsu, *On the statistical theory of electromagnetic waves in a fluctuating medium*, J. Res. NBS **D667** (1963), 303.

[31] C. W. Gardiner, *Handbook of stochastic methods*, Springer, Berlin, 1996.

[32] K. Geist, U. Parlitz, and W. Lauterborn, *Comparison of different methods for computing Lyapunov exponents*, Prog. Theor. Phys. **83** (1990), no. 5, 875.

[33] J. Guckenheimer and P. Holmes, *Nonlinear oscillations, dynamical systems, and bifurcations of vector fields*, Springer, N. Y., 1986.

[34] H. Kantz and T. Schreiber, *Nonlinear time series analysis*, Cambridge University Press, Cambridge, 1997.

[35] T. Kostyrko, M. Bartkowiak, and G. D. Mahan, *Localization in carbon nanotubes within a tight-binding model*, Phys. Rev. B **60** (1999), 735.

[36] T. Kottos, F. M. Izrailev, and A. Politi, *Finite-length Lyapunov exponents and conductance for quasi-1D disordered solids*, Physica D **131** (1999), 155–169.

[37] B. Kramer and A. MacKinnon, *Localization: theory and experiment*, Rep. Prog. Phys. **56** (1993), 1469.

[38] P. S. Landa and A. A. Zaikin, *Noise-induced phase transitions in a pendulum with a randomly vibrating suspension axis*, Phys. Rev. E **54** (1996), 3535–3544.

[39] R. Landauer, Phil. Mag. **21** (1970), 683.

[40] D. W. Lewis, *Matrix theory*, World Scientific, Singapore, 1991.

[41] I. M. Lifshitz, S. A. Gredeskul, and L. A. Pastur, *Introduction to the theory of disordered systems*, Wiley, New York, 1988.

[42] Z. Liu, Y.-C. Lai, and M. A. Matías, *Universal scaling of Lyapunov exponents in coupled chaotic oscillators*, Phys. Rev. E **67** (2003), 045203.

[43] R. Livi, A. Politi, and S. Ruffo, *Scaling law for the maximal Lyapunov exponent*, J. Phys. A: Math., Gen. **25** (1992), 4813.

[44] P.-G. Luan and Z. Ye, *Statistics of the Lyapunov exponent in one-dimensional layered systems*, Phys. Rev. E **64** (2001), 066609.

[45] E. A. Novikov, *Functionals and the random-force method in turbulence theory*, JETP **20** (1965), no. 5, 1290.

[46] V. I. Oseledec, *A multiplicative ergodic theorem: Lyapunov characteristic numbers for dynamical systems*, Trans. Moscow Math. Soc. **19** (1968), 197–231.

[47] E. Ott, *Chaos in dynamical systems*, Cambridge Univ. Press, Cambridge, 1992.

[48] G. Paladin and S. Vaienti, *Looking at the equilibrium measures in dynamical systems.*, J. Phys. A **21** (1988), 4609.

[49] G. Paladin and A. Vulpiani, *Scaling law and asymptotic distribution of Lyapunov exponents in conservative dynamical systems with many degrees of freedom.*, J. Phys. A **19** (1986), no. 10, 1881.

[50] S. Papazoglou, Master's thesis, Universität Hamburg, 2003.

[51] J.-L. Pichard, Ph. D. thesis, Université de Paris Orsay, Orsay, 1984.

[52] A. Pikovsky, *On the interaction of strange attractors*, Z. Phys. B **55** (1984), no. 2, 149–154.

[53] A. Pikovsky and U. Feudel, *Characterizing strange nonchaotic attractors*, Chaos **5** (1995), no. 1, 253.

[54] A. Pikovsky and A. Politi, *Dynamic localization of Lyapunov vectors in space-time chaos*, Nonlinearity **11** (1998), no. 4, 1049.

[55] W. H. Press, S. A. Teukolsky, W. T. Vetterling, and B. P. Flannery, *Numerical recipes in C: The art of scientific computing*, Cambridge University Press, Cambridge, 1992.

[56] Y. Quéré, *Physics of materials*, Gordon and Breach, Amsterdam, 1998.

[57] L. E. Reichl, *The transition to chaos in conservative classical systems: Quantum manifestations*, Springer, New York, 1992.

[58] H. Risken, *The Fokker–Planck equation*, Springer, Berlin, 1989.

[59] J. G. Rivas, R. Sprik, A. Lagendijk, L. D. Noordam, and C. W. Rella, *Static and dynamic transport of light close to the Anderson localization transition*, Phys. Rev. E **63** (2001), 046613.

[60] H. Schomerus and M. Titov, *Statistics of finite-time Lyapunov exponents in a random time-dependent potential*, Phys. Rev. E **66** (2002), 066207.

[61] H. Schomerus and M. Titov, *Band-center anomaly of the conductance distribution in one-dimensional Anderson localization*, Phys. Rev. B **67** (2003), 100201.

[62] K. Slevin, P. Markoš, and T. Ohtsuki, *Reconciling conductance fluctuations and the scaling theory of localization*, Phys. Rev. Lett. **86** (2001), no. 16, 3594.

[63] R. L. Stratonovich, *Topics in the theory of random noise*, Gordon and Breach, New York, 1963.

[64] L. Tessieri and F. M. Izrailev, *One-dimensional quantum models with correlated disorder versus classical oscillators with colored noise*, Phys. Rev. E **64** (2001), 066120.

[65] N. G. van Kampen, *Stochastic processes in physics and chemistry*, Elsevier-Science, Amsterdam, 1997.

[66] T. Yamada and H. Fujisaka, *Intermittency caused by chaotic modulation. I. Analysis with a multiplicative noise model*, Prog. Theor. Phys. **76** (1986), no. 3, 582–591.

[67] R. Zillmer, *Lyapunov-Exponenten in gekoppelten und rauschgetriebenen Systemen*, Master's thesis, Universität Potsdam, 1999.

[68] R. Zillmer, V. Ahlers, and A. Pikovsky, *Scaling of Lyapunov exponents of coupled chaotic systems*, Phys. Rev. E **61** (2000), no. 1, 332.

[69] R. Zillmer, V. Ahlers, and A. Pikovsky, *Stochastic approach to Lyapunov exponents in coupled chaotic systems*, Stochastic Processes in Physics, Chemistry, and Biology (J. A. Freund and T. Pöschel, eds.), Lecture Notes in Physics, vol. 557, Springer, 2000, p. 400.

[70] R. Zillmer, V. Ahlers, and A. Pikovsky, *Coupling sensitivity of localization length in one-dimensional disordered systems*, Europhys. Lett. **60** (2002), no. 6, 889.

[71] R. Zillmer and A. Pikovsky, *Multiscaling of noise-induced parametric instability*, Phys. Rev. E **67** (2003), 061117.

Acknowledgements

Many people have made indispensable contributions to the completion of this work. In particular I sincerely thank:

Prof. Dr. Arkady Pikovsky for giving me the opportunity to join his research group, for introducing me to new fields of science, and for sharing many valuable ideas concerning this work;

my colleagues of the statistical physics group for the cooperative atmosphere;

Ines Katzorke, Dr. Volker Ahlers, and Jörg-Uwe Tessmer for their advice in computational matters;

Marlies Path, Marita Dörrwand, and Birgit Nader for their organizational support;

the members of the *Sonderforschungsbereich 555* (Complex Nonlinear Processes), in particular the main organizers Prof. Dr. Lutz Schimansky-Geier, Prof. Dr. Jürgen Kurths, and Prof. Dr. Eckehard Schöll, for establishing a stimulating scientific environment in Berlin and Potsdam;

Dr. Volker Ahlers for the perfect cooperation during the first half of my PhD work and beyond;

Dr. Markus Abel, Dr. Bernd Blasius, Dr. habil. Frank Spahn, Prof. Dr. Fritz Haake, Dr. Dima Shepelyansky, Dr. Stefan Kettemann, Dr. Henning Schomerus, Prof. Dr. Leonid Bunimovich, Dr. Oleksandr Popovych, Nina Kuckländer, Dr. Dmitri Topaj, and many others for enlightening discussions;

Prof. Dr. Günter Radons, Prof. Dr. Igor Sokolov, and Prof. Dr. Arkady Pikovsky for acting as referees of this thesis;

Dr. Volker Ahlers and Nina Kuckländer for their critical reading of parts of the manuscript;

the *Max-Planck-Institut für Physik komplexer Systeme* in Dresden for promoting cooperations with other scientists during well organized workshops;

the *Deutsche Forschungsgemeinschaft* for providing my salary (project SFB 555);

and, of course, my family, in particular my parents, for their invaluable support throughout my studies.